The American Journal of Human Genetics, Volume *109*

Supplemental information

Enrichment analyses identify shared associations for 25 quantitative traits in over 600,000 individuals from seven diverse ancestries

Samuel Pattillo Smith, Sahar Shahamatdar, Wei Cheng, Selena Zhang, Joseph Paik, Misa Graff, Christopher Haiman, T.C. Matise, Kari E. North, Ulrike Peters, Eimear Kenny, Chris Gignoux, Genevieve Wojcik, Lorin Crawford, and Sohini Ramachandran

S1 Supplemental Note for Smith et al. 2021 - "Enrichment analyses identify shared associations for 25 quantitative traits in over 600,000 individuals from seven diverse ancestries"

S0.1 SNP-level results for height and C-reactive protein

In Figure S5A and Figure S5D, we found that, across 25 traits analyzed, height had the greatest number of genome-wide significant SNP-level associations (76,910 unique associations) in at least one ancestry. Of these SNP-level associations, 8.90% (7,377 SNPs) replicate based off of rsID in at least two ancestry cohorts. Height is not the only trait in which the standard GWA SNP-level association test detects associations that replicate extensively across ancestries. In fact, SNP-level associations replicate in each of the 25 continuous traits that we analyze in this study.

We analyzed SNP-level associations with C-reactive protein in six ancestry cohorts: African-American (PAGE), European, South Asian, East Asian, Native Hawaiian, and Hispanic and Latin American cohorts. C-reactive protein is an example of a trait with a sparse and highly conserved genetic architecture across ancestries, as shown in Figure 2. Many SNPs within the *CRP* gene have been previously associated with C-reactive protein plasma levels[1,3]. In our analysis, rs3091244 is genome-wide significant in only the European ancestry cohort, and has been functionally validated as influencing C-reactive protein levels[4,5]. The SNP rs3091244 is located in a promoter region slightly upstream of *CRP*, and it has clinical implications for both atrial fibrillation[6] and lupus erythematosus[7] (European $p = 1.54 \times 10^{-116}$; East Asian $p = 1.15 \times 10^{-9}$).

We expanded our search for replicated GWA SNP-level association signals across ancestry cohorts by scanning for 1 Mb regions that contained associations to the same phenotype in two or more ancestries—a process often referred to as "clumping". These windows were centered at every unique genome-wide significant SNP in any ancestry for a given trait (we refer the 1Mb window around the significant SNP as a "clump", Figure S5B and Figure S5E). In addition to the largest number of unique SNP-level associations, height also had the largest proportion of clumps containing a significant SNP-level GWA association signal that replicated in at least two ancestry cohorts (see Figure S5B and Figure S5E). The three traits with the greatest proportion of clumps containing SNP-level GWA signals that replicate in multiple ancestry cohorts were height (77.09% of clumps), urate (65.89%), and low density lipoprotein (54.40%).

In addition to the SNP-level associations on chromosome 1 surrounding the *CRP* gene across all six ancestry cohorts (displayed in Figure 2), there are other regions of the genome that contain significant GWA associations with C-reactive protein that replicate in multiple ancestry cohorts. On chromosome 2, there is a cluster of four SNPs significantly associated with C-reactive protein levels in the European, East Asian, and

Hispanic and Latin American ancestry cohorts. Of these, rs1260326 (European $p = 1.01 \times 10^{-55}$; East Asian $p = 1.70 \times 10^{-9}$; Hispanic and Latin American $p = 1.24 \times 10^{-20}$), rs780094 (European $p = 9.95 \times 10^{-51}$; East Asian $p = 1.70 \times 10^{-9}$; Hispanic and Latin American $p = 1.14 \times 10^{-16}$), and rs6734238 (African-American (PAGE) $p = 3.04 \times 10^{-10}$; European $p = 8.38 \times 10^{-34}$; South Asian $p = 2.17 \times 10^{-9}$) were statistically significant in three of the six ancestry cohorts that we analyzed. Each of these three SNPs has been previously associated with C-reactive protein levels in a European ancestry cohort[8,10]. Of these three SNPs, only one (rs6734238) had previously been replicated in other ancestries (in African-American, and Hispanic and Latin American cohorts[11]).

On chromosome 19 there are 23 SNPs that are associated with CRP in the African-American PAGE, European, and Hispanic and Latin American ancestry cohorts. Two other SNPs are associated with C-reactive protein in the African-American (PAGE), European, and Hispanic and Latin American cohorts, as well as the East Asian ancestry cohort. One of these two SNPs, rs7310409 (African-American (PAGE) $p = 8.57 \times 10^{-9}$; European $p = 3.57 \times 10^{-210}$; East Asian $p = 2.72 \times 10^{-27}$; Hispanic and Latin American $p = 5.35 \times 10^{-29}$) located in the HNF1 homeobox A (*HNF1A*) gene, has been previously associated with C-reactive protein levels in only a European ancestry cohort[9,10]. Three additional significant SNPs in our analysis have been previously associated with European ancestry cohorts in previous studies, including: rs1169310[11] (European $p = 1.52 \times 10^{-172}$; East Asian $p = 1.28 \times 10^{-18}$; Hispanic and Latin American $p = 1.17 \times 10^{-27}$), rs1183910[8,12] (European $p = 5.50 \times 10^{-177}$; East Asian $p = 3.16 \times 10^{-29}$; Hispanic and Latin American $p = 7.47 \times 10^{-29}$), and rs7953249[13] (European $p = 1.19 \times 10^{-177}$; East Asian $p = 1.10 \times 10^{-19}$; Hispanic and Latin American $p = 4.80 \times 10^{-29}$). Two SNPs, rs2259816 (European $p = 2.77 \times 10^{-172}$; East Asian $p = 9.33 \times 10^{-18}$; Hispanic and Latin American $p = 1.90 \times 10^{-27}$) and rs7979473 (African $p = 1.49 \times 10^{-9}$; East Asian $p = 6.06 \times 10^{-29}$; Hispanic and Latin American $p = 1.56 \times 10^{-30}$), have been previously associated with C-reactive protein in both African-American and Hispanic and Latin American ancestry cohorts[11]. There is one final group of three SNPs associated with C-reactive protein in the African-American (PAGE), European, East Asian, and Hispanic and Latin American ancestry cohorts on chromosome 19. One of them, rs4420638 (East Asian $p = 9.93 \times 10^{-29}$; Hispanic and Latin American $p = 2.03 \times 10^{-30}$), has been previously associated in a European ancestry cohort[8,10,12]. These four regions indicate a highly conserved SNP-level architecture of C-reactive protein across six ancestry cohorts. Interestingly, we were unable to replicate associations with C-reactive protein across ancestries at the gene or pathway levels.

Gene and pathway association results

Three genes, *GP6*, *RDH13*, and *AGPAT5*, were significantly associated with platelet count (PLC) in the African-American (PAGE) ancestry cohort and the East Asian ancestry cohort (Figure S13. Of these, no

significant SNPs in glycoprotein VI platelet (*GP6*) have been reported in the GWAS catalog for either ancestry cohort. However, a single SNP within *GP6*, rs1613662, has previously been associated with mean platelet volume in a GWA study analyzing a European ancestry cohort[14]. *GP6* plays a critical role in platelet aggregation, and mutations have been previously associated with fetal loss[15]. Retinol dehydrogenase 13 (*RDH13*) has no reported GWAS catalog associations with platelet count, but is within 60kb of a SNP significantly associated with platelet aggregation[16]. Of the three genes significantly associated with PLC in both the European and AIAN cohorts, 1-Acylglycerol-3-Phosphate O-Acyltransferase 5 (*AGPAT5*) is a member of a gene family known to play a role in immunity and inflammation response[17].

Alcohol dehydrogenase 2 (*ALDH2*) has additionally been associated with hypertension in an elderly Japanese cohort[18]. A member of the RAS oncogene family (*RAB8A*) has been shown to play a role in the inhibition of inflammatory response. In contrast, cut like homeobox 2 *CUX2* contains a significantly associated SNP in the array used in this study for the East Asian ancestry cohort, but it has no previous associations in a European ancestry cohort. However, *CUX2* is significantly associated at the gene-level in both the European and East Asian ancestry cohorts. Although not reported as being associated with PLC in the GWAS Catalog, a single SNP, rs61745424 which encodes a missense mutation, has been previously identified as being related to the trait[19]. The gene-ε association statistics for the seven genes significantly associated with PLC are available in Table S24.

Finally, a single gene, acyl-CoA dehydrogenase family member 10 (*ACAD10*) associated in our gene-level analysis of PLC, was significant in both the European and East Asian ancestry cohorts (European gene-ε $p = 1.47 \times 10^{-10}$; East Asian gene-ε $p = 2.00 \times 10^{-10}$) but contained no previous associations in the GWAS catalog. The African-American and Hispanic and Latin American ancestry cohorts analyzed in Qayyum et al.[20] both contain SNPs within *ACAD10* that are significantly associated with PLC.

In our analysis of triglyceride levels in six ancestry cohorts (African-American (PAGE), European, East Asian, South Asian, Hispanic and Latin American, and Native Hawaiian), we identified shared genetic architecture at the SNP, gene, and subnetwork level. Replicated SNPs and genes between the six ancestry cohorts are shown in Figure S15-Figure S16. We focus our discussion of results at the network level in the European, East Asian, and Native Hawaiian ancestry cohorts (Figure 3). In the European and East Asian ancestry cohorts, we identified 55 shared genome-wide significant associations at the gene-level. Of these results, eight genes lie in the same significantly mutated subnetwork (Hierarchical HotNet $p < 10^{-3}$) when analyzing each ancestry cohort independently. Five of those eight genes belong to the apolipoprotein family of genes, including: apolipoprotein A1 (*APOA1*), apolipoprotein A4 (*APOA4*), apolipoprotein A5 (*APOA5*), apollipoprotein C3 (*APOC3*), apolipoprotein E (*APOE*). Specifically, the apolipoprotein play a central role in lipoprotein biosynthesis and transport. All of these genes contain SNPs previously associated

with triglyceride levels in a European ancestry cohort[21,26]. All five genes also contain SNPs previously associated with triglyceride levels in non-European ancestry cohorts. Specifically, *APOA1*, *APOC3*, and *APOE* each contain SNPs previously associated with triglyceride levels in African-American and Hispanic and Latin American ancestry cohorts[21,22]. *APOA5* has previously been associated to triglyceride levels in an East Asian, African-American, and Hispanic and Latin American ancestry cohorts[24,27].

The other three genes that were significantly associated with triglyceride levels in the European and East Asian ancestry cohorts are members of the largest significantly mutated subnetwork including phospholipid transfer protein (*PLTP*; European gene-ε $p = 4.29 \times 10^{-9}$; East Asian gene-ε $p = 6.66 \times 10^{-15}$), lipoprotein lipase (*LPL*; European gene-ε $p = 4.08 \times 10^{-13}$; East Asian gene-ε $p = 1.00 \times 10^{-20}$), and angiopoietin like 3 (*ANGPTL3*; European gene-ε $p = 8.86 \times 10^{-8}$; East Asian gene-ε $p = 1.00 \times 10^{-20}$). *PLTP* has previously been associated with triglyceride levels in European, African-American, and Hispanic and Latin American ancestry cohorts[21,22,24,28,32]. *LPL* is one of the most well-studied genes in the regulation of triglyceride levels. It has previously been associated with triglyceride levels in European ancestry cohorts[21,26,28,32,32,45], East Asian ancestry cohorts[27,46], and African ancestry cohorts as well as Hispanic and Latin American ancestry cohorts[21,24,28,29,42,44,45,47,48]. The final gene that was genome-wide significant in both the European and East Asian ancestry cohorts, *ANGPTL3*, has no previous associations in the GWAS catalog and presents a novel candidate gene within the network. While not significant in any gene-level analysis, *ANGPTL4* (European gene-ε $p = 1.00 \times 10^{-20}$; East Asian gene-ε $p = 9.99 \times 10^{-1}$) is from the same family is present in the largest subnetwork in the European cohort and also has also been previously identified as having associations in European, African, and Hispanic and Latin American ancestry cohorts[24,28,42,44,45,49].

In our analysis of the European ancestry cohort from the UK Biobank, we additionally identified a set of eight genes that are connected to the core network discussed above. One of these genes is *ANGPTL4*, which we discussed above. Five of these genes were significant at the gene-level in the European ancestry cohort, including four apoliprotein genes (*APOC1*; European gene-ε $p = 1.67 \times 10^{-16}$, *APOC2*; European gene-ε $p = 3.57 \times 10^{-13}$, *APOC4*; European gene-ε $p = 3.72 \times 10^{-13}$, and *APOB*; European gene-ε $p = 1.00 \times 10^{-20}$) and lipase maturation factor 1 (*LMF1*; European gene-ε $p = 8.03 \times 10^{-7}$). Each of these genes have been previously associated with triglyceride levels in a European ancestry cohort[24]. Additional associations were also found in that same study which conducted a meta-analysis of European, African-American, and Hispanic and Latin American ancestry cohorts. The final two genes included in the significantly mutated subnetwork of the European ancestral cohort, *APOL1* and *HBA1*, were not were not identified as genome-wide significant by gene-ε and have no previous SNP-level associations with triglyceride levels in the GWAS Catalog. Interestingly, both *APOL1* (Native Hawaiian gene-ε $p = 8.89 \times 10^{-11}$) and *HBA1* (Native Hawaiian gene-ε $p = 2.46 \times 10^{-10}$) were both identified as genome-wide significant by gene-ε in our analysis of the Native

Hawaiian ancestry cohort and the interaction between them was identified in our Hierarchical HotNet[50] analysis as present in both the European and Native Hawaiian ancestry cohorts.

In addition to *APOL1* and *HBA1*, six more genes are connected to the core network of genes that overlap in the East Asian and European significantly mutated subnetworks. Of these, both *HBA2* and *B4GALT3* are significant at the gene-level in the Native Hawaiian ancestry cohort alone. They are each connected to genes identified in both the European and Native Hawaiian ancestry cohorts as members of the largest significantly mutated subnetwork. The final three genes include kallikrein related peptidase 8 (*KLK8*), pancreatic lipase *PNLIP*, and wnt family member 4 (*WNT4*) which were not significant at the gene-level and did not contain previous SNP-level associations in the GWAS catalog.

Three of the genes within the network identified in the East Asian ancestry cohort contain previously associated SNPs in both European and non-European ancestry cohorts, including: cholesteryl ester transfer protein (*CETP*), proprotein convertase subtilisin/kexin type 6 (*PCSK6*), and proprotein convertase subtilisin/kexin type 7 (*PCSK7*)[21,29]. The final three genes in the significantly mutated subnetwork identified in the East Asian ancestry cohort were not significant at the gene-level and do not contain previously associated SNPs in the GWAS catalog in any ancestral cohort. Lecithin-cholesterol acyltransferase (*LCAT*) is involved in cholesterol biosynthesis and apolipoprotein F (*APOF*) encodes one of the minor apolipoprotein genes present in plasma. Finally, tyrosine-protein kinase receptor 3 (*TYRO3*) plays a role in ligand recognition and cell metabolism[51]. The gene-ε p-values in each ancestry cohort for each of the 28 genes discussed here are shown in Table S26.

Supplemental Figures

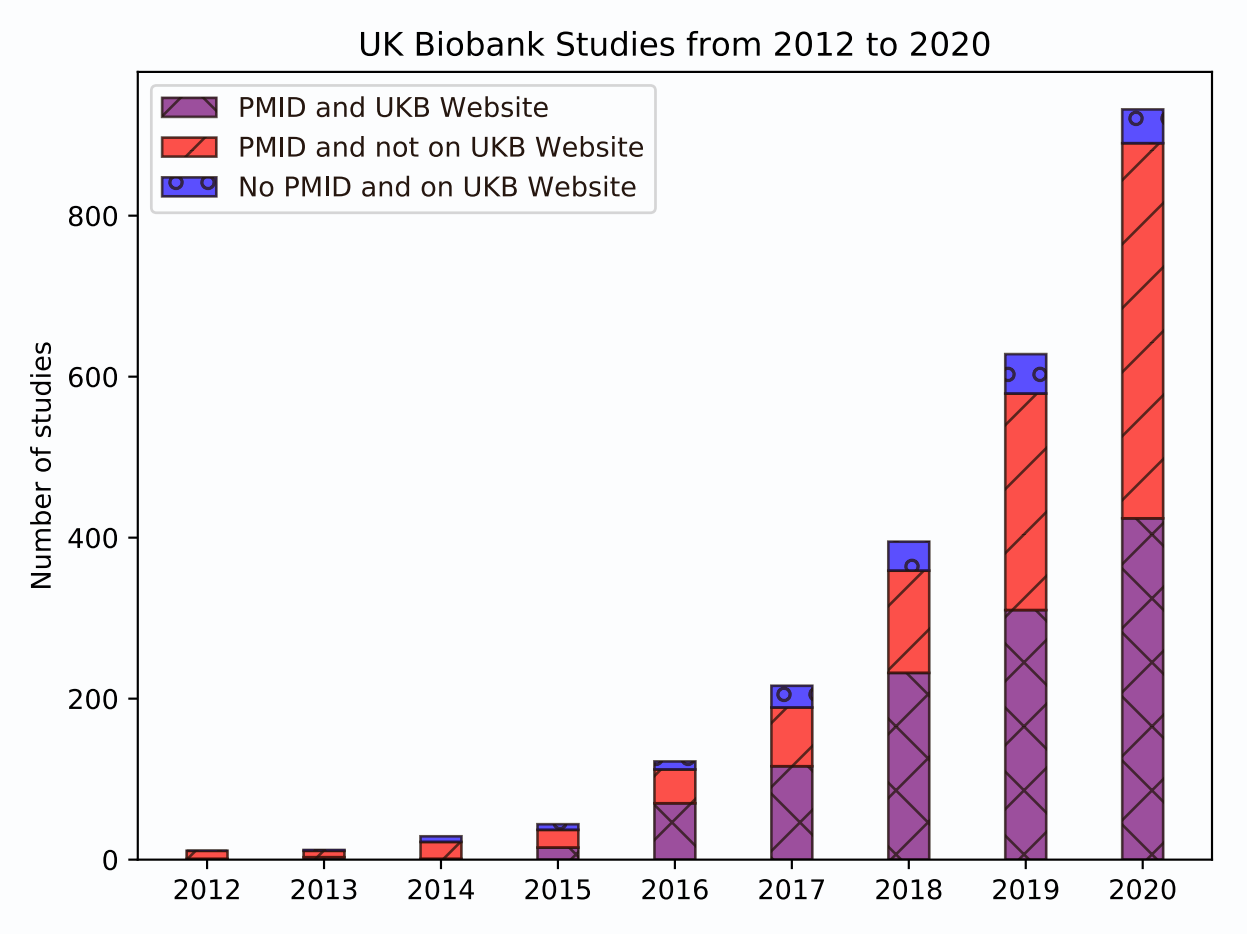

Figure S1: Number of publications we identified using UK Biobank data from 2012 to 2020. Studies identified using PMIDs as described in the Supplemental Information. Studies that are displayed on the UK Biobank website (`https://www.ukbiobank.ac.uk/`) and identified on PubMed are shown in purple. Studies listed on the UK Biobank website but do not have a PMID are shown in blue, and studies only identified using PubMed but not listed on the UK Biobank website are shown in red. The protocols for identifying studies both on PubMed and the UK Biobank website are detailed in the Supplemental Information. Data from both the UK Biobank website and PubMed were accessed on January 12, 2021.

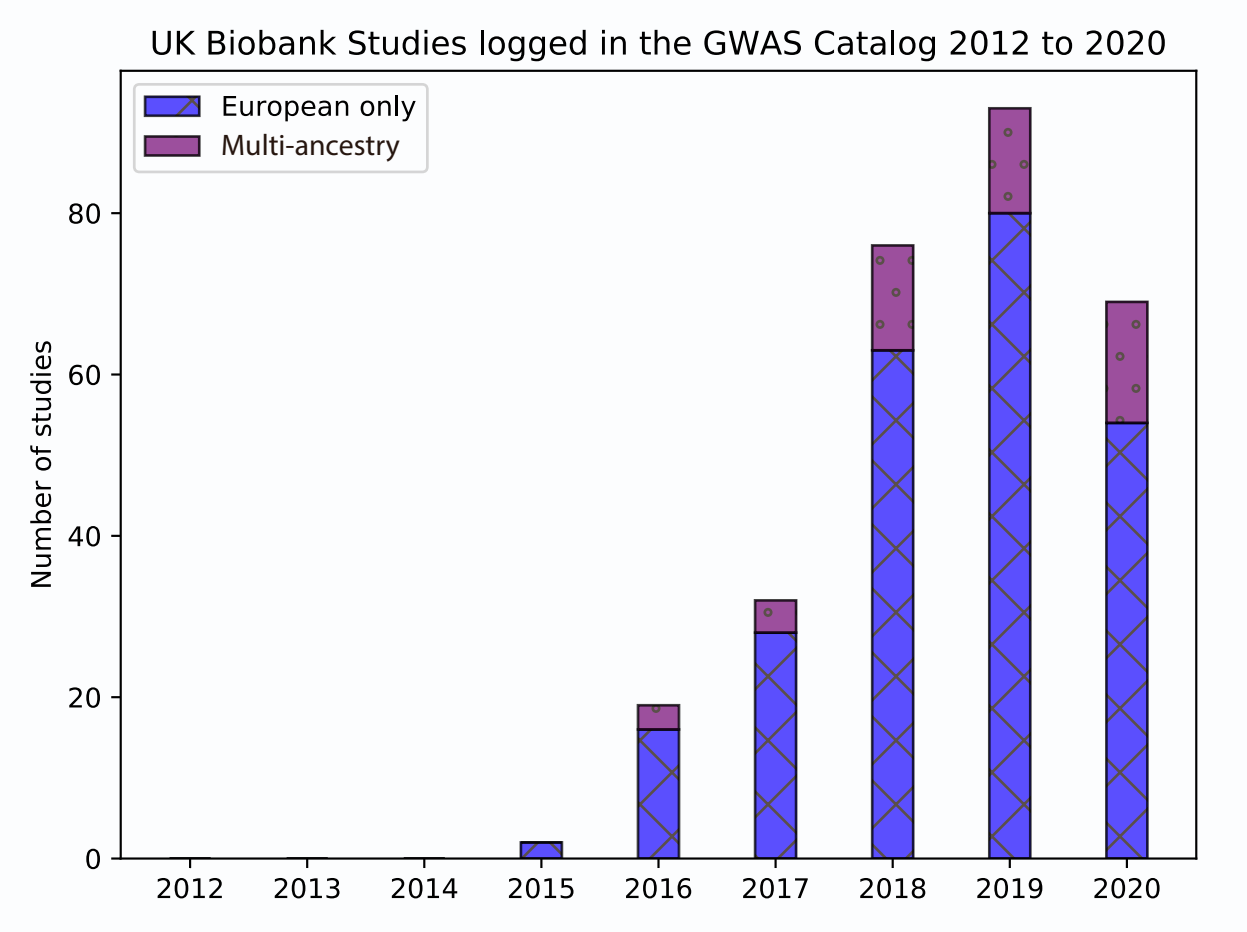

Figure S2: Number of studies published using UK Biobank data from 2012 to 2020 that have available metadata in the GWAS Catalog. Our protocols for identifying studies from the GWAS Catalog are detailed in the Supplemental Information. Multi-ancestry studies are shown in purple and include those that list samples of more than one ancestral group in the GWAS catalog (as defined according to the protocol using Popejoy and Fullerton[52], available on the GitHub page `https://github.com/ramachandran-lab/redefining_replication`). Studies that only list samples of European ancestry in the GWAS catalog are shown in blue. Every multi-ancestry analysis includes samples of European ancestry and of at least one other ancestry. GWAS Catalog data was accessed on January 10, 2021 from the website `https://www.ebi.ac.uk/gwas/docs/file-downloads` using the final release file of 2020 (see file named `gwas_catalog_v1.0.2-associations_e100_r2020-12-15.tsv`).

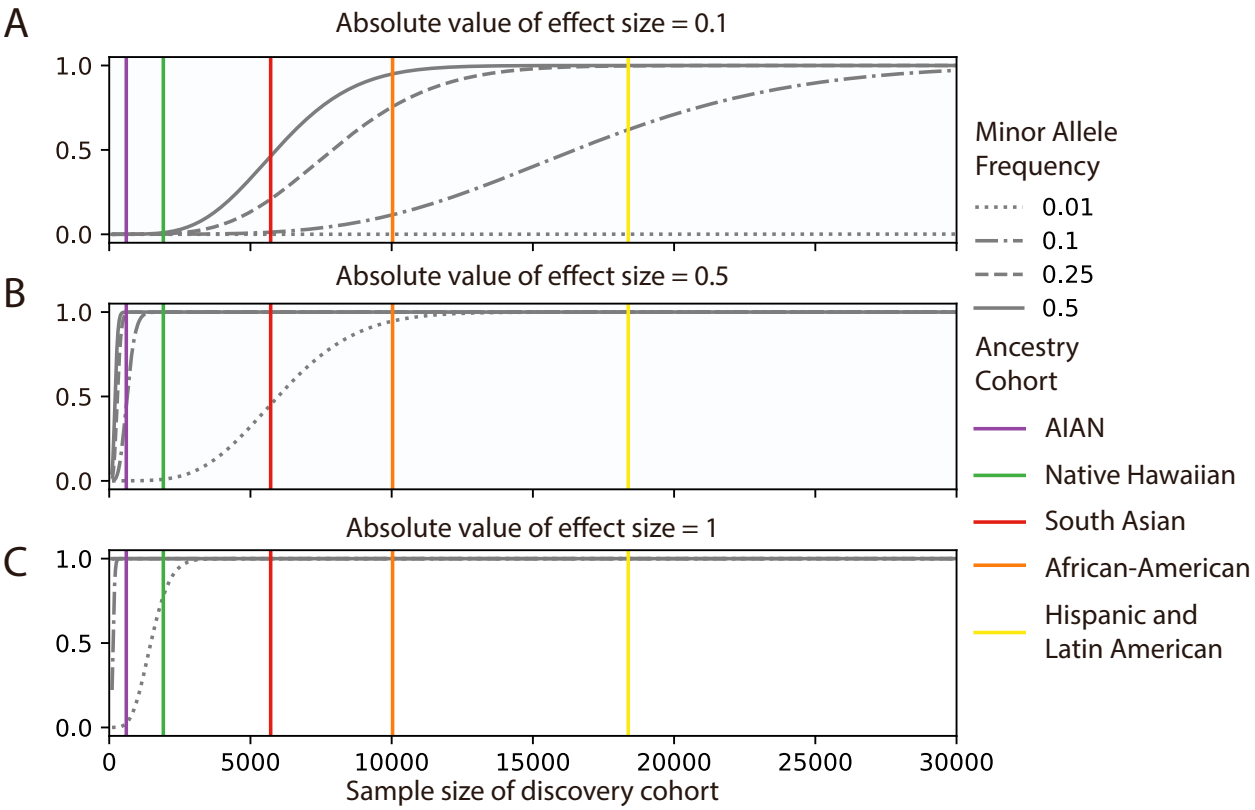

Figure S3: Power calculations for the standard GWA framework as a function of sample sizes using a range of effect sizes and minor allele frequencies. A. For an absolute value of effect size equal to 0.1 we performed power calculations for the standard GWA framework for cohorts with sample sizes of up to 30,000 individuals. Similar plots for absolute value of effect size set to 0.5 and 1 are shown in **B.** and **C.**, respectively. A full description of the power calculations is given in the Materials and Methods.

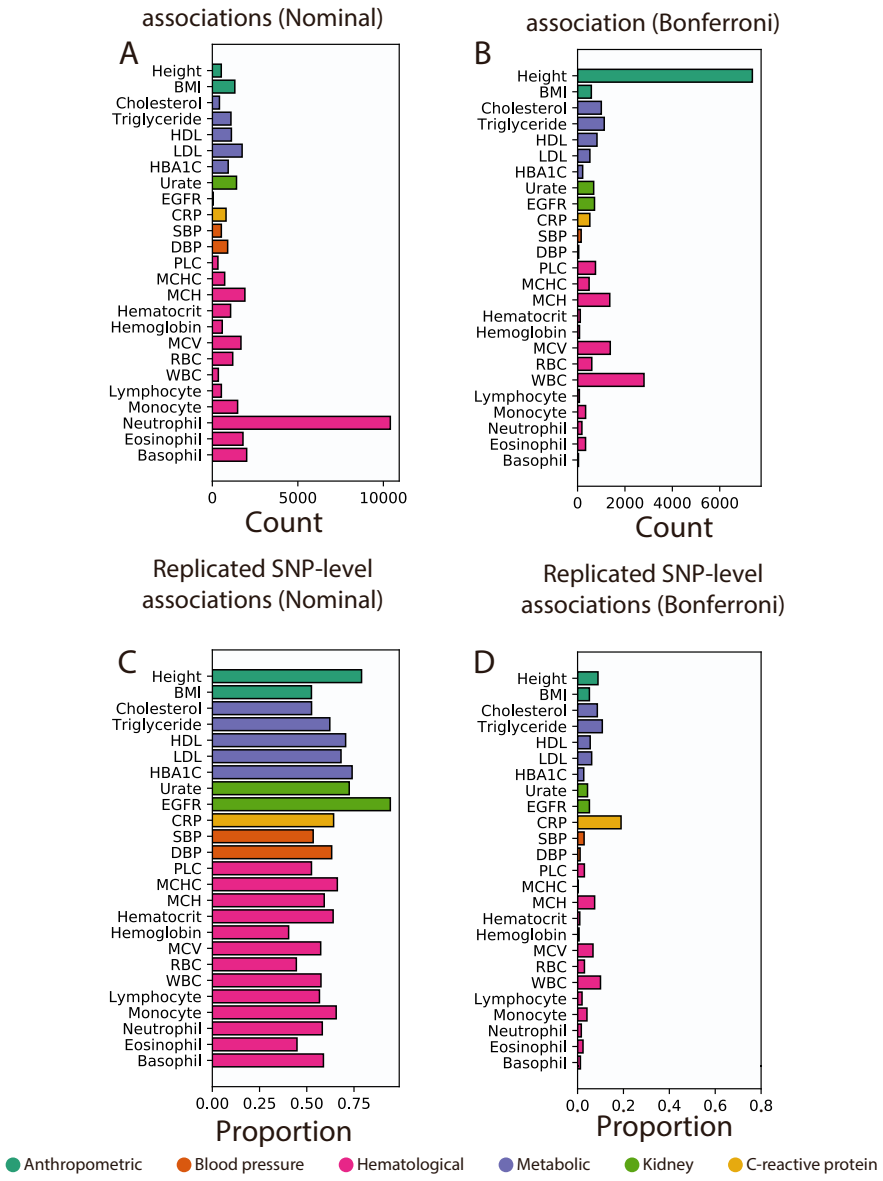

Figure S4: Summaries of replicated SNP-level associations when using two-stage GWA study design a nominal significance threshold. (**A**) Number and (**C**) proportion of nominally significant SNPs associated with a phenotype in the European ancestry cohort that were replicated in at least one other ancestry cohorts using a nominal p-value threshold calculated as 0.05 divided by the number of SNPs significantly associated with that trait in the European ancestry cohort. The corresponding thresholds for each trait are listed in Table S12. For ease of comparison, (**B**) number and (**D**) proportion of Bonferroni significant SNP-level associations that replicate among ancestry cohorts using the ancestry-trait Bonferroni-correction thresholds shown Table S11. Expansion of three letter trait codes are given in Table S2. Expansion of three letter trait codes are given in Table S2

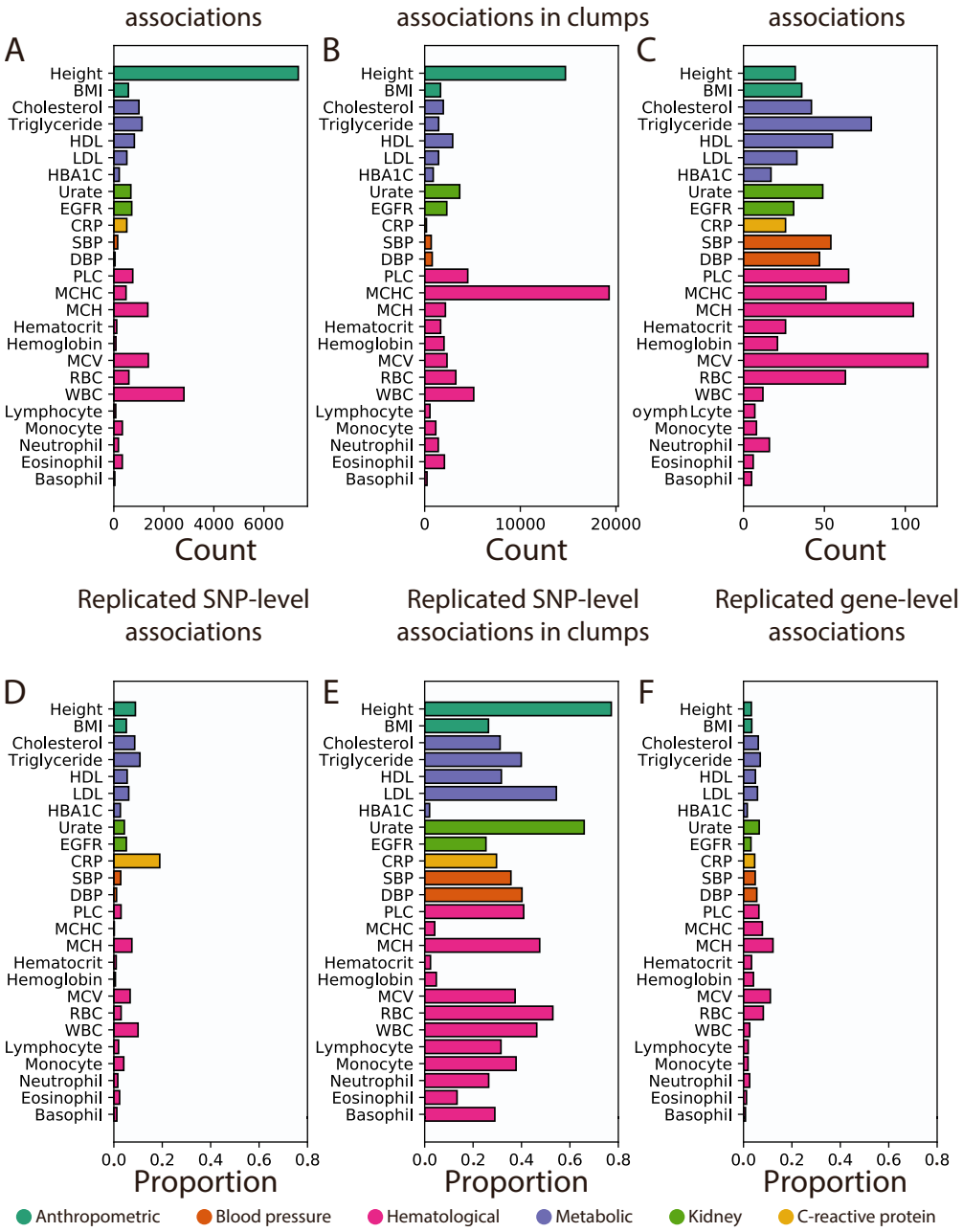

Figure S5: Summaries of replicated associations at multiple genomic scales among ancestry cohorts for all 25 traits analyzed using Bonferroni-corrected thresholds. Expansion of three letter trait codes are given in Table S2. (**A**) Number and (**D**) proportion of genome-wide significant SNPs associated with a phenotype in at least one ancestry cohort that were replicated in at least two ancestry cohorts. In all 25 traits, genome-wide significant SNPs replicate in at least two ancestry cohorts. Height contains over 7,000 replicated SNPs among the seven ancestry cohorts analyzed, illustrating its highly polygenic architecture. For many traits across all categories, with the exception of other biochemical (i.e., CRP), the replication rate of genes is higher in gene-level associations than at the SNP-level. (**B**) Number and (**E**) proportion of 1Mb windows, or "clumps", that contain at least one genome-wide significant SNP-level associations for a given phenotype in at least two ancestry cohorts. (**C**) Number and (**F**) proportion of genome-wide significant gene-level associations that replicate among ancestry cohorts. Replicated associations in hematological are common at the gene-level in hematological and metabolic traits. For instance, in three of the four cohorts with mean corpuscular hemoglobin (MCH) measurements *HBA1* and *HBA2* were identified as significant associated with MCH in the African, European, and East Asian ancestry cohorts Table S3. The denominator of the proportion is calculated as the total number of unique SNPs, clumps, or genes that are significantly associated with a trait in at least on ancestral cohort. Note that **D** and **F** correspond to Figure 1**A** and **B**, with an altered x-axis upper limit of 0.8 in this figure.

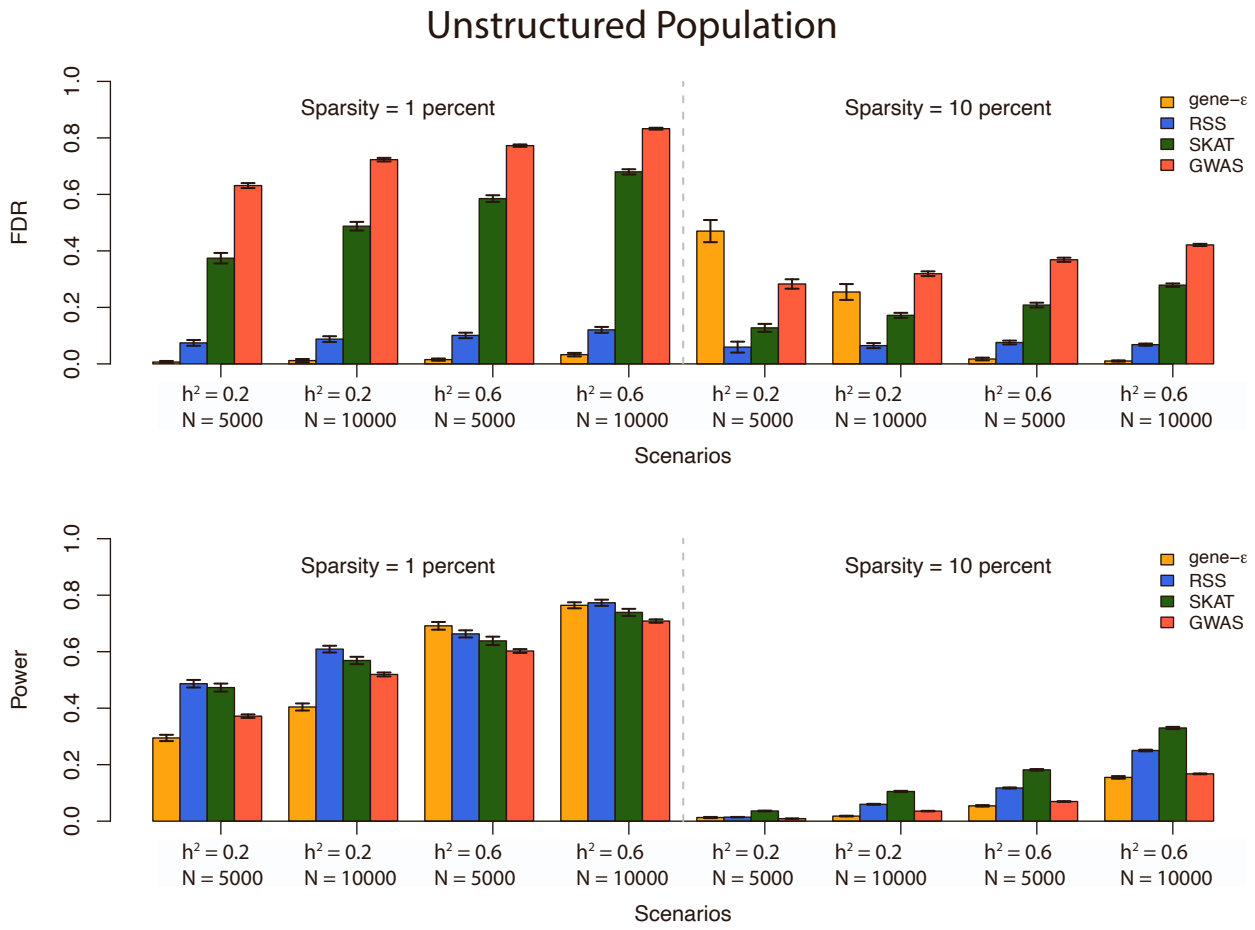

Figure S6: gene-ε outperforms and controls false discovery rate (FDR) better than other association methods in simulations with varying heritability and sample size. Simulations were designed to assess gene versus SNP-level association false discovery rate (FDR) and power in an unstructured population as described by the protocols in the Supplemental Information. The top and bottom panels show the FDR and power of four different association methods on 100 simulated datasets, respectively. We compared performance of three gene-level association test methods (gene-ε[53], RSS[54], SKAT[55]) with outputs from the standard GWA association test under different simulation parameters (sample size N, narrow-sense heritability h^2, and sparsity). We define sparsity as the proportion of SNPs that are ground-truth causal. Standard errors across the simulated replicates are shown using black whisker plots. Simulation protocol is described in the Supplemental Information.

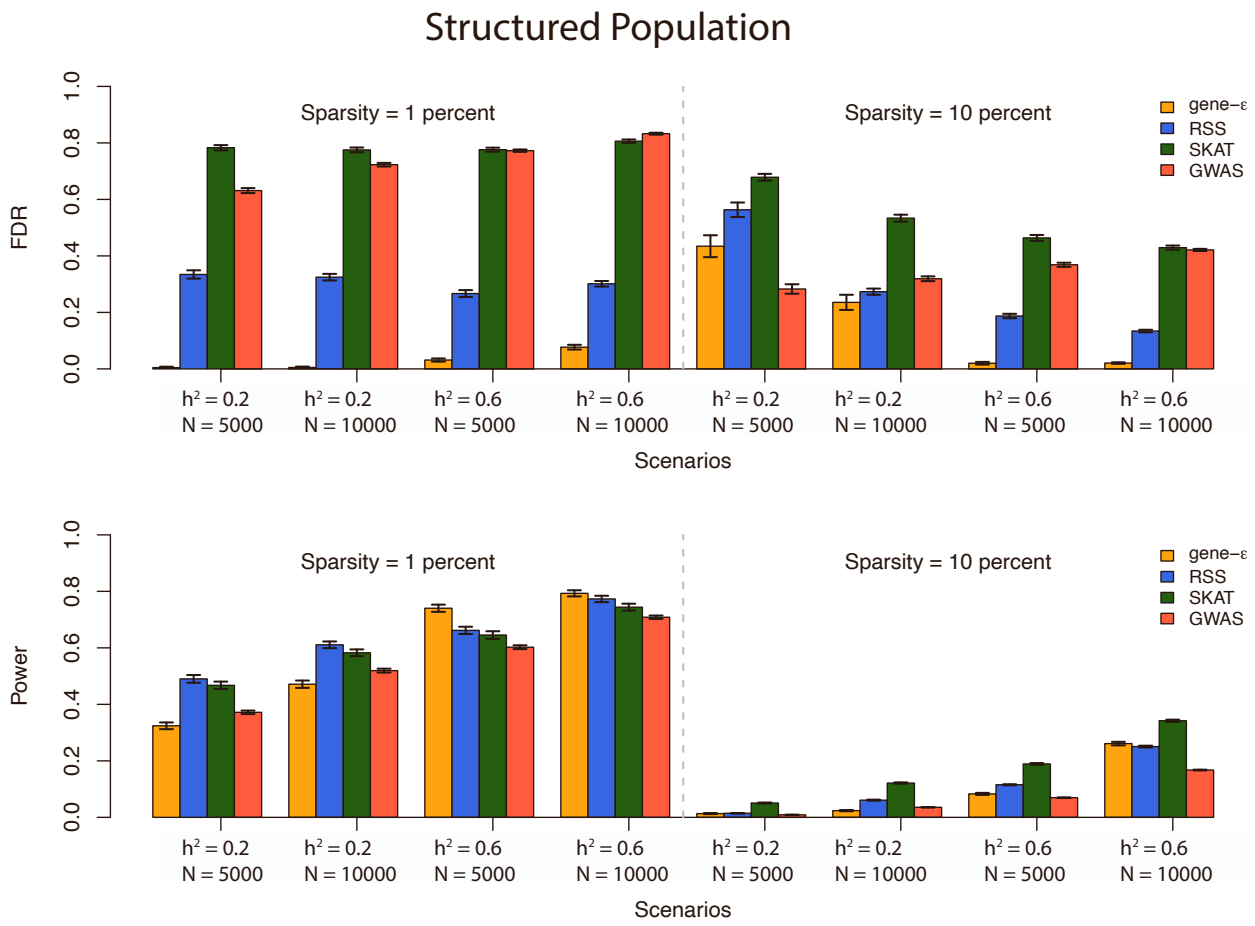

Figure S7: gene-ε outperforms and controls false discovery rate (FDR) better than other association methods in simulations with varying heritability and sample size. Simulations are designed to assess gene versus SNP-level association false discovery rate (FDR) and power in an structured population as described by the protocols in the Supplemental Information. The top and bottom panels show the FDR and power of four different association methods on 100 simulated datasets, respectively. We compared performance of three gene-level association test methods (gene-ε[53], RSS[54], SKAT[55]) with outputs from the standard GWA association test under different simulation parameters (sample size N, narrow-sense heritability h^2, and sparsity). We define sparsity as the proportion of SNPs that are designated to be causal. Standard errors across the simulated replicates are shown using black whisker plots.

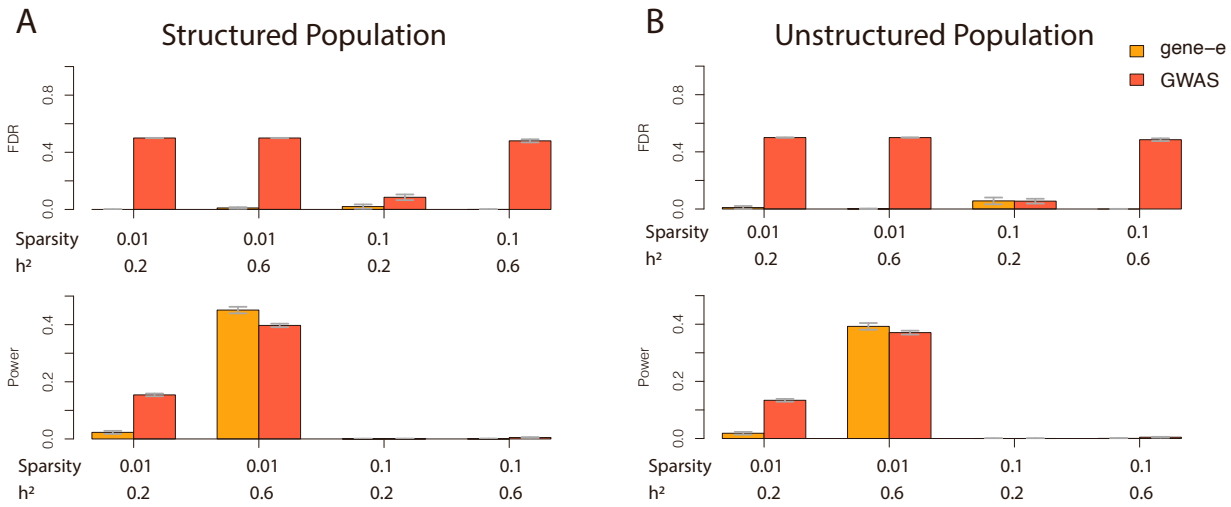

Figure S8: gene-ε outperforms and controls false discovery rate (FDR) better than the standard GWA framework in simulations with varying heritability and sparsity. All simulations were done with 2,000 individuals to test the power of gene-ε to detect associations in a small cohort. The FDR (top) and power (bottom) for each parameter set are calculated across 100 simulated replicates. A. Results from simulated populations where population structure is present. B. Results from simulated populations when population structure is not present. Mean power and false discovery rate, as well as corresponding standard errors, are shown in Table S23 for clarity.

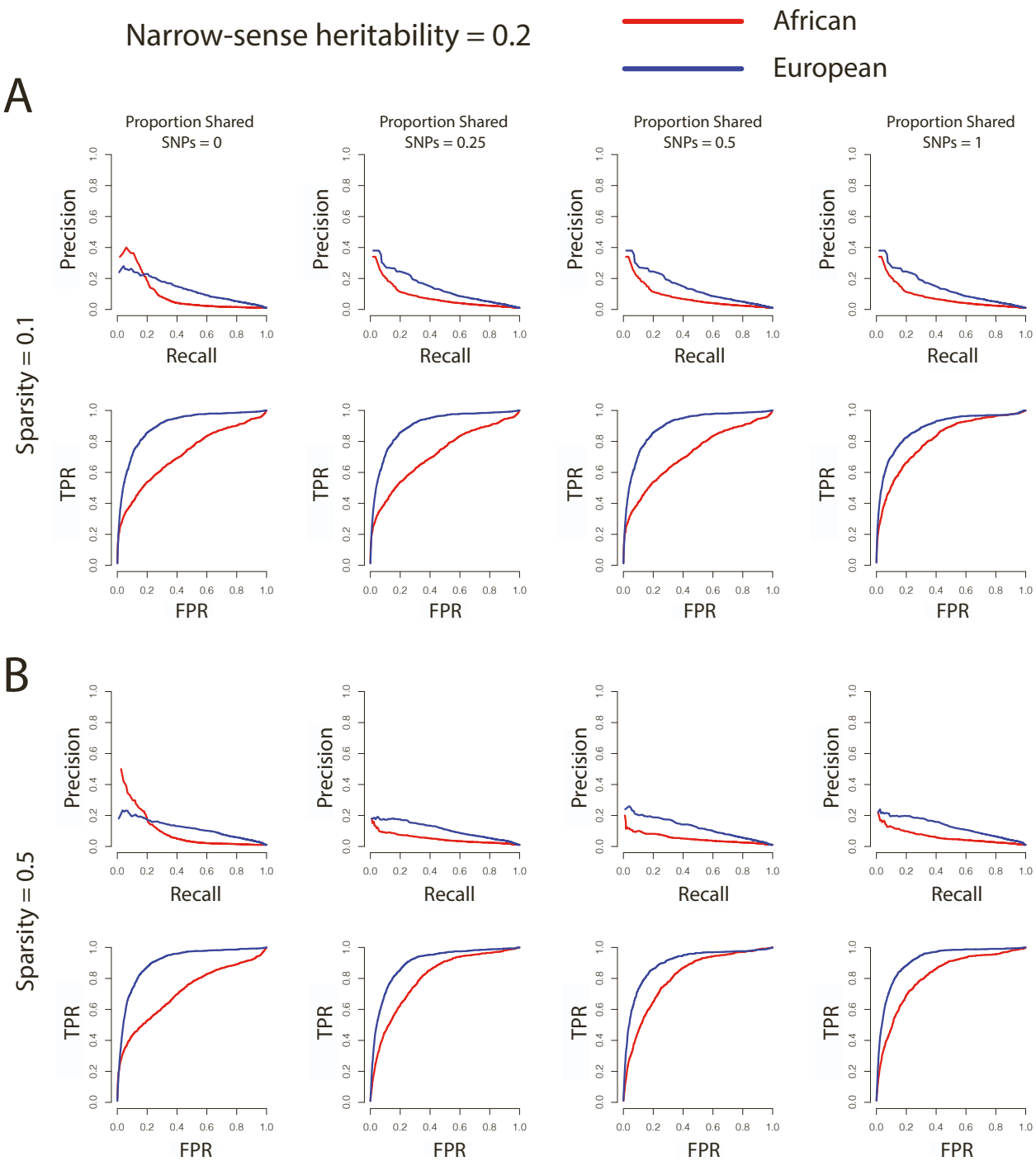

Figure S9: gene-ε identifies associated genes in two simulated ancestry cohorts under a variety of genetic architectures with low narrow sense heritability. A. Precision-recall (top row) and receiver operating curves (bottom row) for gene-ε analysis of cohorts simulated using genotypes from individuals of European (N = 10,000; blue line) and African (N = 4,967; red line) ancestry, respectively. Narrow-sense heritability was set to $h^2 = 0.2$ in each simulation. Sparsity of causal SNPs was set to a proportion of 0.1 and the proportion of causal SNPs shared was tested at different values. 50 replicates of each set of simulations under each parameter were performed. **B.** Precision-recall (top row) and receiver operating curves (bottom row) for gene-ε analysis of 50 replicated simulations of a European and African cohort using a causal SNP sparsity of 0.5.

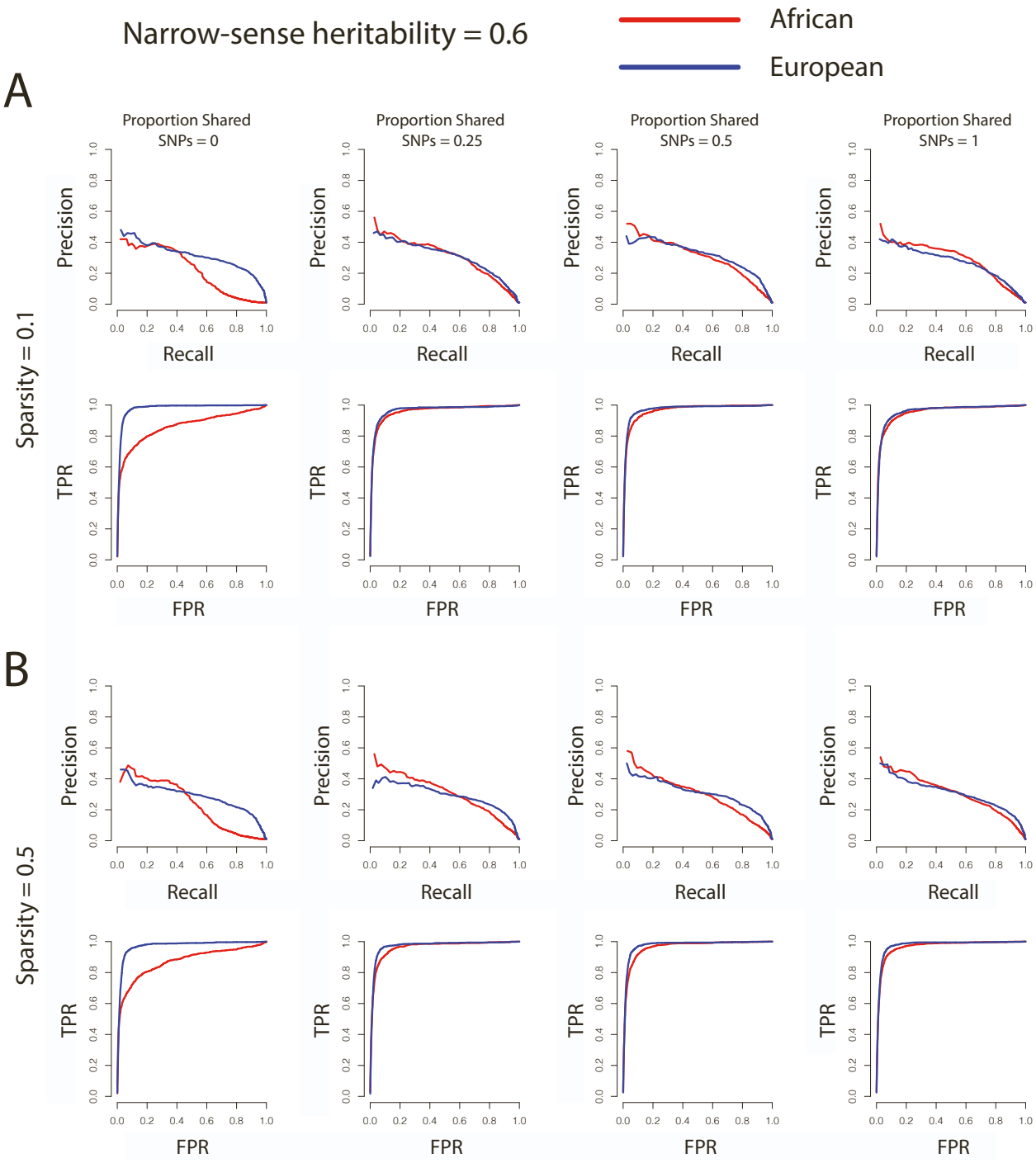

Figure S10: gene-ε identifies associated genes in two simulated ancestry cohorts under a variety of genetic architectures with high narrow sense heritability. A. Precision-recall (top row) and receiver operating curves (bottom row) for gene-ε analysis of cohorts simulated using genotypes from individuals of European (N = 10,000; blue line) and African (N = 4,967; red line) ancestry, respectively. Narrow-sense heritability was set to h^2 = 0.6 in each simulation. Sparsity of causal SNPs was set to a proportion of 0.1 and the proportion of causal SNPs shared was tested at different values. 50 replicates of each set of simulations under each parameter were performed. **B.** Precision-recall (top row) and receiver operating curves (bottom row) for gene-ε analysis of 50 replicated simulations of a European and African cohort using a causal SNP sparsity of 0.5.

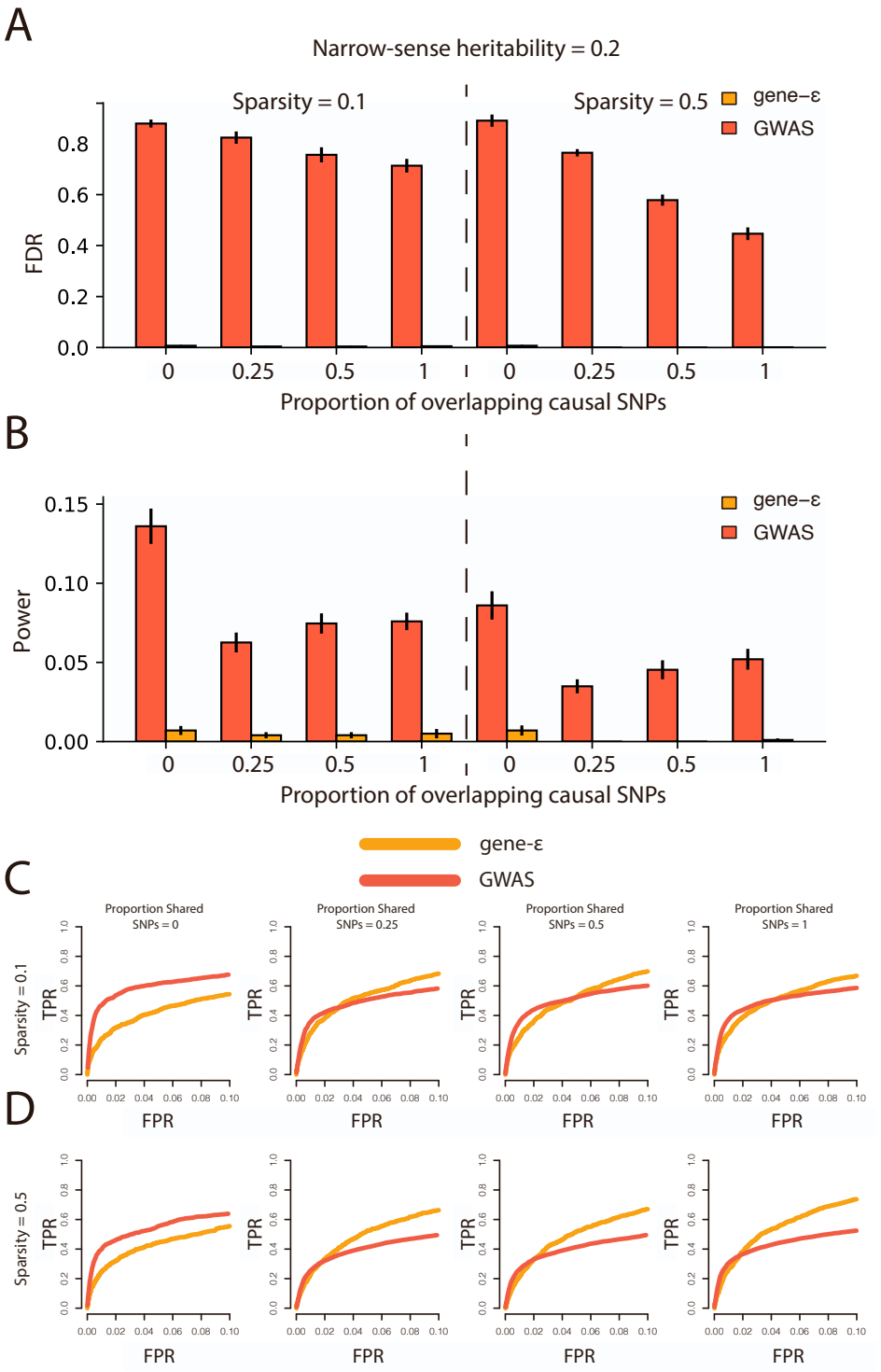

Figure S11: gene-ε (orange) has a lower false discovery rate for identification of shared genetic determinants between cohorts than the standard GWA framework (red). Narrow-sense heritability (percent variance explained by the genotype matrix) was set to $h^2 = 0.2$ for all simulations. **A.** False discovery rate of shared genetic determinants between two ancestry cohorts using varying levels of causal SNP sparsity and proportion of shared causal SNPs between the cohorts. **B.** Power of gene-ε and the standard GWA framework to detect shared genetic determinants between two cohorts. Error bars were calculated using the results from 50 simulations of each parameter set of sparsity and proportion of shared causal SNPs for both FDR(**A**) and Power(**B**). **C.** Receiver operating curves corresponding to simulations of genetic architecture when causal SNP sparsity is equal to 0.1 (corresponding to the left-hand panels of **A** and **B**). **D.** Receiver operating curves corresponding to simulations of genetic architecture when causal SNP

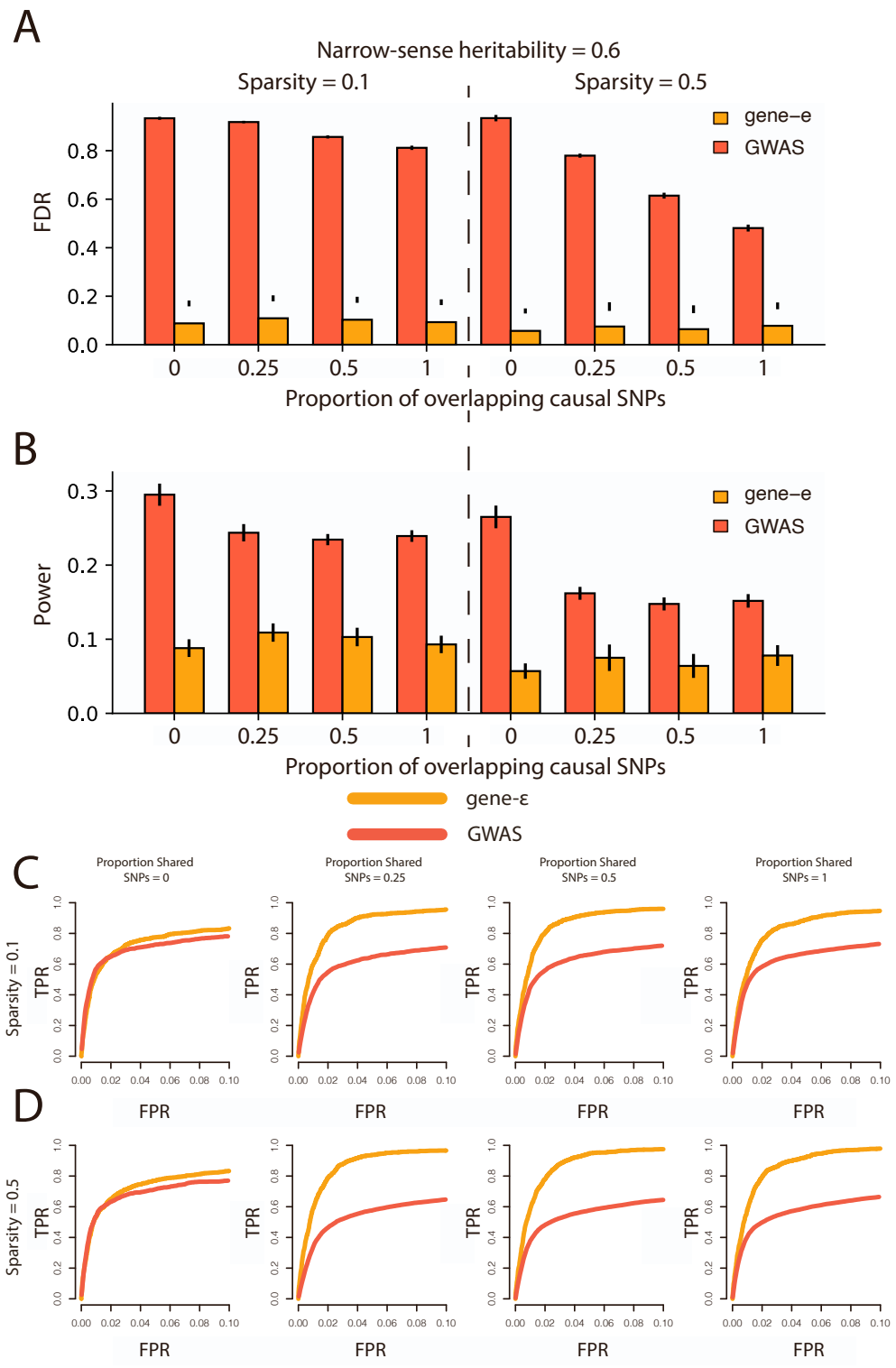

Figure S12: gene-ε (orange) has a lower false discovery rate for identification of shared genetic determinants between cohorts than the standard GWA framework (red). Narrow-sense heritability (percent variance explained by the genotype matrix) was set to $h^2 = 0.6$ for all simulations. **A.** False discovery rate of shared genetic determinants between two ancestry cohorts using varying levels of causal SNP sparsity and proportion of shared causal SNPs between the cohorts. **B.** Power of gene-ε and the standard GWA framework to detect shared genetic determinants between two cohorts. Error bars were calculated using the results from 50 simulations of each parameter set of sparsity and proportion of shared causal SNPs for both FDR(**A**) and Power(**B**). **C.** Receiver operating curves corresponding to simulations of genetic architecture when causal SNP sparsity is equal to 0.1 (corresponding to the left-hand panels of **A** and **B**). **D.** Receiver operating curves corresponding to simulations of genetic architecture when causal SNP sparsity is equal to 0.5 (corresponding to the right-hand panels of **A** and **B**).

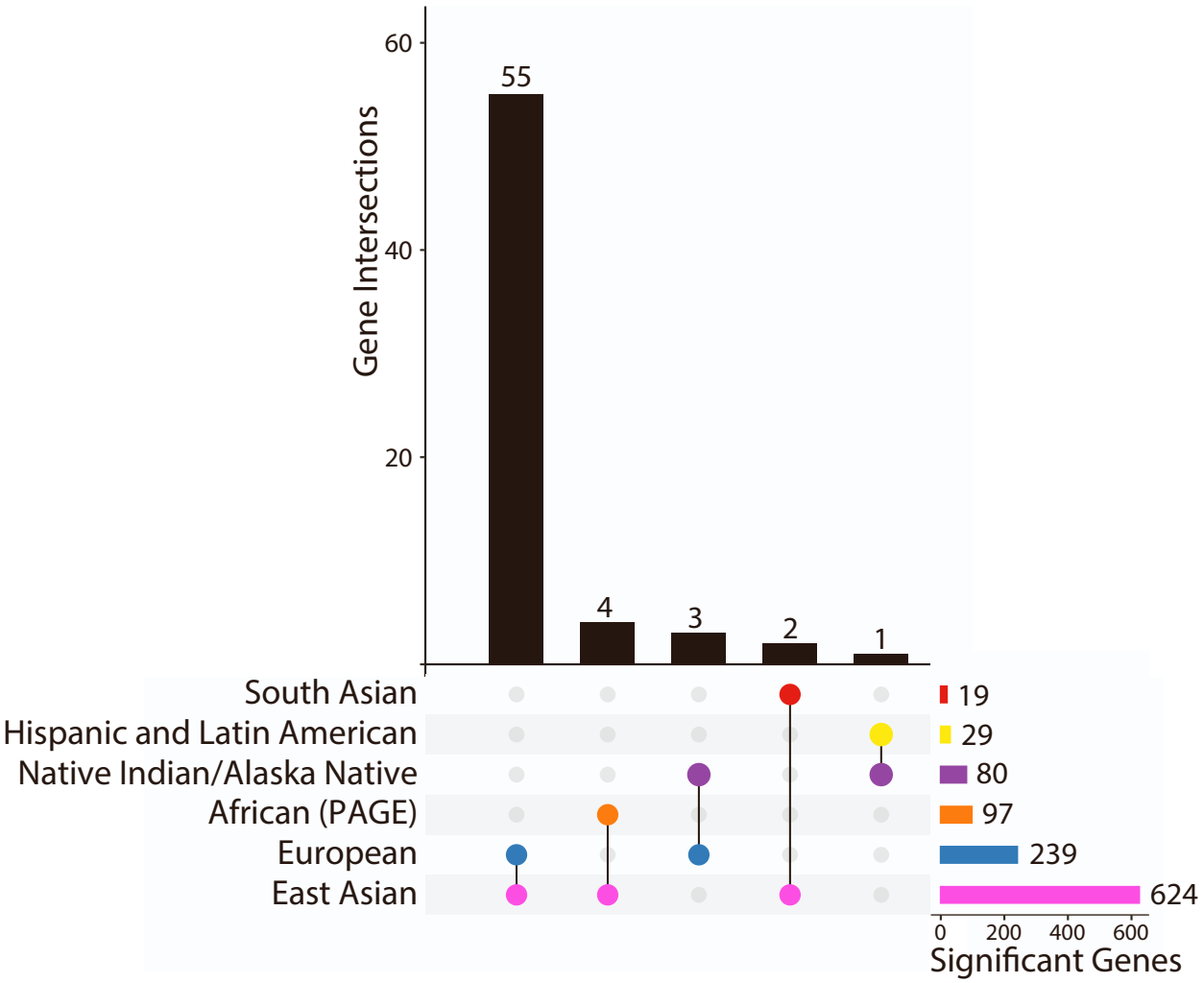

Figure S13: All six ancestries have gene-level associations with platelet count that replicate in at least one other ancestry. Total number of genome-wide significant genes in each ancestry, after correcting for total number of regions tested, are given in the bar plot located in the bottom right (significance thresholds are given in Table S16, sample sizes are given in Table S6 - Table S9). Shared gene-level association statistics between pairs of ancestries are shown in the vertical bar plot; the pair of ancestries represented by each bar can be identified using the dots and links below the barplot. Of the 65 genome-wide significant gene-level association statistics that replicate in at least two ancestry cohorts, only 25 contain SNPs that have been previously associated with platelet count in at least one ancestry in at least one study in the GWAS catalog (`https://www.ebi.ac.uk/gwas/home`) This plot was generated using the UpSetR package[56].

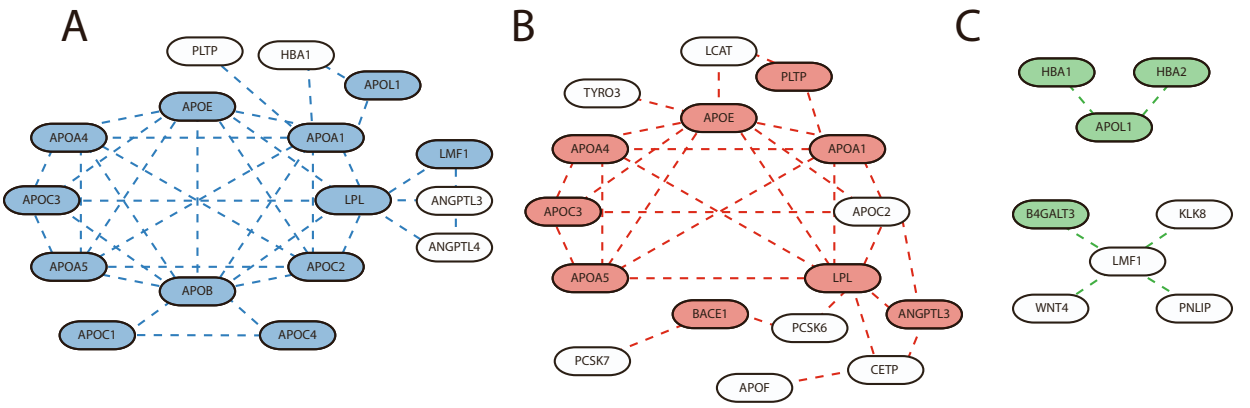

Figure S14: Significantly mutated subnetworks associated with triglyceride levels identified in the (A) European, (B) East Asian, and (C) Native Hawaiian ancestry cohorts. Significantly mutated subnetworks were identified using the Hierarchical HotNet method[50]. Genes that were identified in each ancestry as significantly associated with triglyceride levels using the gene-ε method are shaded using ancestry-specific color coding (also used in Figure 3, European—blue, East Asian—pink, Native Hawaiian—green). Significantly mutated subnetworks in the (**A**) European and (**B**) East Asian cohorts were identified using the ReactomeFI[57] protein-protein interaction network, and the significantly mutated subnetwork in the (**C**) the Native Hawaiian cohort was identified using the iRefIndex 15.0[58] protein-protein interaction networks. Genes that are present in any of the significantly mutated subnetworks that contain SNPs previously associated with triglyceride levels in the GWAS Catalog are listed with corresponding citations in Table S25.

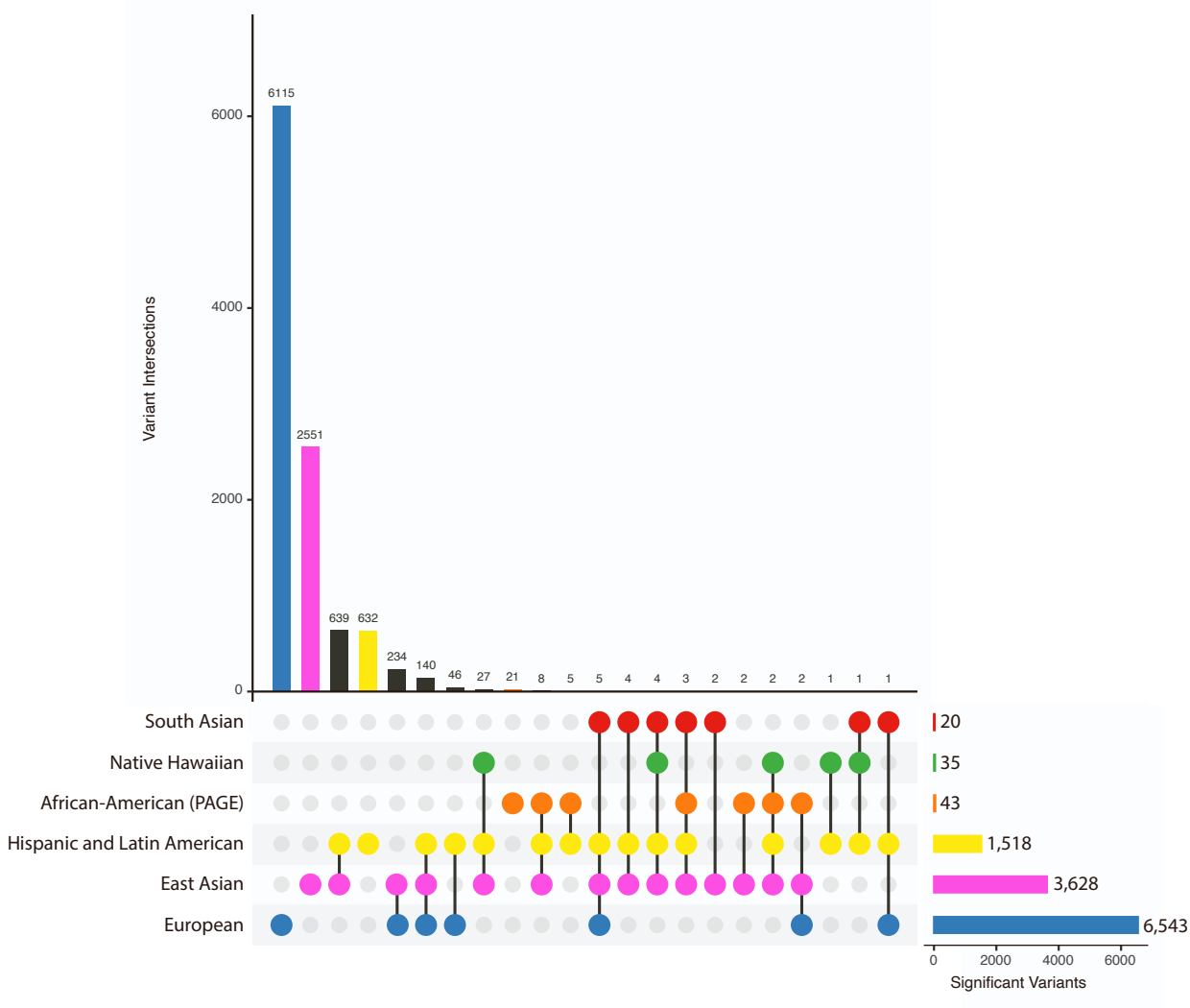

Figure S15: Shared SNP-level associations with triglyceride levels in six ancestral cohorts. Total number of genome-wide significant genes in each ancestry, after correcting for total number of regions tested, are given in the bar plot located in the bottom right (significance thresholds are given in Table S11 and sample sizes are given in Table S6 - Table S9). Shared SNP-level association statistics between pairs of ancestries are shown in the vertical bar plot. The pair of ancestries represented by each bar can be identified using the dots and links below the vertical barplot. This plot was generated using the UpSetR package[56].

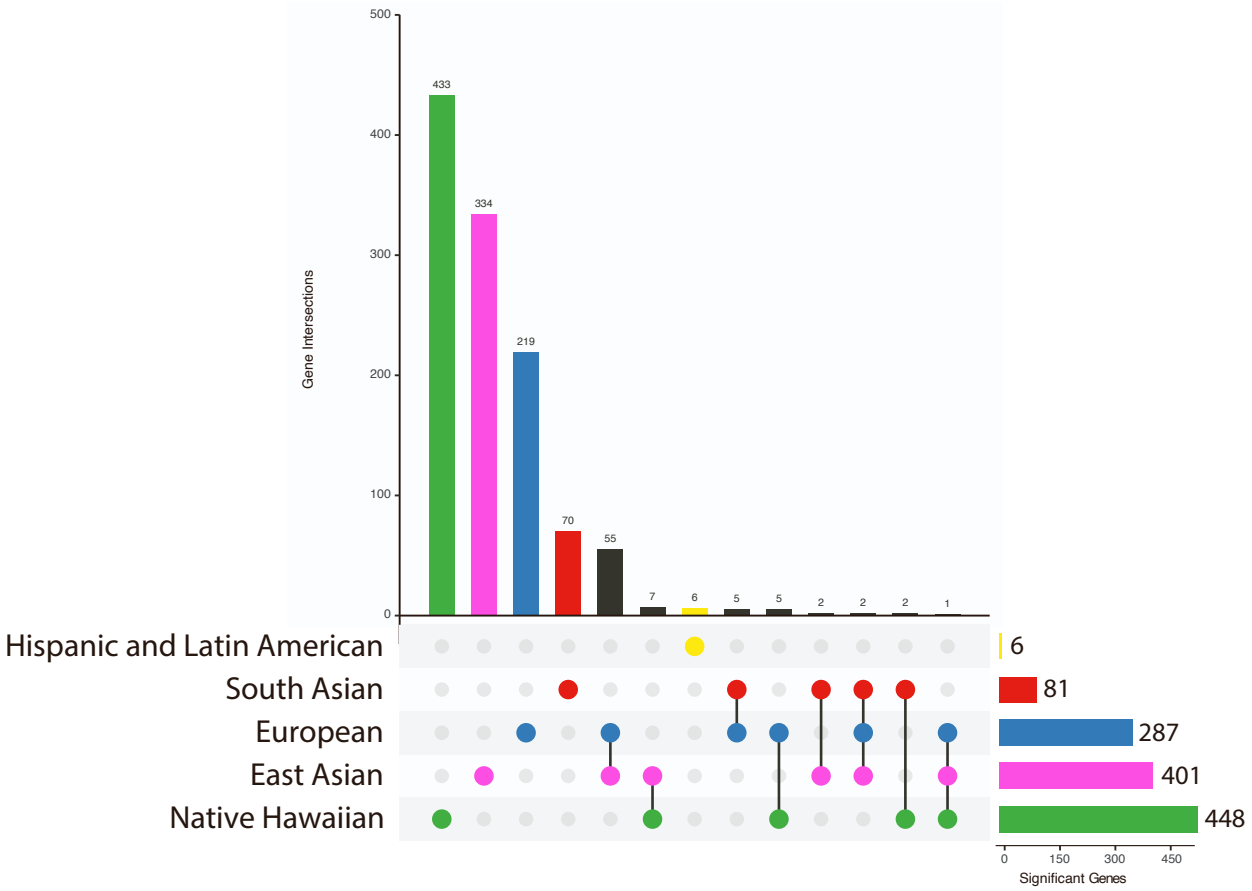

Figure S16: Shared gene-level associations with triglyceride levels in five ancestral cohorts. Total number of genome-wide significant genes in each ancestry, after correcting for total number of regions tested, are given in the bar plot located in the bottom right (significance thresholds are given in Table S16 and sample sizes are given in Table S6 - Table S9). Shared gene-level association statistics between pairs of ancestries are shown in the vertical bar plot. The pair of ancestries represented by each bar can be identified using the dots and links below the vertical barplot. This plot was generated using the UpSetR package[56].

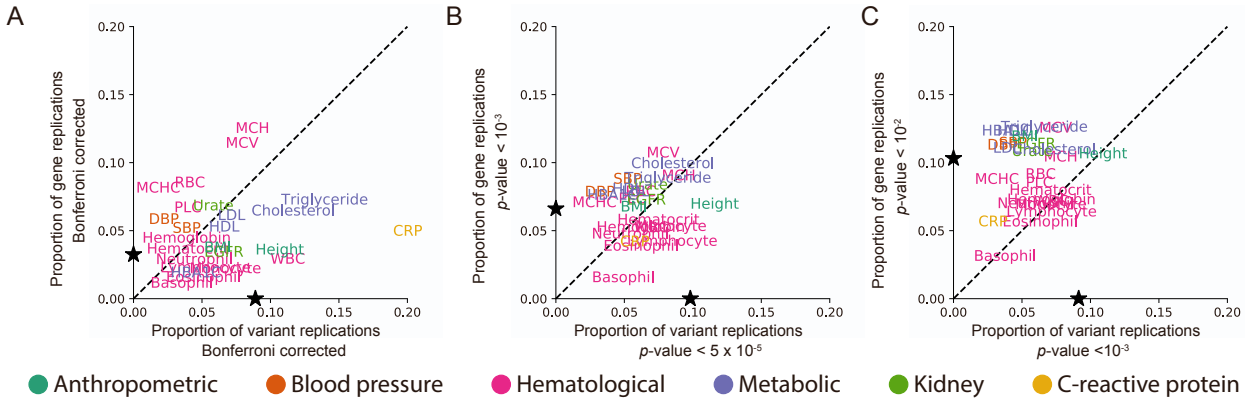

Figure S17: Less stringent significance thresholds lead to a decrease in the proportion of replicated SNP-level associations and an increase in the proportion of gene-level associations among ancestries for each of the 25 traits analyzed. A. Proportion of all SNP-level Bonferroni-corrected genome-wide significant associations in any ancestry that replicate in at least one other ancestry is shown on the x-axis (see Table S11 for ancestry-trait specific Bonferroni corrected p-value thresholds). On the y-axis we show the proportion of significant gene-level associations that were replicated for a given phenotype in at least two ancestries (see Table S16 for Bonferroni corrected significance thresholds for each ancestry-trait pair). The black stars on the x- and y-axes represent the mean proportion of replicates in SNP and gene analyses, respectively. C-reactive protein (CRP) contains the greatest proportion of replicated SNP-level associations of any of the phenotypes. **B.** The x-axis indicates the proportion of SNP-level associations that surpass a nominal threshold of p-value $< 10^{-5}$ in at least one ancestry cohort that replicate in at least one other ancestry cohort. The y-axis indicates the proportion of gene-level associations that surpass a nominal threshold of p-value $< 10^{-3}$ in at least one ancestry cohort and replicate in at least one other ancestry cohort. Nominal p-value thresholds tend to decrease the proportion of replicated SNP-level associations and tend to increase the proportion of replicated gene-level associations. The number of unique SNPs and genes that replicated in each cohort is given in Figure S18. **C.** The x-axis indicates the proportion of SNP-level associations that surpass a nominal threshold of p-value $< 10^{-3}$ in at least one ancestry cohort that replicate in at least one other ancestry cohort. The y-axis indicates the proportion of gene-level associations that surpass a nominal threshold of p-value $< 10^{-2}$ in at least one ancestry cohort and replicate in at least one other ancestry cohort. The number of unique SNPs and genes that replicated in each cohort is given in Figure S19. As shown in panel **B**, nominal p-value thresholds tend to decrease the proportion of replicated SNP-level associations and tend to increase the proportion of replicated gene-level associations. Expansion of three letter trait codes are given in Table S2.

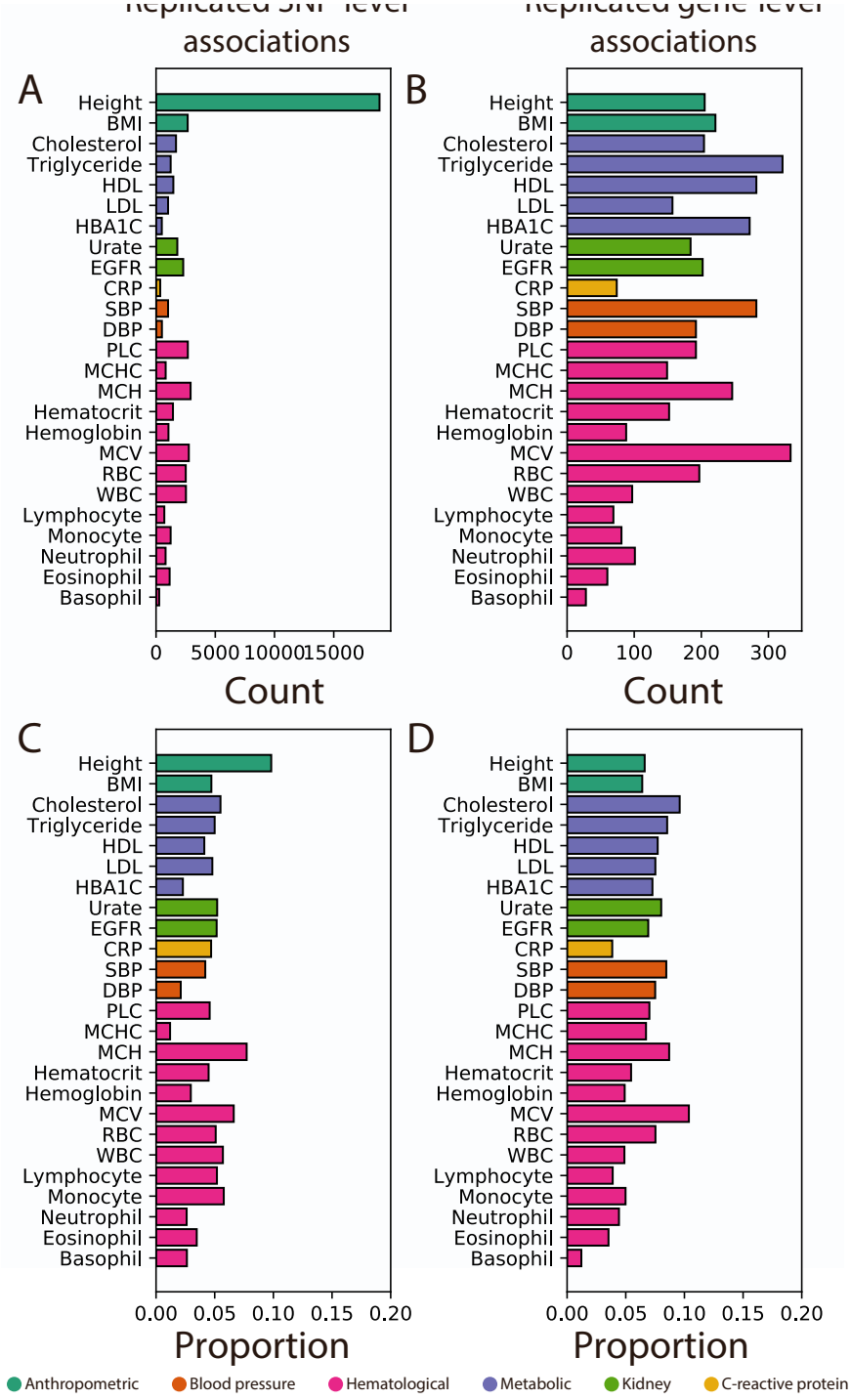

Figure S18: Summaries of replicated associations at multiple genomic scales among ancestry cohorts for all 25 traits analyzed using nominal p-value thresholds (SNP p-value $< 5 \times 10^{-5}$, gene p-value $< 10^{-3}$). (**A**) Number and (**C**) proportion of genome-wide significant SNPs associated with a phenotype in at least one ancestry cohort that were replicated in at least two ancestry cohorts using a nominal p-value threshold of 5×10^{-5}. (**B**) Number and (**D**) proportion of genome-wide significant gene-level associations that replicate among ancestry cohorts using a nominal p-value threshold of 10^{-3}. Expansion of three letter trait codes are given in Table S2.

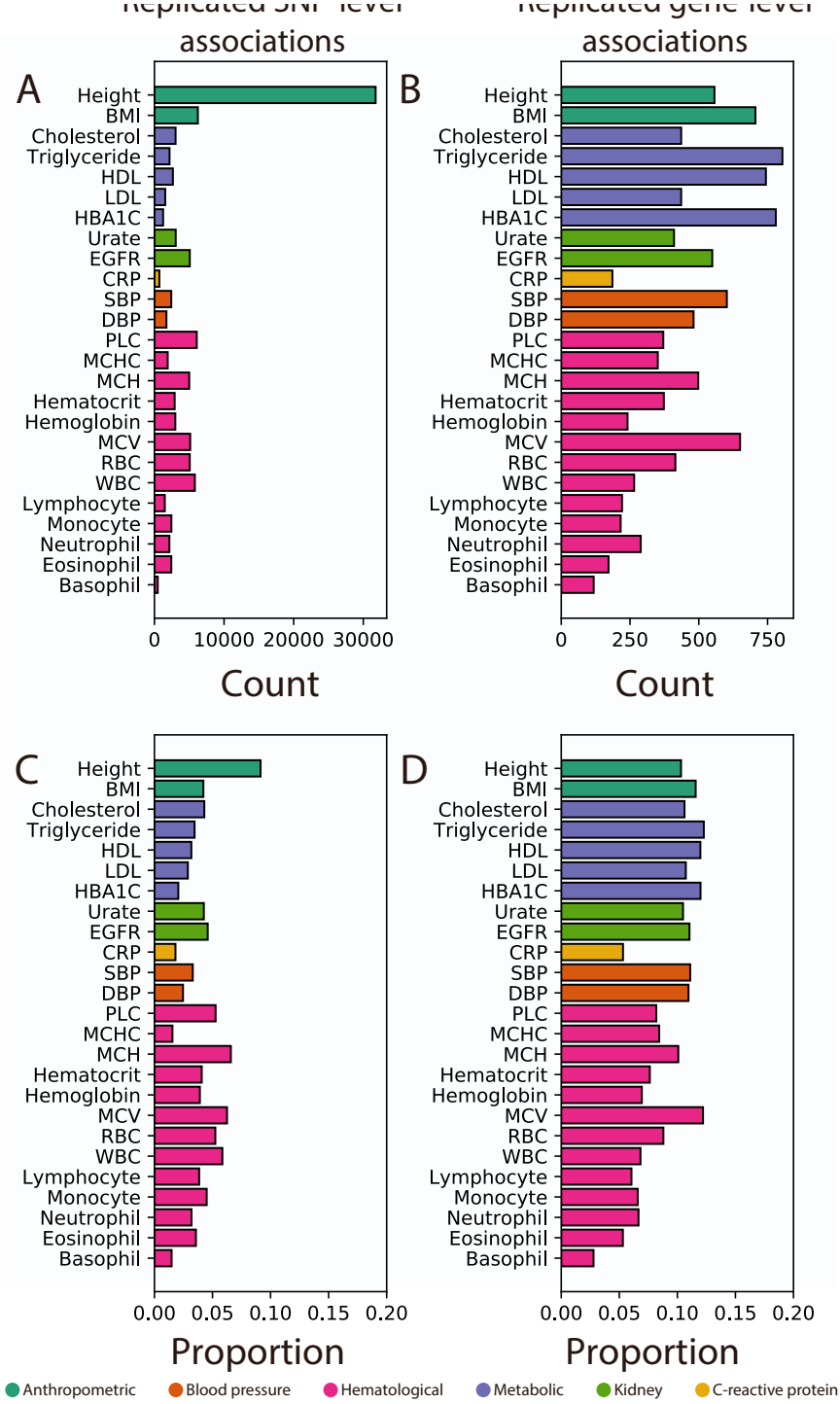

Figure S19: Summaries of replicated associations at multiple genomic scales among ancestry cohorts for all 25 traits analyzed using nominal p-value thresholds (SNP p-value $< 10^{-3}$, gene p-value $< 10^{-2}$). (**A**) Number and (**C**) proportion of genome-wide significant SNPs associated with a phenotype in at least one ancestry cohort that were replicated in at least two ancestry cohorts using a nominal p-value threshold of 10^{-3}. (**B**) Number and (**D**) proportion of genome-wide significant gene-level associations that replicate among ancestry cohorts using a nominal p-value threshold of 10^{-2}. Expansion of three letter trait codes are given in Table S2. Expansion of three letter trait codes are given in Table S2.

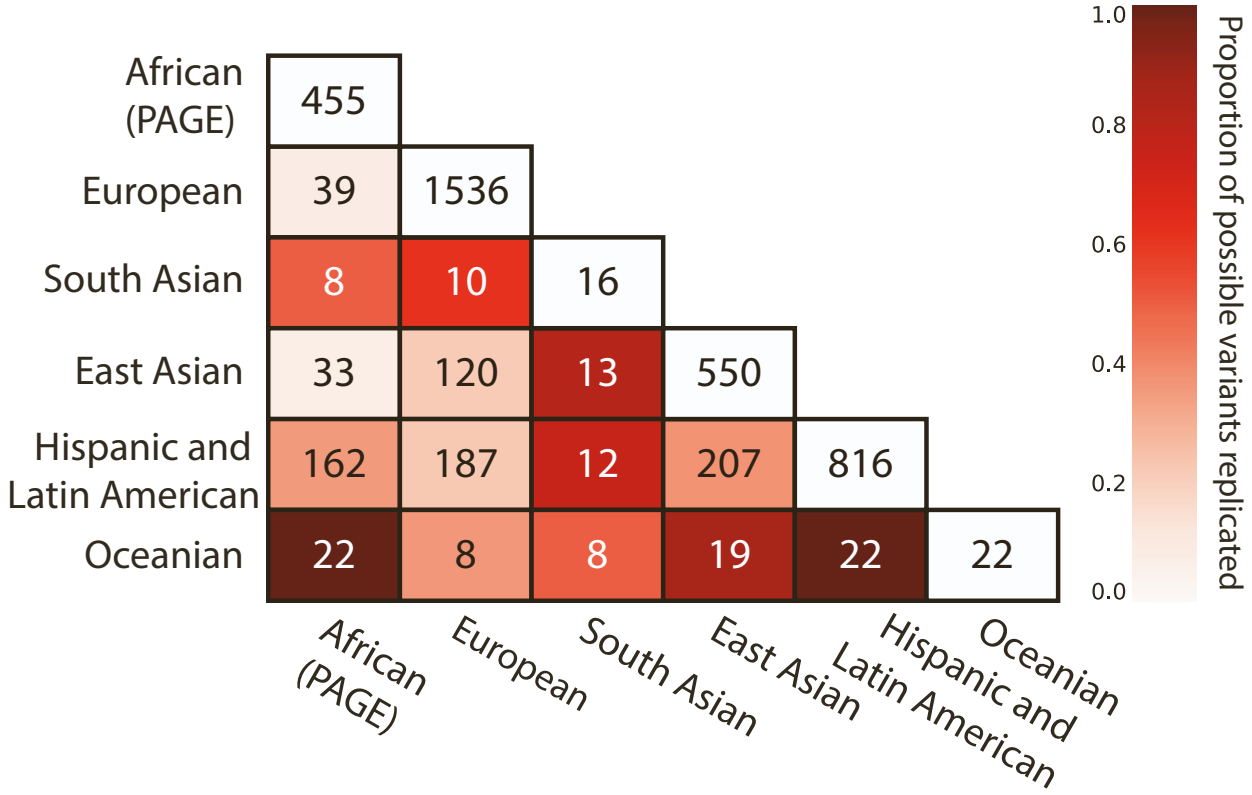

Figure S20: Pairwise replication of SNP-level association signals for C-reactive protein in six ancestral cohorts using genotype and imputed data. Imputed data was available and included in this analysis for each of the six cohorts. The inclusion of imputed SNPs in GWA analysis of C-reactive protein increases both the number of significant SNPs in each ancestry (along the diagonal) as well as the number of replicating significant SNP-level associations among pairs of ancestry cohorts (lower triangular). The corresponding analysis of pairwise SNP-level replication using only genotype data from each cohort is shown in Figure 2C.

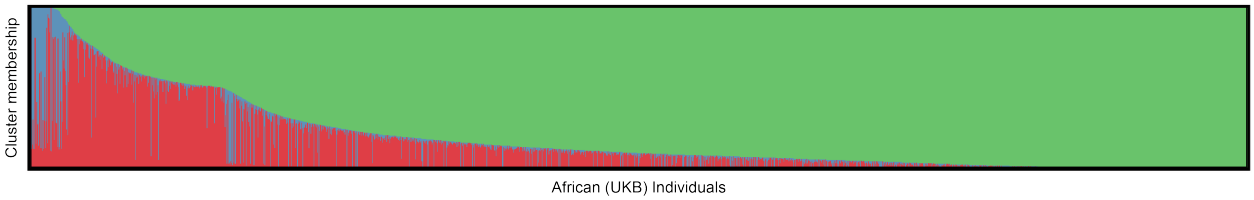
Cluster membership
African (UKB) Individuals

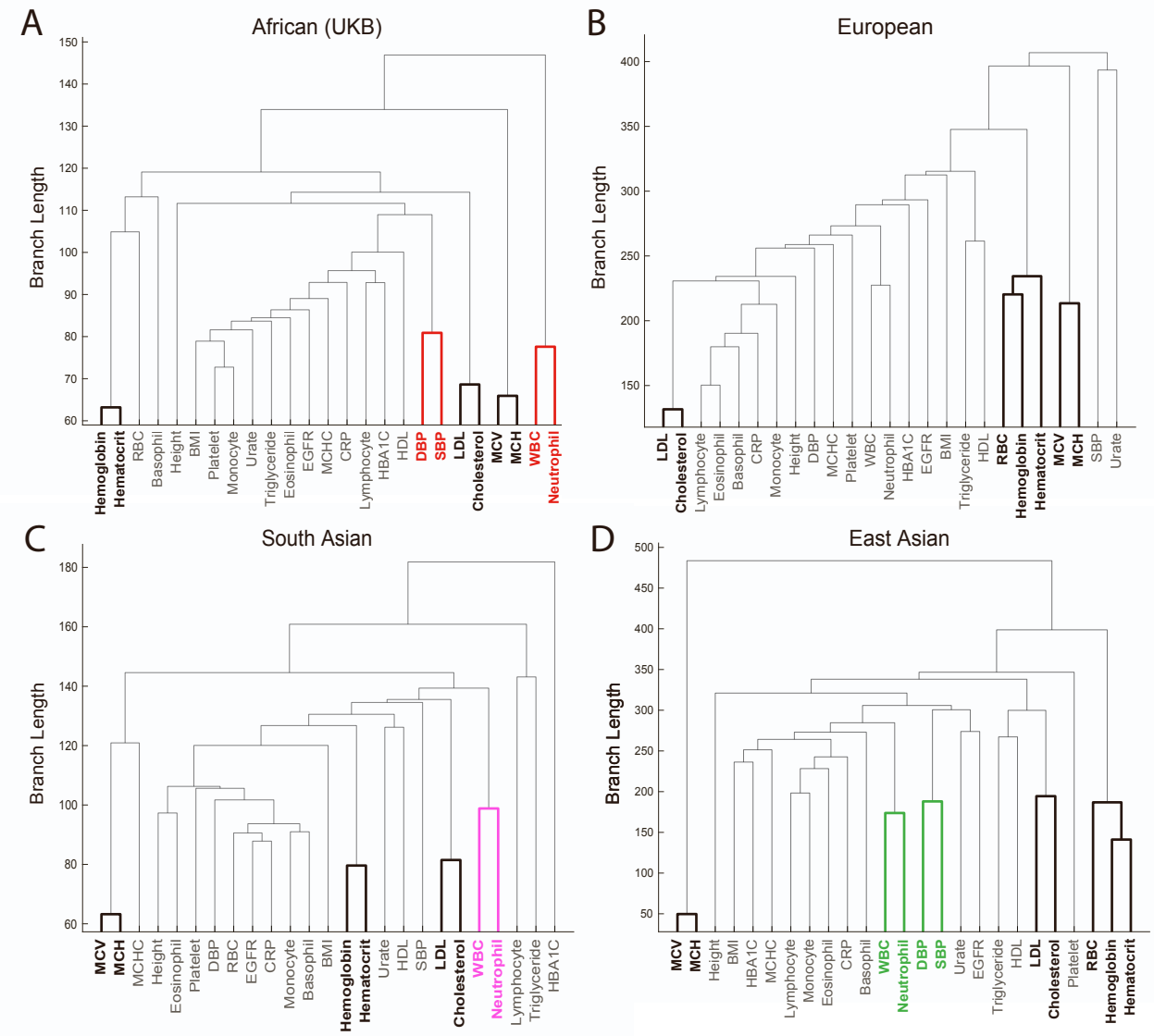

Figure S21: Multiple prioritized trait clusters with shared core genetic trait architecture replicate in the (A) African (UKB), (B) European, (C) South Asian, and (D) East Asian ancestry cohorts. The WINGS algorithm identified prioritized phenotype clusters in each of these ancestry cohorts, denoted in each dendrogram as clades with emboldened lines. Three clusters of phenotypes were found in all ancestries (shown and labeled in black), comprising: mean corpuscular volume (MCV) and mean corpuscular hemoglobin (MCH), hemoglobin and hematocrit, and the metabolic traits low-density lipoprotein (LDL) and cholesterol levels. In both the European and East Asian ancestry cohorts, red blood cell count (RBC) was also a member of the hemoglobin and hematocrit phenotype cluster. Two other phenotype clusters were identified in at least two ancestry cohorts. One of these clusters contains white blood cell count (WBC) and neutrophil count, and the other contains diastolic and systolic blood pressure (DBP and SBP). These two clusters are color-coded according to the ancestry cohorts in which they are prioritized. The WINGS algorithm was applied to traits from each ancestry cohort separately as described in the Supplemental Information.

Supplemental Tables

Ancestry cohort label in this study	Study	Label from original study	Sample Size	Number of SNPs
European	UK Biobank	Self-identified white british	349,411	1,933,096
East Asian	Biobank Japan	East Asian	19,190 - 206,692	4,823,101 - 6,628,005
Hispanic and Latin American	PAGE	Admixed Hispanic and Latin American	15,522 - 21,955	8,576,622 - 8,822,607
African-American (PAGE)	PAGE	African-American	3,750 - 17,280	12,107,345 - 12,274,127
South Asian	UK Biobank	Self-identified South Asian	5,716	958,375
African (UKB)	UK Biobank	African	4,967	578,320
Native Hawaiian	PAGE	Native Hawaiian	1,777 - 3,938	6,656,996 - 6,966,169
American Indian/Alaska Native	PAGE	AIAN	574 - 645	3,970,247 - 8,504,923

Table S1: Ancestry cohorts analyzed in this study. In studies where GWA summary statistics were available to us, sample size and number of SNPs differ due to original study design. The specific sample size and number of SNPs for each trait in studies from Biobank Japan and PAGE are provided in Table S5- Table S10.

Trait Name	Code
Body mass index	BMI
High density lipoprotein	HDL
Low density lipoprotein	LDL
Hemoglobin A1c	HBA1C
Estimated glomerular filtration rate	EGFR
C-reactive protein	CRP
Systolic blood pressure	SBP
Diastolic blood pressure	DBP
Platelet count	PLC
Mean corpuscular hemoglobin concentration	MCHC
Mean corpuscular hemoglobin	MCH
Mean corpuscular volume	MCV
Red blood cell count	RBC
White blood cell count	WBC

Table S2: Abbreviations used throughout this study for 14 quantitative traits analyzed in this study. The remaining 11 traits analyzed were Basophil count, Cholesterol, Eosinophil count, Height, Hematocrit, Hemoglobin, Lymphocyte count, Monocyte count, Neutrophil count, and Triglyceride levels, respectively. These are not abbreviated in the main text.

Trait Name or Code	AIAN	Native Hawaiian	Hispanic
BMI	Yes	Yes	Yes
Basophil count	No	No	No
CRP	Yes	Yes	Yes
Cholesterol	Yes	Yes	Yes
DBP	Yes	No	Yes
EGFR	Yes	No	Yes
Eosinophil count	No	No	No
HBA1C	Yes	Yes	Yes
HDL	Yes	Yes	Yes
Height	Yes	Yes	Yes
Hematocrit	No	No	No
Hemoglobin	No	No	No
LDL	Yes	Yes	Yes
Lymphocyte count	No	No	No
MCH	Yes	No	Yes
MCHC	No	No	No
MCV	No	No	No
Monocyte count	No	No	No
Neutrophil count	No	No	No
PLC	Yes	No	Yes
RBC	No	No	No
SBP	Yes	No	Yes
Triglyceride	No	Yes	Yes
Urate	No	No	No
WBC	Yes	No	Yes

Table S3: Traits assayed in the PAGE study data by ancestry cohort. Data were available for each of the 25 listed traits in the UK Biobank European, South Asian, and African cohorts, as well as, the East Asian cohort from the Biobank Japan. Thus, each trait was analyzed in a minimum of four ancestries and a maximum of seven ancestries.

Trait	Number of significant SNPs in at least the European or East Asian cohort	Number of SNPs with same direction of effect	Percentage of SNPs with same direction of effect
BMI	6,374	4,456	69.91
Basophil	884	520	58.82
CRP	694	463	66.71
Cholesterol	3,451	2,379	68.94
DBP	1,962	1,320	67.28
EGFR	7,129	5,038	70.67
Eosinophil	5,890	3,608	61.26
HBA1C	3,030	2,206	72.81
HDL	5,995	4,077	68.01
Height	33,577	22,090	65.79
Hematocrit	5,382	3,602	66.93
Hemoglobin	5,280	3,601	68.20
LDL	2,521	1,929	76.56
Lymphocyte	2,214	1,237	55.87
MCH	6,763	4,674	69.11
MCHC	1,760	1,124	63.86
MCV	7,489	5,208	69.54
Monocyte	3,929	2,565	65.28
Neutrophil	5,431	3,850	70.89
PLC	11,014	7,161	65.02
RBC	9,211	6,263	67.99
SBP	1,807	1,182	65.41
Triglyceride	3,743	2,686	71.76
WBC	6,017	4,105	68.22
Urate	5,864	3,787	64.58

Table S4: Effect size homogeneity in variants identified as significant in the European or East Asian cohorts. In each of the 25 traits analyzed in this study a majority of variants that are significant in at least the European or East Asian cohorts had the same direction of effect in the other ancestry cohort.

Trait Name or Code	Sample Size	Total SNPs	Pruned SNPs	Regions	Citations
Basophil count	62,076	5,653,566	410,465	23,106	[59]
BMI	158,284	5,653,566	410,465	23,085	[60]
CRP	75,391	5,608,701	408,166	23,108	[59]
DBP	136,615	5,653,566	410,465	23,085	[59]
eGFR	143,658	5,608,701	408,166	23,108	[59]
Eosinophil count	62,076	5,653,566	410,465	23,106	[59]
HDL	70,657	5,608,701	408,166	23,108	[59]
Height	159,095	6,296,332	354,647	23,679	[61]
Hematocrit	108,757	5,653,566	410,465	23,106	[59]
Hemoglobin	108,769	5,653,566	410,465	23,085	[59]
HbA1c	75,391	5,608,701	408,166	23,108	[59]
LDL	72,866	5,608,701	408,166	23,108	[59]
Lymphocyte count	62,076	5,653,566	410,465	23,106	[59]
MCH	108,054	5,653,566	410,465	23,106	[59]
MCHC	108,738	5,653,566	410,465	23,106	[59]
MCV	108,526	5,653,566	410,465	23,085	[59]
Monocyte count	62,076	5,653,566	410,465	23,106	[59]
Neutrophil count	62,076	5,653,566	410,465	23,106	[59]
PLC	108,208	5,653,566	410,465	23,085	[59]
RBC	108,794	5,653,566	410,465	23,085	[59]
SBP	136,597	5,653,566	410,465	23,085	[59]
Cholesterol	128,305	5,608,701	408,166	23,108	[59]
Triglyceride	105,597	5,608,701	410,465	23,108	[59]
Urate	109,029	5,608,701	408,166	23,108	[59]
WBC	107,694	5,653,566	408,166	23,085	[59]

Table S5: Number of individuals, total SNPs, pruned SNPs used for gene-ε, and genes and transcription factors (regions) included in the analysis for each trait in Biobank Japan data. Regions were defined using the hg19 list provided in Gusev et al.[62].

Trait Name or Code	Sample Size	Total SNPs	Pruned SNPs	Regions
BMI	17,127	12,139,115	404,401	24,216
CRP	8,349	12,274,126	404,572	24,206
DBP	11,380	12,148,801	405,188	24,218
eGFR	8,261	12,128,273	403,371	24,207
Hemoglobin A1c	17,127	12,139,115	404,401	24,215
HDL	10,085	12,114,827	404,089	24,201
Height	17,280	12,139,907	404,522	24,201
LDL	9,720	12,107,344	403,740	24,218
MCHC	3,750	12,132,232	405,558	24,217
PLC	8,850	12,131,935	404,497	24,193
SBP	11,380	12,148,801	405,188	24,218
Cholesterol	10,137	12,110,337	403,674	24,222
Triglyceride	9,980	12,110,879	403,455	24,206
WBC	8,802	12,126,732	404,579	24,219

Table S6: Number of individuals, total SNPs, pruned SNPs used for gene-ε, and genes and transcription factors (regions) included in the analysis for each trait in the African-American cohort of the PAGE study data.

Trait Name or Code	Sample Size	Total SNPs	Pruned SNPs	Region Count
BMI	21,955	8,812,436	432,762	24,138
CRP	15,912	8,576,621	397,941	24,118
DBP	21,549	8,784,112	430,360	24,126
Estimated glomerular filtration rate	18,548	8,702,426	422,598	24,123
HbA1c	21,955	8,812,436	432,762	24,138
HDL	17,751	8,583,603	412,771	24,122
Height	22,187	8,822,606	433,604	24,132
LDL	17,373	8,588,800	413,074	24,116
MCHC	15,522	8,763,739	427,208	24,132
PLC	18,949	8,612,804	415,201	24,115
SBP	21,549	8,784,112	430,360	24,126
Cholesterol	17,802	8,586,887	412,830	24,115
Triglyceride	17,856	8,594,121	413,546	24,104
WBC	18,206	8,603,503	414,462	24,123

Table S7: Number of individuals, total SNPs, pruned SNPs used for gene-ε, and genes and transcription factors (regions) included in the analysis for each trait in the Hispanic and Latin American cohort of the PAGE study data.

Trait Name or Code	Sample Size	Total SNPs	Pruned SNPs	Regions
BMI	645	8,374,976	421,826	24,124
CRP	574	8,504,922	417,287	24,136
DBP	636	8,376,521	421,528	24,136
eGFR	602	8,336,044	417,540	24,132
Hemoglobin A1c	645	8,374,976	421,826	24,124
HDL	604	8,315,912	415,939	24,121
Height	645	8,375,624	421,750	24,117
LDL	591	8,360,719	419,544	24,123
MCHC	620	3,970,246	62,339	17,381
PLC	603	8,294,302	414,530	24,133
Systolic blood pressure	636	8,376,521	421,528	24,136
Cholesterol	604	8,586,887	415,939	24,121
WBC	602	8,289,567	414,462	24,133

Table S8: Number of individuals, total SNPs, pruned SNPs used for gene-ε, and genes and transcription factors (regions) included in the analysis for each trait in the AIAN cohort of the PAGE study data.

Trait Name or Code	Sample Size	Total SNPs	Pruned SNPs	Regions
BMI	3,936	6,664,738	415,221	23,885
CRP	1,777	6,966,169	428,517	23,834
Hemoglobin A1c	3,936	6,664,738	415,221	23,885
HDL	1,912	6,656,996	416,255	23,894
Height	3,938	6,660,920	415,172	23,878
LDL	1,900	6,662,802	416,810	23,895
Cholesterol	1,915	6,660,807	416,425	23,899
Triglycerides	1,915	6,660,807	416,425	23,899

Table S9: Number of individuals, total SNPs, pruned SNPs used for gene-ε, and genes and transcription factors (regions) included in the analysis for each trait in the Native Hawaiian (Native Hawaiian) cohort of the PAGE study data.

Trait Name or Code	Sample Size	Total SNPs	Pruned SNPs	Regions
BMI	4,647	15,362,633	433,356	24,085
CRP	1,811	14,374,461	428,656	24,116
DBP	1,086	12,470,507	416,273	24,112
eGFR	150	8,314,417	337,167	24,017
HbA1c	4,647	15,362,633	433,356	24,085
HDL	2,378	13,413,244	428,598	24,072
Height	4,679	15,366,710	433,005	24,103
LDL	2,316	13,327,313	428,741	24,075
MCHC	128	8,089,136	315,583	23,946
PLC	541	10,528,072	421,929	24,098
SBP	1,086	12,470,507	416,273	24,112
Cholesterol	2,387	13,436,190	428,656	24,078
Triglyceride	2,381	13,423,953	429,246	24,073
WBC	543	10,570,051	421,776	24,095

Table S10: Number of individuals, total SNPs, pruned SNPs used for gene-ε, and genes and transcription factors (regions) included in the analysis for each trait in the Asian cohort of the PAGE study data.

Trait Name or Code	African or African-American ($\times 10^{-8}$)	East Asian ($\times 10^{-8}$)	AIAN ($\times 10^{-8}$)	Native Hawaiian ($\times 10^{-9}$)	Hispanic ($\times 10^{-8}$)
Basophil count	8.646*	8.844	NA	NA	NA
BMI	0.412	8.844	0.597	7.502	5.674
CRP	0.407	8.915	0.588	7.176	5.830
Cholesterol	0.414	8.915	0.601	7.507	5.823
DBP	0.412	8.844	0.597	NA	5.692
EGFR	0.412	8.915	0.600	NA	5.746
Eosinophil count	8.646*	8.844	NA	NA	NA
HBA1C	0.412	8.915	0.597	7.502	5.674
HDL	0.413	8.915	0.601	7.511	5.825
Height	0.412	7.941	0.597	7.506	5.667
Hematocrit	8.646*	8.844	NA	NA	NA
Hemoglobin	8.646*	8.844	NA	NA	NA
LDL	0.413	8.914	0.598	7.504	5.822
Lymphocyte count	8.646*	8.843	NA	NA	NA
MCH	8.646*	8.844	NA	NA	NA
MCHC	0.412	8.844	1.259	NA	5.705
MCV	8.646*	8.844	NA	NA	NA
Monocyte count	8.646*	8.844	NA	NA	NA
Neutrophil count	8.646*	8.844	NA	NA	NA
PLC	0.412	8.844	0.603	NA	5.805
RBC	8.646*	8.844	NA	NA	NA
SBP	0.412	8.844	0.597	NA	5.692
Triglyceride	0.413	8.915	NA	7.507	5.818
Urate	8.646*	8.915	NA	NA	NA
WBC	0.412	8.844	NA	NA	5.812

Table S11: Bonferroni *p*-value threshold corrected for number of SNP-level association tests performed for each ancestry-trait pair. Thresholds are calculated as 0.05 divided by the number of SNPs tested in each ancestry-trait pair. The term"NA" indicates that there was no data for that ancestry-trait pair. The threshold for Bonferroni-corrected significance was the same for every trait in the European (p-value $< 2.587 \times 10^{-8}$) and South Asian (p-value $< 5.217 \times 10^{-8}$) cohorts from the UK Biobank. Traits for which the UK Biobank African cohort was used are denoted with a *; otherwise, the African-American cohort from the PAGE study data was used. See Table S2 for expansion of trait codes.

Trait Name or Code	Nominal Significance Threshold	Number of Variants Tested	Number of Replicated Variants	Proportion of Replicated Variants	Unidentified non-European Associations
MCV	1.46×10^{-05}	3,414	2,008	0.588	7,830
PLC	1.25×10^{-05}	3,998	1,792	0.448	6,073
Height	2.80×10^{-06}	17,877	10406	0.582	37,360
BMI	2.22×10^{-05}	2,254	1,478	0.656	2,762
DBP	5.37×10^{-05}	931	528	0.567	719
SBP	8.17×10^{-05}	612	352	0.575	1,315
WBC	1.87×10^{-05}	2,680	1,192	0.445	17,800
RBC	1.71×10^{-05}	2,918	1,674	0.574	3514
Hemoglobin	3.48×10^{-05}	1,436	5,80	0.404	368
Hematocrit	2.99×10^{-05}	1,670	1,068	0.640	524
MCH	1.56×10^{-05}	3,214	1,904	0.592	7,851
MCHC	4.58×10^{-05}	1,091	722	0.662	26,507
Lymphocyte	8.03×10^{-05}	623	327	0.525	536
Monocyte	3.53×10^{-05}	1,418	896	0.632	1,568
Neutrophil	5.07×10^{-05}	987	527	0.534	1,550
Eosinophil	4.00×10^{-05}	1,249	802	0.642	2,143
Basophil	9.62×10^{-04}	52	49	0.942	2,017
Urate	2.56×10^{-05}	1,951	1,414	0.725	6,530
Triglyceride	3.99×10^{-05}	1,254	928	0.740	3,902
Cholesterol	1.96×10^{-05}	2,557	1,742	0.681	2,847
LDL	3.16×10^{-05}	1,580	1,115	0.706	1,735
HDL	2.86×10^{-05}	1,751	1,089	0.622	4,737
HBA1C	6.31×10^{-05}	7,92	4,16	0.525	899
EGFR	2.00×10^{-05}	2,506	1,315	0.525	2,227

Table S12: Nominal *p*-value threshold corrected for number of Bonferroni-corrected SNP-level associations found in the European ancestry cohort. To illustrate how SNP-level statistical replication among ancestry cohorts is prohibited by external factors (e.g. sample sizes, genotype array design), We calculated the number of SNP-level replications when thresholds for non-European cohorts are calculated as 0.05 divided by the number of significant SNPs in the European cohort. This design is analogous to a two-stage GWA framework, where non-European ancestry cohorts are not used for discovery and associations discovered in the European ancestry cohort are used to find replicates. Replication of SNP-level association signals increases when less stringent thresholds are used. Number of variants that were tested in the European ancestry cohort and at least one another cohort were included in this calculation and are given here. We also include the number of variants that were identified in non-European ancestry cohorts using a Bonferroni-corrected significance threshold to illustrate how this study design may miss signals in other ancestries. See Table S2 for expansion of trait codes.

Gene	European	East Asian	South Asian	African-American	Hispanic and Latin American	AIAN	Native Hawaiian
MCV	0.013-0.153	0.024-0.153	0.136-0.268	0.113-0.522	NA	NA	NA
PLC	0.0132-0.190	0.024-0.140	0.124-0.171	5.715-17.196	3.732-18.805	100.736-100.736	0.0
Height	0.009-0.115	0.0178-0.150	NA	0.064-0.267	0.051-0.113	NA	NA
BMI	0.0133-0.113	0.020-0.110	NA	0.068-0.068	0.064-0.101	NA	NA
DBP	0.0136-0.070	0.022-0.074	NA	NA	0.787-0.806	NA	NA
SBP	0.0129-0.066	0.022-0.064	NA	NA	4.64-4.643	NA	NA
WBC	0.0135-0.122	0.024-0.104	0.117-0.145	0.027-0.198	0.018-0.112	NA	NA
RBC	0.012-0.107	0.025-0.142	NA	0.115-0.297	NA	NA	NA
Hemoglobin	0.0108-0.129	0.025-0.083	NA	0.162-0.232	NA	NA	NA
Hematocrit	0.011-0.093	0.024-0.085	NA	0.241-0.241	NA	NA	NA
MCH	0.013-0.159	0.024-0.153	0.104-0.277	0.109-0.541	NA	NA	NA
MCHC	0.014-0.115	0.024-0.106	NA	0.152-1.28	0.088-0.489	0.118-9.222	MA
Lymphocyte	0.014-0.078	0.033-0.264	0.503-0.503	0.647-0.647	NA	NA	NA
Monocyte	0.0133-0.195	0.0329-0.123	NA	0.423-0.423	NA	NA	NA
Neutrophil	0.014-0.160	0.033-0.106	0.123-0.142	0.108-0.518	NA	NA	NA
Eosinophil	0.013-0.149	0.033-0.188	NA	NA	NA	NA	NA
Basophil	0.014-0.120	0.033-0.167	0.363-0.581	0.241-0.626	NA	NA	NA
Urate	0.0112-0.097	0.024-0.346	0.092-0.251	0.104-0.682	NA	NA	NA
Triglyceride	0.013-0.204	0.0247-0.318	0.113-0.311	0.043-0.616	0.032-0.159	NA	0.102-0.169
Cholesterol	0.013-0.309	0.023-0.285	0.118-0.268	4.280-30.434	2.734-15.098	NA	NA
LDL	0.0136-0.121	0.030-0.514	0.139-0.367	3.785-29.006	2.371-18.999	16.273-33.101	14.133-16.297
HDL	0.013-0.296	0.030-0.529	0.106-0.369	1.368-23.818	0.838-32.374	NA	22.726-46.409
HBA1C	0.013-0.090	0.039-0.139	NA	0.068-0.068	0.064-0.101	NA	NA
EGFR	0.0133-0.195	0.021-0.095	0.119-0.162	NA	1.102-1.102	12.494-27.656	0.0
CRP	0.0137-0.122	0.0300-0.127	0.106-0.263	0.094-0.418	0.0626-0.434	NA	0.211-0.254

Table S13: Range of effect sizes for significant SNPs in each ancestry cohort.

Trait Name or Code	African	South Asian	Native Hawaiian	AIAN	Hispanic and Latin American
Hemoglobin	1.464×10^{-7}	NA	0.0	0.0	0.0
Height	**0.999**	7.930×10^{-5}	0.0006	NA	**0.948**
PLC	**0.958**	0.0006	0.0	NA	**0.993**
MCV	0.1123	0.0004	0.0	0.0	0.0
BMI	0.079	0.056	0.005	NA	**0.970**
DBP	0.0009	NA	0.0	NA	0.015
SBP	9.078×10^{-6}	NA	0.0	NA	0.027
WBC	0.227	0.048	0.0	NA	**0.914**
RBC	0.001	0.010	0.0	0.0	0.0
Hematocrit	1.287×10^{-7}	NA	0.0	0.0	0.0
MCH	0.321	0.016	0.0	0.0	0.0
MCHC	0.001	NA	0.0	6.814×10^{-8}	0.285
Lymphocyte	NA	4.931×10^{-6}	0.0	0.0	0.0
Monocyte	0.093	0.137	0.0	0.0	0.0
Neutrophil	1.722×10^{-7}	6.244×10^{-6}	0.0	0.0	0.0
Eosinophil	0.044	1.499×10^{-5}	0.0	0.0	0.0
Basophil	NA	9.739×10^{-5}	0.0	0.0	0.0
Urate	0.002	0.005	0.0	0.0	0.0
Triglyceride	0.462	0.171	NA	0.0	**0.997**
Cholesterol	0.897	0.210	NA	NA	**0.998**
LDL	**0.963**	NA	NA	NA	**0.997**
HDL	0.345	0.146	NA	NA	**0.930**
HBA1C	NA	NA	3.092×10^{-6}	NA	0.024
EGFR	NA	0.031	0.0	NA	0.886
CRP	0.267	0.137	0.002	1.686×10^{-5}	**0.981**

Table S14: Maximum power under the standard GWA framework to detect variants that were significant in both the European ancestry cohort and at least one other cohort. For each ancestry-trait pair, power calculations were performed for all variants that were significant using a Bonferonni-corrected significance threshold and were significant in the corresponding ancestry (sorted by column). Power was calculated assuming the marginal European effect size to be the true effect size. Non-European ancestry minor allele frequencies and sample sizes were used in the power calculations. Calculations were performed using then framework defined in Sham and Purcell[63]. Comparisons where a variant had power to detect greater than 0.9 are shown in bold.

Trait Name or Code	African	South Asian	Native Hawaiian	AIAN	Hispanic and Latin American
Hemoglobin	0(1)	NA	0.0	0.0	0.0
Height	4(56)	0(2)	0(5)	NA	16(408)
PLC	1(163)	0(8)	0.0	NA	6(262)
MCV	0(18)	0(7)	0.0	0.0	0.0
BMI	0(3)	0(1)	0(35)	NA	48(212)
DBP	0(1)	NA	0.0	NA	0(109)
SBP	0(1)	NA	0.0	NA	0(99)
WBC	0(71)	0(25)	0.0	NA	35(104)
RBC	0(3)	0(3)	0.0	0.0	0.0
Hematocrit	0(1)	NA	0.0	0.0	0.0
MCH	0(22)	0(8)	0.0	0.0	0.0
MCHC	0(3)	NA	0.0	0(135)	0(110)
Lymphocyte	NA	0(7)	0.0	0.0	0.0
Monocyte	0(1)	0(2)	0.0	0.0	0.0
Neutrophil	0(2)	0(32)	0.0	0.0	0.0
Eosinophil	0(7)	0(1)	0.0	0.0	0.0
Basophil	NA	0(2)	0.0	0.0	0.0
Urate	0(1)	0(8)	0.0	0.0	0.0
Triglyceride	0(30)	0(61)	NA	0.0	124(311)
Cholesterol	0(85)	0(11)	NA	NA	16(943)
LDL	7(132)	NA	NA	NA	17(634)
HDL	0(21)	0(31)	NA	NA	2(241)
HBA1C	NA	NA	0(39)	NA	0(73)
EGFR	NA	0(86)	0.0	NA	0(5)
CRP	0(136)	0(32)	0(27)	0(8)	12(358)

Table S15: Number of variants that had greater than 90% power under the standard GWA framework that were significant in the European ancestry cohort and at least one other cohort. Numbers in parentheses are the total number of variants that could be compared between the European and correponding (column) ancestry cohort. Power was calculated assuming the marginal European effect size to be the true effect size. Non-European ancestry minor allele frequencies and sample sizes were used in the power calculations. Calculations were performed using then framework defined in Sham and Purcell[63].

Trait	African or African-American ($\times 10^{-6}$)	East Asian ($\times 10^{-6}$)	AIAN ($\times 10^{-6}$)	Native Hawaiian ($\times 10^{-6}$)	Hispanic and Latin American ($\times 10^{-6}$)
Basophil count	1.121	2.197	NA	NA	NA
BMI	2.096	2.197	2.073	2.093	2.072
CRP	2.097	2.085	2.072	2.100	2.073
Cholesterol	2.096	2.198	2.073	2.092	2.073
DBP	2.096	2.197	2.072	NA	2.073
EGFR	2.097	2.198	2.073	NA	2.073
Eosinophil count	2.121*	2.197	NA	NA	NA
HBA1C	2.096	2.198	2.073	2.093	2.072
HDL	2.097	2.198	2.073	2.093	2.073
Height	2.097	2.131	2.073	2.094	2.072
Hematocrit	2.121*	2.197	NA	NA	NA
Hemoglobin	2.121*	2.197	NA	NA	NA
LDL	2.096	2.198	2.073	2.093	2.073
Lymphocyte count	2.121*	2.197	NA	NA	NA
MCH	2.121*	2.197	NA	NA	NA
MCHC	2.096	2.197	2.877	NA	2.072
MCV	2.121*	2.197	NA	NA	NA
Monocyte count	2.121*	2.197	NA	NA	NA
Neutrophil count	2.121*	2.197	NA	NA	NA
PLC	2.097	2.197	2.072	NA	2.073
RBC	2.121*	2.197	NA	NA	NA
SBP	0.412	8.844	0.597	NA	5.692
Triglyceride	2.096	2.197	NA	2.072	2.073
Urate	2.121*	2.197	NA	NA	NA
WBC	2.092	2.197	2.072	NA	2.073

Table S16: Bonferroni *p*-value threshold corrected for number of gene-level association tests performed for each ancestry-trait pair. Thresholds are calculated as 0.05 divided by the number of SNPs tested in each ancestry-trait pair. The term"NA" indicates that there was no data for that ancestry-trait pair. The threshold for Bonferroni-corrected significance was the same for every trait in the European (p-value $< 2.092 \times 10^{-6}$) and South Asian (p-value $< 1.085 \times 10^{-6}$) cohorts from the UK Biobank. Traits for which the UK Biobank African cohort was used are denoted with a *; otherwise, the African-American cohort from the PAGE study data was used. See Table S2 for expansion of trait codes.

Trait Name or Code	Initial gene-level associations	Pruned gene-level associations $r^2 > 0.25$	Number of replicated associations	Proportion of replicated associations
MCV	434	336	174	0.400
PLC	241	295	116	0.481
Height	192	327	119	0.620
BMI	347	482	93	0.268
DBP	215	717	63	0.293
SBP	524	375	53	0.101
WBC	167	279	49	0.293
RBC	233	476	77	0.330
Hemoglobin	175	525	79	0.451
Hematocrit	267	356	72	0.270
MCH	246	562	161	0.654
MCHC	205	388	106	0.517
Lymphocyte	38	52	23	0.605
Monocyte	179	122	71	0.397
Neutrophil	211	549	124	0.588
Eosinophil	87	482	56	0.644
Basophil	88	237	35	0.398
Urate	391	444	54	0.138
Triglyceride	285	346	136	0.477
Cholesterol	167	477	136	0.814
LDL	120	443	67	0.558
HDL	213	496	136	0.638
HBA1C	235	421	89	0.379
CRP	105	526	34	0.324
EGFR	294	181	77	0.262

Table S17: Number and proportion of gene$-\varepsilon$ gene-level associations that are replicated under a more stringent pruning threshold. In our initial analysis of the European ancestry cohort we pruned all variants using an $r^2 > 0.5$ threshold. Here, we set the threshold as $r^2 > 0.25$ and recalculated the gene$-\varepsilon$ gene-level association statistics for each trait (see). Replication of associated genes using different r^2 thresholds varies by trait, the inclusion of as many SNPs as computationally possible in the gene-ε framework is optimal in identifying trait associated genes.

Trait	PESCA EUR only and EUR GWA nominal significance	PESCA EAS only and EAS GWA nominal significance	PESCA both and EUR GWA nominal significance	PESCA both and EAS GWA nominal significance	PESCA both and GWA nominal significance in both
BMI	0	0	97	539	94
Cholesterol	2	13	14	54	11
HDL	5	8	29	74	27
LDL	0	6	16	43	13
MCH	3	14	39	180	39
MCV	1	11	44	215	44
Triglyceride	4	8	15	49	15

Table S18: Overlap between SNPs identified by PESCA and GWA analyses in the European ancestry cohort from the UK Biobank and the East Asian ancestry cohort from the Biobank Japan. For seven continuous traits, we compared SNP-level association p-values from our analysis to the posterior probabilities calculated in Shi et al.[64] using the PESCA framework. For each of the seven traits, there were SNPs that had a posterior probability > 0.8 of being causal in both ancestries and were also nominally significant (p-value $5 < 10^{-6}$) using the standard GWA SNP-level framework.

Trait Name or Code	Median Effect Size Correlation	Effect Sizes > 0.1 (Mean)	Median PIP Correlation	PIPs > 0.01 (Mean)
BMI	0.0143	0	0.073	67.3
Basophil	3.69×10^{-6}	0	0.002	211.8
CRP	0.096	0.7	0.159	142.6
Cholesterol	0.966	1	0.232	53.1
DBP	0.001	0.6	0.012	173.1
EGFR	4.71×10^{-6}	0	0.005	149
Eosinophil	0.0179	0.2	0.042	325.8
HBA1C	0.012	0.2	0.025	26.8
HDL	0.325	0.1	0.219	57.6
Height	9.20×10^{-5}	1.6	0.010	187.7
Hematocrit	-4.16×10^{-6}	0.5	0.015	40.3
Hemoglobin	-1.13×10^{-5}	0.6	0.014	45.8
LDL	0.949	1	0.331	60.9
Lymphocyte	-1.01×10^{-6}	1.5	0.001	1368.5
MCH	7.098×10^{-6}	0.6	0.007	60.9
MCHC	-2.00×10^{-6}	0.9	0.01	58.7
MCV	1.71×10^{-5}	0.6	0.01	70
Monocyte	0.002	0.1	0.017	349.4
Neutrophil	0.038	0.1	0.071	66.5
PLC	0.609	0.9	0.154	112.5
RBC	9.650×10^{-5}	0.9	0.028	49.7
SBP	0.001	0.6	0.019	166.8
Triglyceride	0.348	0.0	0.247	164.7
Urate	0.252	0.5	0.24	39.9
WBC	0.0002	0.1	0.01	347.8

Table S19: Replication of effect sizes and posterior inclusion probabilities (PIPs) among ten independent subsamples of the UK Biobank European ancestry cohort using SuSiE[65] for fine-mapping. The sample size of the ten independent, non-overlapping subsamples of the UK Biobank European ancestry cohort was set to 10,000. For the 1,895,051 SNPs that were analyzed in every European ancestry cohort subsample (Table S1) and the effect sizes and PIPs (columns 2 and 4, respectively) generated using the SuSiE method[65], we calculated the median correlation coefficient between all possible pairwise comparisons (10 choose 2) of the European ancestry cohort subsamples. Column 3 reports the mean number of SNPs with effect sizes greater than 0.1 across all ten European ancestry cohort subsamples for each trait. Column 5 reports the mean number of SNPs with a posterior inclusion probability greater than 0.01 across the ten European ancestry cohort subsamples for each trait.

Trait Name or Code	Number of Shared Effect Sizes > 0.1	Median Effect Size Correlation	African Effect Sizes > 0.1	European Effect Sizes > 0.1 (Mean)	Number of Shared PIPs > 0.01	Median PIP Correlation	African PIPs > 0.01	European P > 0.01 (Mea
BMI	0	5.12×10^{-5}	2	0	1	0.027	1206	8.9
Basophil	0	-3.01×10^{-5}	0	0	0	0.001	403	40.3
CRP	0	-3.68×10^{-6}	0	0.4	0	5.88×10^{-5}	95	33.6
Cholesterol	1	0.5	1	0.9	5	0.467	1144	8.4
DBP	0	1.58×10^{-5}	10	0.3	0	0.008	1249	20.3
EGFR	0	2.41×10^{-6}	1	0	0	0.001	984	24.7
Eosinophil	0	-1.97×10^{-5}	0	0	0	0.003	979	29.3
HBA1C	0	-1.15×10^{-6}	5	0.2	0	0.004	959	6.5
HDL	0	0.014	0	0.1	2	0.014	31	11.6
Height	0	-1.22×10^{-5}	19	0.7	0	0.003	208	33.7
Hematocrit	0	-1.14×10^{-5}	1	0	0	0.016	199	12.2
Hemoglobin	0	-6.31×10^{-6}	1	0	0	0.022	568	12.5
LDL	1	0.674	1	1	8	0.497	995	13.5
Lymphocyte	0	2.71×10^{-5}	0	0	1	0.001	60	115.5
MCH	0	1.14×10^{-5}	1	0.2	0	0.005	1332	11.8
MCHC	0	-1.56×10^{-6}	1	0.2	0	0.008	646	13.6
MCV	0	2.58×10^{-6}	1	0.2	0	0.005	917	11.8
Monocyte	0	-2.44×10^{-5}	0	0	2	0.002	2215	27.7
Neutrophil	0	-0.0001	1	0	0	0.001	2386	10.2
PLC	0	-0.017	1	0.6	3	0.035	2088	13.7
RBC	0	-6.35×10^{-6}	1	0.1	0	-0.002	3	12.7
SBP	0	4.31×10^{-5}	13	0.1	0	0.008	1133	20
Triglyceride	0	0.004	0	0.1	8	0.009	2231	25.6
Urate	1	0.01	2	0.3	3	0.051	334	9.8
WBC	0	-0.0001	1	0	5	0.0006	2862	48.3

Table S20: Replication of effect sizes and posterior inclusion probabilities (PIPs) between the UK Biobank African ancestry cohort and ten independent subsamples of the UK Biobank European ancestry cohort using SuSiE[65] for fine-mapping. Each of the ten independent, non-overlapping subsamples of the UK Biobank European ancestry cohort was set to be equal in size to the sample size of the African ancestry cohort (N = 4,967), Table S1. Column headers containing "(mean)" indicate a mean is generated averaging over the ten independent European ancestry cohort subsamples. For the 496,997 SNPs that were analyzed in both the African ancestry cohort and every European ancestry cohort subsample, we compared the SuSiE[65] effect size estimates and PIPs. For both effect sizes and PIPs, the median correlation coefficient between the African ancestry cohort and the pairwise comparison to each European ancestry cohort subsample is reported in the third and seventh columns, respectively. Column 3 reports the total number of SNPs with effect sizes greater than 0.1 in the African cohort. Column four gives the mean number of effect sizes greater than 0.1 in the European ancestry cohort subsamples for each trait. We performed the same comparison for the PIPs using a threshold of 0.01. Column 2 reports the number of SNPs that surpassed an effect size of 0.1 in both the African ancestry cohort and at least one of the European ancestry cohort subsamples. Column 6 reports the number of SNPs that surpasses a PIP of 0.01 in the African ancestry cohort and at least one European ancestry cohort subsample.

Trait Name or Code	Number of Shared Effect Sizes > 0.1	Median Effect Size Correlation	South Asian Effect Sizes > 0.1	European Effect Sizes > 0.1 (Mean)	Number of Shared PIPs > 0.01	Median PIP Correlation	South Asian PIPs > 0.01	European P > 0.01 (Mea
BMI	0	7.07×10^{-5}	1	0	0	0.0173	180	18
Basophil	0	-1.10×10^{-5}	0	0	0	0.0008	210	78.4
CRP	0	0.0309	0	0.4	17	0.121	181	64.7
Cholesterol	0	0.004	0	0.9	2	0.0127	20	9
DBP	0	-2.12×10^{-5}	0	0.6	0	0.013	115	40
EGFR	0	-1.26×10^{-5}	0	0	0	5.12×10^{-5}	452	44.2
Eosinophil	0	2.16×10^{-5}	0	0	0	0.006	63	69.1
HBA1C	0	-3.33×10^{-5}	2	0.3	0	0.011	133	13.3
HDL	0	0.525	0	0.1	3	0.505	78	12.2
Height	0	-2.13×10^{-5}	12	1.1	1	0.001	754	66.8
Hematocrit	0	-4.78×10^{-6}	1	0.3	0	6.24×10^{-5}	24	17.4
Hemoglobin	0	-4.19×10^{-6}	1	0.3	0	0.011	19	16.1
LDL	0	0.491	1	1	14	0.386	44	15.6
Lymphocyte	0	-4.40×10^{-6}	0	1.1	0	0.0001	113	343.1
MCH	0	5.29×10^{-6}	2	0.5	0	0.008	78	22.3
MCHC	0	-5.77×10^{-6}	1	0.9	0	0.007	45	20.3
MCV	0	1.74×10^{-5}	3	0.5	0	0.005	81	26.3
Monocyte	0	-4.05×10^{-6}	0	0.1	0	0.001	156	76.8
Neutrophil	0	0.221	0	0	16	0.172	70	25.7
PLC	0	0.577	0	0.8	1	0.679	126	22.7
RBC	0	2.79×10^{-6}	0	0.3	0	-0.011	41	20.9
SBP	0	-0.0004	0	0.3	0	0.037	116	43.2
Triglyceride	0	0.158	0	0	53	0.173	189	46.4
Urate	0	0.137	1	0.4	6	0.150	52	15.8
WBC	0	0.001	0	0	18	0.008	52	93

Table S21: Replication of effect sizes and posterior inclusion probabilities (PIPs) between the UK Biobank South Asian ancestry cohort and ten independent subsamples of the UK Biobank European ancestry cohort using SuSiE[65] for fine-mapping. Each of the ten independent, non-overlapping subsamples of the UK Biobank European ancestry cohort was set to be equal in size to the sample size of the South Asian ancestry cohort (N = 5,660), Table S1. Column headers containing "(mean)" indicate a mean is generated averaging over the ten independent European ancestry cohort subsamples. For the 863,569 SNPs that were analyzed in both the South Asian ancestry cohort and every European ancestry cohort subsample, we compared the SuSiE[65] effect size estimates and PIPs. For both effect sizes and PIPs, the median correlation coefficient between the South Asian ancestry cohort and the pairwise comparison to each European ancestry cohort subsample is reported in the third and seventh columns, respectively. Column 3 reports the total number of SNPs with effect sizes greater than 0.1 in the South Asian cohort. Column four gives the mean number of effect sizes greater than 0.1 in the European ancestry cohort subsamples for each trait. We performed the same comparison for the PIPs using a threshold of 0.01. Column 2 reports the number of SNPs that surpassed an effect size of 0.1 in both the South Asian ancestry cohort and at least one of the European ancestry cohort subsamples. Column 6 reports the number of SNPs that surpasses a PIP of 0.01 in the South Asian ancestry cohort and at least one European ancestry cohort subsample.

Trait Name or Code	Cochran's Q among European subsamples (p-value)	Cochran's Q between African and European subsamples (p-value)	Cochran's Q between South Asian and European subsamples (p-value)
Height	641.91 (2.10e-132)	395.01 (1.09e-78)	4036.8(0.0)
BMI	316.69 (7.48e-63)	6,916.75 (0.0)	1076.76 (5.39e-225)
MCV	160.05 (7.25e-30)	11,489.97 (0.0)	155.06 (3.37e-28)
PLC	51.29 (6.15e-08)	13,141.96 (0.0)	386.07 (8.67e-77)
DBP	254.32 (1.22e-49)	9,725.02 (0.0)	241.54 (3.26e-46)
SBP	126.20 (7.16e-23)	1,0479.39 (0.0)	286.38 (1.17e-55)
WBC	1458.39 (1.87e-308)	20,351.80 (0.0)	374.37 (2.65e-74)
RBC	102.75 (4.36e-18)	29.34 (0.001)	153.12 (8.51e-28)
Hemoglobin	114.35 (1.91e-20)	5,022.47 (0.0)	76.74 (2.18e-12)
Hematocrit	149.67 (1.03e-27)	1,205.09 (1.15e-252)	93.03 (1.34e-15)
MCH	90.29 (1.42e-15)	14,366.33 (0.0)	158.25 (7.44e-29)
MCHC	260.58 (5.80e-51)	14,674.80 (0.0)	112.79 (1.46e-19)
Lymphocyte	3105.01 (0.0)	396.931 (4.23e-79)	1,062.61 (6.05e-222)
Monocyte	811.20 (8.26e-169)	9,186.25 (0.0)	433.65 (6.41e-87)
Neutrophil	95.72 (1.15e-16)	24,580.86 (0.0)	141.67 (1.92e-25)
Eosinophil	4,919.90 (0.0)	3,615.16 (0.0)	873.53 (3.16e-181)
Basophil	833.69 (1.18e-173)	1,879.65 (0.0)	541.10 (7.19e-110)
Urate	73.29 (3.44e-12)	93.37 (1.15e-15)	110.03 (5.26e-19)
HBA1C	100.17 (1.45e-17)	14,073.79 (0.0)	639.21 (6.93e-131)
EGFR	361.48 (2.23e-72)	11,478.25 (0.0)	3,012.83 (0.0)
CRP	288.30 (7.91e-57)	117.51 (1.62e-20)	509.40 (4.33e-103)
Triglyceride	138.42 (2.19e-25)	9,133.51 (0.0)	564.80 (6.09e-115)
HDL	175.95 (3.54e-33)	30.98 (0.00059)	292.39 (6.32e-57)
LDL	101.33 (8.45e-18)	3,935.88 (0.0)	86.14 (3.12e-14)
Cholesterol	158.82 (1.30e-29)	5,919.75 (0.0)	43.87 (3.47e-06)

Table S22: Cochran's Q Statistics and p-values for comparisons of SuSiE[65] for fine-mapping posterior inclusion probabilities among UKB ancestry cohorts. We calculated the Cochran's Q statistic for posterior inclusion probabilities > 0.01 for each pairwise comparison of European cohort subsamples. We reported the median value of these comparisons for each trait. We then calculated the median Cochran's Q when comparing the ten European subsamples to the African and South Asian ancestry cohorts in the UK Biobank.

False discovery rate					
gene-ε					
Structured Population			Unstructured Population		
Sparsity	0.01	0.1		0.01	0.1
$h^2 = 0.2$	0 (0)	0.010 (0.044)	$h^2 = 0.2$	0.418 (0.183)	0.618 (0.085)
$h^2 = 0.6$	0.020 (0.141)	0 (0)	$h^2 = 0.6$	0.097 (0.284)	0.327 (0.245)
GWAS					
Sparsity	0.01	0.1	Sparsity	0.01	0.1
$h^2 = 0.2$	0.447 (0.153)	0.636 (0.075)	$h^2 = 0.2$	0.01 (0.1)	0.001 (0.011)
$h^2 = 0.6$	0.127 (0.324)	0.38 (0.241)	$h^2 = 0.6$	0.057 (0.227)	0 (0)
Power					
gene-ε					
Structured Population			Unstructured Population		
Sparsity	0.01	0.1	Sparsity	0.01	0.1
$h^2 = 0.2$	0.023 (0.043)	0.045 (0.104)	$h^2 = 0.2$	0.002 (0.038)	0.392 (0.108)
$h^2 = 0.6$	0.0006 (0.0006)	0.0002 (0.002)	$h^2 = 0.6$	0.0006 (0.0006)	0.0004 (0.002)
GWAS					
Sparsity	0.01	0.1	Sparsity	0.01	0.1
$h^2 = 0.2$	0.154 (0.038)	0.397 (0.052)	$h^2 = 0.2$	0.010 (0.038)	0.001 (0.108)
$h^2 = 0.6$	0.0002 (0.0008)	0.005 (0.004)	$h^2 = 0.6$	0.057 (0.0006)	0 (0.002)

Table S23: Performance of the standard GWA framework and gene-ε in simulations of a small cohort with $N = 2,000$ individuals. Mean false discovery rate and power for 100 simulations of a population under each parameter set shown in Figure S8. Standard errors are given in parentheses.

Gene	African-American	European	South Asian	East Asian	AIAN	Hispanic and Latin American
RDH13	4.14×10^{-10}	9.95×10^{-1}	8.80×10^{-2}	1.76×10^{-6}	1	7.88×10^{-1}
AGPAT5	1	1.30×10^{-6}	7.83×10^{-1}	5.00×10^{-1}	7.33×10^{-8}	1
GP6	7.20×10^{-10}	9.93×10^{-1}	1.47×10^{-1}	9.07×10^{-7}	1	6.92×10^{-1}
ALDH2	1	1.00×10^{-20}	1.13×10^{-2}	1.00×10^{-20}	1	1
RAB8A	9.57×10^{-1}	1.00×10^{-20}	1	5.76×10^{-6}	1	9.97×10^{-1}
CUX2	1	5.13×10^{-7}	1.16×10^{-1}	3.44×10^{-11}	1	1
ACAD10	1	1.47×10^{-10}	1.10×10^{-2}	2.00×10^{-10}	1	1

Table S24: Gene-level association *p*-values for seven genes associated with platelet count in at last two ancestry cohorts. Of the 65 genes that were associated with platelet count in at least two ancestry cohorts, these seven contained previously identified SNP-level associations in studies submitted to the GWAS Catalog. Previous associations in the GWAS Catalog are discussed in the Supplemental Information. Ancestry-specific Bonferroni corrected significance thresholds for gene-level association analysis of platelet count are shown in Table S16.

Gene	African or African-American	European	East Asian	Hispanic
ANGPTL4	[42]	[28]	NA	[28]
APOA1	[21]	[21]	NA	[21]
APOA4	NA	[22]	NA	NA
APOA5	[24]	[23] [26]	[27]	[24]
APOB	[29]	[29]	NA	[29]
APOC1	[21]	[22]	NA	[21]
APOC2	[24]	[24]	NA	[24]
APOC3	[21]	[21] [22]	NA	[21]
APOC4	[22]	[22]	NA	[22]
APOE	[22]	[22] [24]	NA	[22]
CETP	[21]	[22]	NA	[21]
LMF1	NA	[22]	NA	NA
LPL	[21]	[22]	[27]	[21]
PCSK6	[42]	[22]	NA	[42]
PCSK7	[24]	[24]	[27]	[24]
PLTP	[21] [24] [28] [29]	[21] [22] [28] [31]	NA	[21] [24] [28] [29]

Table S25: Genes shown in Figure 3 as associated with triglyceride levels are supported by publications in the GWAS Catalog. Each of the genes listed is present in the significantly mutated subnetworks identified using Hierarchical HotNet[50] as enriched for associations with triglyceride levels in the European, East Asian, or Native Hawaiian ancestry cohorts. We mapped SNP-level associations from the GWAS Catalog to the 29 genes present in the significantly mutated subnetworks shown in Figure 3 (using the gene list provided by Gusev et al.[62]) to generate the results for the 16 genes shown here.

Gene	African-American (PAGE)	European	South Asian	East Asian	Native Hawaiian	Hispanic and Latin American
APOA1	4.99×10^{-1}	1.00×10^{-20}	9.91×10^{-1}	1.00×10^{-20}	7.52×10^{-1}	4.99×10^{-1}
APOA4	4.99×10^{-1}	1.00×10^{-20}	2.51×10^{-5}	1.00×10^{-20}	9.15×10^{-1}	4.99×10^{-1}
APOA5	4.99×10^{-1}	1.42×10^{-11}	1.60×10^{-6}	9.95×10^{-1}	3.67×10^{-12}	4.99×10^{-1}
APOC3	4.99×10^{-1}	1.00×10^{-20}	9.82×10^{-1}	9.83×10^{-1}	3.05×10^{-15}	4.99×10^{-1}
APOE	4.99×10^{-1}	1.00×10^{-20}	8.65×10^{-1}	1.00×10^{-20}	1	1
PLTP	4.99×10^{-1}	4.29×10^{-9}	9.66×10^{-1}	6.66×10^{-15}	1.00×10^{-2}	4.99×10^{-1}
LPL	4.99×10^{-1}	4.08×10^{-13}	3.00×10^{-3}	1.00×10^{-20}	6.59×10^{-1}	4.99×10^{-1}
ANGPTL3	4.99×10^{-1}	8.86×10^{-8}	2.00×10^{-3}	1.00×10^{-20}	4.00×10^{-3}	1
ANGPTL4	4.99×10^{-1}	1.00×10^{-20}	9.78×10^{-1}	9.99×10^{-1}	9.89×10^{-1}	1
APOC1	4.99×10^{-1}	1.67×10^{-16}	4.99×10^{-1}	1.00×10^{-20}	9.81×10^{-1}	4.99×10^{-1}
APOC2	4.99×10^{-1}	3.57×10^{-13}	7.71×10^{-1}	1.11×10^{-1}	9.11×10^{-1}	4.99×10^{-1}
APOC4	4.99×10^{-1}	3.72×10^{-13}	7.36×10^{-1}	2.58×10^{-14}	9.73×10^{-1}	4.99×10^{-1}
APOB	4.99×10^{-1}	1.00×10^{-20}	9.99×10^{-1}	7.32×10^{-12}	1.00×10^{-3}	1
LMF1	9.98×10^{-1}	8.03×10^{-7}	1	3.21×10^{-2}	3.79×10^{-5}	9.98×10^{-1}
APOL1	4.99×10^{-1}	5.30×10^{-2}	6.40×10^{-2}	1	8.89×10^{-11}	4.99×10^{-1}
HBA1	4.99×10^{-1}	3.75×10^{-5}	9.99×10^{-1}	4.51×10^{-1}	2.46×10^{-10}	1
HBA2	4.99×10^{-1}	1.30×10^{-5}	9.99×10^{-1}	4.51×10^{-1}	3.93×10^{-10}	4.99×10^{-1}
B4GALT3	4.99×10^{-1}	6.80×10^{-2}	7.21×10^{-1}	4.99×10^{-1}	1.23×10^{-6}	1
KLK8	1	1	1.62×10^{-6}	9.89×10^{-1}	1.00×10^{-3}	1
PNLIP	4.99×10^{-1}	9.99×10^{-1}	9.26×10^{-1}	7.75×10^{-1}	1.00×10^{-3}	4.99×10^{-1}
WNT4	4.99×10^{-1}	9.61×10^{-1}	9.99×10^{-1}	4.99×10^{-1}	3.29×10^{-5}	4.99×10^{-1}
BACE1	4.99×10^{-1}	5.55×10^{-17}	2.20×10^{-2}	9.99×10^{-16}	6.69×10^{-1}	4.99×10^{-1}
CETP	4.99×10^{-1}	1.00×10^{-3}	9.99×10^{-1}	1.41×10^{-6}	9.99×10^{-1}	4.99×10^{-1}
PCSK6	4.99×10^{-1}	1	9.99×10^{-1}	1.83×10^{-5}	1.00×10^{-3}	4.99×10^{-1}
PCSK7	4.99×10^{-1}	1.66×10^{-8}	9.97×10^{-1}	1.00×10^{-20}	9.99×10^{-1}	4.99×10^{-1}
LCAT	4.99×10^{-1}	5.00×10^{-1}	1	6.24×10^{-3}	4.38×10^{-1}	4.99×10^{-1}
APOF	4.99×10^{-1}	5.78×10^{-1}	7.79×10^{-1}	4.10×10^{-3}	9.64×10^{-1}	4.99×10^{-1}
TYRO3	4.99×10^{-1}	9.28×10^{-1}	9.99×10^{-1}	1.20×10^{-2}	8.57×10^{-1}	4.99×10^{-1}

Table S26: Gene-ε p-values for the 28 genes present in the significantly mutated subnetworks associated with triglyceride level in the European, East Asian, and Native Hawaiian cohorts. Each of these genes is present in Figure 3 which depicts the overlapping significantly mutated subnetworks identified using Hierarchical HoNet[50] identified in an analysis of triglyceride levels in the European, East Asian, and Native Hawaiian cohorts. Known SNP-level associations identified within the bounds of these genes in previous studies submitted to the GWAS Catalog are discussed in the Supplemental Information. Ancestry-specific Bonferroni corrected significance thresholds for gene-level association analysis of triglyceride levels are shown in Table S16.

Supplemental Subjects and Methods

UK Biobank Data

We downloaded individual genotype data using the UK Biobank's (UKB) `ukbgene` resource, https://biobank.ctsu.ox.ac.uk/crystal/download.cgi. European individuals from the UK Biobank data were selected using the self-identified ancestry (data field 21000) using values outlined at https://biobank.ctsu.ox.ac.uk/crystal/field.cgi?id=21000. Using the relatedness file provided by the UK Biobank, one individual from each related pair was then randomly removed. This process was repeated for individuals whose self-identified ancestry was South Asian.

We performed unsupervised genome-wide ancestry estimation using ADMIXTURE by setting $K = 3$[66] on the self-identified African ancestry cohort. We also included YRI and CEU individuals in the ADMIXTURE runs from the 1000 Genomes Project, to identify the ancestry components corresponding to African and European ancestry. We removed individuals containing less than 5% membership in the African ancestry component and more than 5% membership in the third component, which corresponds to American Indian/Alaskan Native (AIAN) ancestry (??). We downloaded imputed SNP data from the UK Biobank for all remaining individuals and removed SNPs with an information score below 0.8. Information scores for each SNP are provided by the UK Biobank (http://biobank.ctsu.ox.ac.uk/crystal/refer.cgi?id=1967). The remaining genotype and high-quality imputed SNPs were put through a stringent quality control pipeline in each ancestry cohort to obtain cohort-specific SNPs to be used for further analysis as detailed in the main text (detailed below).

We performed the following quality control filters in the European, South Asian, and African cohorts from the UK Biobank (Application number 22419). Genotype data for 488,377 individuals in the UK Biobank were downloaded using the UK Biobank's `ukbgene` (https://biobank.ctsu.ox.ac.uk/crystal/download.cgi) tool and converted using the provided `ukbconv` tool (https://biobank.ctsu.ox.ac.uk/crystal/refer.cgi?id=149660). Phenotype data was also downloaded for those same individuals using the `ukbgene` tool. Individuals identified by the UK Biobank to have high heterozygosity, excessive relatedness, or aneuploidy were removed (1,550 individuals). After then separating individuals into self-identified ancestral groups using data field 21000. Within these cohorts, unrelated individuals were then selected by randomly selecting an individual from each pair of related individuals. This resulted in 349,469 European individuals, 5,716 South Asian individuals, and 4,967 African individuals.

Genotype quality control was then performed on each cohort separately using the following steps. All structural variants were first removed, leaving only single nucleotide polymorphisms in the genotype data. Next, all AT/CG SNPs were removed to avoid possible confounding due to sequencing errors. Then, SNPs

with minor allele frequency less than 1% were removed using the plink2[67] `--maf 0.01`. We then removed all SNPs found to be in Hardy-Weinberg equilibrium, using the plink `--hwe 0.000001` flag to remove all SNPs with a Fisher's exact test p-value $> 10^{-6}$. Finally, all SNPs with missingness greater than 1% were removed using the plink `--mind 0.01` flag.

Finally, we note that the number of filtered SNPs in the African cohort is smaller than the number of filtered SNPs in the European cohort. These results stand in contrast to expectation about number of independent variants in these two populations. We believe this to be due to ascertainment bias on the genotyping array.

Biobank Japan Data

We downloaded summary statistics for 25 quantitative traits from the Biobank Japan (BBJ) website (`http://jenger.riken.jp/en/result`)[59–61,68]. The sample descriptions and number of SNPs included in our analyses are given in Table S5. The number of SNPs included in the analysis of each trait represent those SNPs that: (*i*) contained an rsid number that could be mapped to the hg19 genome build, (*ii*) overlapped with SNPs contained within the 1000 Genomes Project phase 3 genotype data, and (*iii*) had a minor allele frequency greater than 0.01 in Japanese (JPT) individuals in the 1000 Genomes Project. We used the 1000 Genomes phase 3 data from 93 JPT individuals to estimate the linkage disequilibrium (LD) between SNPs in BioBank Japan for which we had the summary statistic data; LD was estimated separately for each of the 25 quantitative traits using the trait specific SNP arrays. LD estimates were used in the calculation of regional association statistics.

Population Architecture using Genomics and Epidemiology (PAGE) Study Data

Summary statistics for genotyped and imputed SNPs in five admixed populations were downloaded from the Population Architecture using Genomics and Epidemiology (PAGE)[69] with permission granted via approval of manuscript proposal. We included summary statistics for up to 14 quantitative traits for African-American, Hispanic and Latin American, Native Hawaiian, American Indian/Alaska Native, and Asian ancestry cohorts when available. All AT/CG SNPs were omitted, and SNPs with an IMPUTE2 information score greater than 0.8 were included in this analysis. Number of individuals and SNPs varied across ancestry-trait combinations and are given in Table S5 - Table S10.

Individuals from the 1000 Genomes Project phase 3[70] and the Human Genome Diversity Panel (HGDP)[71] were used to obtain LD estimates between SNPs for each ancestry cohort. To construct the LD reference panel for PAGE summary statistics from the African-American ancestry cohort, unrelated individuals from the 1000 Genomes Americans of African Ancestry in SW USA (ASW) and African Caribbeans in Barbados

(ACB) were used. Only SNPs found in both the 1000 Genomes imputed data and PAGE summary statistics files were used in gene-level association and heritability analyses. We used the same approach to compute reference LD estimates between SNPs for the Hispanic and Latin American, AIAN, and Asian ancestry cohorts, with the following 1000 Genomes reference population, respectively: Mexican Ancestry from Los Angeles USA (MXL) and Puerto Ricans from Puerto Rico (PUR); Colombians from Medellin, Colombia (CLM) and Peruvians from Lima, Peru (PEL); and the East Asian superpopulation (EAS). For the Native Hawaiian individuals from the PAGE study, there were no appropriate reference populations in the 1000 Genomes data. In order to construct a reference LD matrix for the Native Hawaiian ancestry cohort, we randomly sampled individuals from populations in the most recent release of the HGDP proportional to the global ancestry of the Native Hawaiian cohort. The Native Hawaiian cohort's global ancestry proportions were determined using ADMIXTURE runs to be 47.89% Oceanian, 25.16% East Asian, 25.51% European, 0.90% African, and 0.54% AIAN in a separate publication (Wojcik preprint - in prep.). We did not sample from populations with less than 1% of the total ancestry in the admixture analysis referenced above. The resulting sample from which LD was estimated included 39 individuals from the Papuan Sepik in New Guinea and Melanesian in Bougainville, 14 individuals from the French in France, and 14 individuals from the Yoruba in Nigeria.

WHI study cohort description

The Women's Health Initiative (WHI) is a long-term, prospective, multi-center cohort study investigating post-menopausal women's health in the US. WHI was funded by the National Institutes of Health and the National Heart, Lung, and Blood Institute to study strategies to prevent heart disease, breast 124 cancer, colon cancer, and osteoporotic fractures in women 50-79 years of age. WHI involves 161,808 women recruited between 1993 and 1998 at 40 centers across the US. The study consists of two parts: the WHI Clinical Trial which was a randomized clinical trial of hormone therapy, dietary modification, and calcium/Vitamin D supplementation, and the WHI Observational Study, which focused on many of the inequities in women's health research and provided practical information about incidence, risk factors, and interventions related to heart disease, cancer, and osteoporotic fractures. For this project, women who self identified as European were excluded from the study sample (dbGaP study accession number: phs000227).

HCHC/SOL study cohort description

The Hispanic Community Health Study / Study of Latinos (HCHS/SOL) is a multi center study of Hispanic/Latino populations with the goal of determining the role of acculturation in the prevalence and development of diseases, and to identify other traits that impact Hispanic/Latino health. The study is sponsored

by the National Heart, Lung, and Blood Institute (NHLBI) and other institutes, centers, and offices of the National Institutes of Health (NIH). Recruitment began in 2006 with a target population of 16,000 persons of Cuban, Puerto Rican, Dominican, Mexican or Central/South American origin. Household sampling was employed as part of the study design. Participants were recruited through four sites affiliated with San Diego State University, Northwestern University in Chicago, Albert Einstein College of Medicine in Bronx, New York, and the University of Miami. Researchers from seven academic centers provided scientific and logistical support. Study participants who were self-identified Hispanic/Latino and aged 18-74 years underwent extensive psycho-social and clinical assessments during 2008-2011. A re-examination of the HCHS/SOL cohort is conducted during 2015-2017. Annual telephone follow-up interviews are ongoing since study inception to determine health outcomes of interest. (dbGaP study accession number: phs000555).

BioMe Biobank study cohort description

The Charles Bronfman Institute for Personalized Medicine at Mount Sinai Medical Center (MSMC), BioMeTM 54 BioBank (BioMe) is an EMR-linked bio-repository drawing from Mount Sinai Medical Center consented patients which were drawn from a population of over 70,000 inpatients and 800,000 outpatients annually. The MSMC serves diverse local communities of upper Manhattan, including Central Harlem (86% African American), East Harlem (88% Hispanic/Latino), and Upper East Side (88% Caucasian/White) with broad health disparities. BioMeTM 58 enrolled over 26,500 participants from September 2007 through August 2013, with 25% African American, 36% Hispanic/Latino (primarily of Caribbean origin), 30% Caucasian, and 9% of Other ancestry. The BioMeTM 60 population reflects community-level disease burdens and health disparities with broad public health impact. Biobank operations are fully integrated in clinical care processes, including direct recruitment from clinical sites waiting areas and phlebotomy stations by dedicate Biobank recruiters independent of clinical care providers, prior to or following a clinician standard of care visit. Recruitment currently occurs at a broad spectrum of over 30 clinical care sites. Study participants of self-reported European ancestry were not included in this analysis. (dbGaP study accession number: phs000925).

MEC study cohort description

The Multiethnic Cohort (MEC) is a population-based prospective cohort study including approximately 215,000 men and women from Hawaii and California. All participants were 45-75 years of age at baseline, and primarily of 5 ancestries: Japanese Americans, African Americans, European Americans, Hispanic/Latinos, and Native Hawaiians. MEC was funded by the National Cancer Institute in 1993 to examine lifestyle risk factors and genetic susceptibility to cancer. All eligible cohort members completed baseline and follow-up

questionnaires. Within the PAGE II investigation, MEC proposes to study: 1) diseases for which we have DNA available for large numbers of cases and controls (breast, prostate, and colorectal cancer, diabetes, and obesity); 2) common traits that are risk factors for these diseases (e.g., body mass index / weight, waist-to-hip ratio, height), and 3) relevant disease-associated biomarkers (e.g., fasting insulin and lipids, steroid hormones). The specific aims are: 1) to determine the population-based epidemiologic profile (allele frequency, main effect, heterogeneity by disease characteristics) of putative causal SNPs in the five racial/ethnic groups in MEC; 2) for SNPs displaying effect heterogeneity across ethnic/racial groups, we will utilize differences in LD to identify a more complete spectrum of associated SNPs at these loci; 3) investigate gene x gene and gene x environment interactions to identify modifiers; 4) examine the associations of putative causal SNPs with already measured intermediate phenotypes (e.g., plasma insulin, lipids, steroid hormones); and 5) for SNPs that do not fall within known genes, start to investigate their relationships with gene expression and epigenetic patterns in small genomic studies. For this project, MEC contributed African American, Japanese American, and Native Hawaiian samples.(dbGaP study accession number: phs000220).

Fine-mapping analyses

Methods: Protocol for implementation of SuSiE and PESCA

To perform SNP-level fine mapping analyses on a given quantitative trait, we applied Sum of Single Effects (SuSiE) variable selection software[65]. SuSiE implements a Bayesian linear regression model on individual level data where sparse prior distributions are placed on the effect size of SNP and posterior inclusion probabilities (PIPs) are used to summarize their statistical relevance to the trait of interest. The software for SuSiE requires an input ℓ which fixes the maximum number of causal SNPs to include in the model. In this work, we consider results when this parameter is chosen conservatively ($\ell = 3000$). We used the three cohorts for which we had genotype data from the UK Biobank (African, European, and South Asian) to test whether there was effect size heterogeneity among ancestries in the 25 traits analyzed in this study. We first selected ten independent, non-overlapping subsamples of 10,000 individuals from the European ancestry cohort and filtered out any SNPs that had a minor allele frequency of less than 0.01. For each subsample, we then applied SuSiE to each of the 25 traits and compared the effect sizes and posterior inclusion probabilities. The average number of SNPs with an effect size greater than 0.01 and average number of SNPs with a PIP greater than 0.01 for each trait across the ten cohorts are reported in Table S19. Table S19 also reports the median correlation coefficient of effect sizes and PIPs among the 45 pairwise comparisons between the 10 subsample cohorts.

We then applied SuSiE to the African and South Asian ancestry cohorts and compared their resulting

effect sizes and PIPs to ten independent, non-overlapping subsamples of the European ancestry cohort. The number of SNPs with an effect size greater than 0.1 and PIPs greater than 0.01 in both the focal cohort (either African or South Asian) and at least one of the ten European ancestry subsamples of the same size are reported in Table S20 and Table S21. Also reported in these tables, are the mean number of effect sizes greater than 0.01 and PIPs greater than 0.01 across the European ancestry subsamples for each trait and the number of unique effect sizes greater than 0.01 and PIPs greater than 0.01 that were only identified in the African or South Asian ancestry cohorts. Finally, Table S20 and Table S21 report the median correlation coefficient of the African or South Asian ancestry cohort effect sizes and PIPs with the ten European ancestry subsample cohorts of the same size.

We report the median Cochran's Q statistic calculated among all pairs of European subsamples for posterior inclusion probabilities (PIPs) Table S22. Additionally, we report the median Cochran's Q for both PIPs and effect sizes between the ten European ancestry subsamples and the South Asian and African ancestry cohorts from the UK Biobank.

We compared the results of two fine-mapping methods, SuSie[65] and PESCA[72], when applied to SNP-level summary statistics in the European (UKB) and East Asian (BBJ) cohorts. SuSie is an iterative Bayesian stepwise selection method that identifies a credible set of SNPs that contribute to a phenotype of interest[65]. Using the effect sizes and standard errors generated from the standard GWA framework for each trait in each ancestry, we applied SuSiE in order to identify probable sets of causal SNPs. We then found the correlation between the posterior inclusion probabilities of each SNP in the European and East Asian cohorts.

Unlike SuSiE, the PESCA framework is explicitly designed for identifying shared SNP-level association signals between multiple ancestry cohorts versus ancestry-specific associations[72]. In addition to GWA summary statistics, PESCA uses information about the correlation structure between SNPs (i.e., LD) to identify SNPs that are likely to be causal in two cohorts of interest. Shi et al.[72] analyzed seven continuous traits in the European (UKB) and East Asian (BBJ) cohorts using PESCA and produced posterior probabilities that individual SNPs were: (*i*) associated with a phenotype in both the both cohorts, (*ii*) associated with the trait of interest only in the European cohort, or (*iii*) associated with the trait of interest only in the East Asian cohort. For each trait, we calculated the number of SNPs that were nominally significant (p-value $< 10^{-}5$, as in the original PESCA analysis) in the standard GWA framework in both the European and East Asian cohorts and had a PESCA posterior probability of being associated in both ancestries > 0.8 (see Table S18). We also found the number of SNPs that had a PESCA posterior probability of being associated in both ancestries > 0.8 that were only identified as significant in one ancestry using the GWA framework.

Finally, we explored the recent proposition of Mathieson[73] that the direction of effect for SNP-level summary statistics might be conserved among ancestry cohorts even if those variants are not genome-wide

significant in either cohort. To that end, for each of the 25 traits that we analyzed, we compared the direction of SNP effect sizes between the European and East Asian ancestry cohorts. We were only able to carry this analysis out for variants that were genotyped in both cohorts (Table S18). For each remaining nominally significant variant, we stored the direction of the effect size and checked the direction of effect size in the other ancestry. When zero was included within the range of the effect size plus or minus one standard deviation, we assumed the SNP did not have the same direction in both cohorts. We note that this test may be confounded by the precision of effect size estimation and warrants further exploration, including an analysis of local false sign discovery rates (see[74,75]).

Results: Fine-mapping methods have variable efficacy in identification of SNP level associations among ancestry cohorts

Often, replication of GWA results across cohorts is tested using genomic regions centered on a SNP. Scans across the region surrounding the SNP of interest are usually defined arbitrarily — using physical windows (or "clumps") to smooth over ascertainment bias and varying LD across cohorts or ancestries instead of using regions that are biologically annotated such as genes or transcriptional elements. While clumping presents an easy way to scan for regional replication of a given GWA finding, the corresponding results are not readily interpretable when prioritizing GWA results for downstream validation. We performed clumping using windows of size 1Mb centered around significant SNP-level associations (see Materials and Methods). Height had the largest proportion of windows that contain a SNP-level association that replicated in at least two ancestries (Figure S5B and Figure S5E). In the three traits with the greatest proportion of windows containing SNP-level replications — height (77.09% of clumps), urate (65.89%), and low density lipoprotein (54.40%) — we then recorded the number of genes and transcriptional elements within the window that contained GWA significant SNP-level associations. We found that for all three traits, the vast majority of 1Mb windows that were used to clump SNP-level associations contained multiple genes and transcriptional elements with significantly associated SNPs: height (94.04% of significant variants are within 1 Mb of two or more genes, 17.93 genes in clump (mean) $\pm$ 15.71 (standard deviation)), urate (97.47%, 18.44 $\pm$ 13.72), and low density lipoprotein (99.12%, 14.85 $\pm$ 12.89). Thus, we find window-based clumping does not easily produce biologically interpretable hypotheses for downstream validation.

Recent analyses of multi-ancestry GWA cohorts have also tested for effect size heterogeneity[64,65,69,76,77]. We applied the fine-mapping method SuSiE[65] to identify signals of effect size heterogeneity in the three ancestry cohorts for which we had access to raw genotype data (UK Biobank European ancestry, African ancestry, and South Asian ancestry individuals; see Table S1). We find little evidence of correlated SuSiE effect size estimates among ancestry cohorts, including among independent subsamples of the UK Biobank

European ancestry individuals Table S19 - Table S21. In addition, we applied PESCA (a method developed by Shi et al.[64]) to the results of our SNP-level analysis to understand how the modeling of LD to affected the power to identify probably causal SNPs shared in the European and East Asian ancestry cohorts. PESCA improves upon standard clumping approaches by modeling the LD in a region to identify SNPs that are likely to be causal for the same trait in multiple ancestries. In a comparison with the results from seven continuous traits analyzed in the original study[64], we found that the vast majority of SNPs identified by PESCA as causal (posterior probability > 0.8) in both ancestries were also nominally significant in our SNP-level association results (see Table S18). Both SuSiE[65] and PESCA[64] demonstrate the utility of modeling variation in LD structure among ancestries when conducting multi-ancestry GWA studies.

Recently, Mathieson[73] proposed the hypothesis that the direction of effect sizes is the same among ancestries, even when the effects are not genome-wide significant. To test this, we compared the direction of effect in SNPs that were significant in either the European or East Asian ancestry cohort to the direction of the effect in the other ancestry where the SNP was tested using the standard GWA framework. We limit the comparison to the European and East Asian cohorts due to their large sample sizes which increases the precision of effect size estimates. Table S18 shows the number of variants that were significantly associated with each trait in at least one of the European and East Asian ancestry cohorts, and also displays the number of those variants that have the same direction of effect as the significant variant in the other ancestry. In the 25 traits that we analyzed, the direction of effect was conserved in both the European and East Asian ancestry cohorts (between effect direction concordance from 55.87% and 76.56% of SNPs across 25 traits). The remaining SNPs where the direction of the effect size was not conserved represent those SNPs that: (*i*) had different direction of effect size, (*ii*) were not tested in both ancestry cohorts, or (*iii*) had effect size estimates within one standard error of zero (Table S18). The observed conservation of effect size direction in multiple ancestry cohorts, even when SNPs are non-significant in one or more cohorts, is a primary assumption of regional enrichment methods and supports Mathieson[73]'s hypothesis and findings. This suggests that regional enrichment methods, which are sensitive to shared patterns of effect size direction among cohorts, are a natural approach to apply to GWA summary statistics even in the absence of replication SNP-level GWA signals among cohorts. We ultimately acknowledge that a more in depth analysis of fine-mapping application to multi-ancestry genetic data is needed to make any conclusions. This precursory analysis using the SuSiE[54] and PESCA[64] highlights that there is widespread heterogeneity in direction of effect.

S0.2 Description of the gene-ε framework

A unique feature of gene-ε is that it treats SNPs with spuriously associated nonzero effects as non-associated. gene-ε assumes a reformulated null distribution of SNP-level effects $\tilde{\beta}_j \sim \mathcal{N}(0, \sigma^2_\varepsilon)$, where σ^2_ε is the SNP-

level null threshold and represents the maximum proportion of phenotypic variance explained (PVE) by a spurious or non-associated SNP. This leads to the reformulated SNP-level null hypothesis $H_0 : \mathbb{E}[\beta_j^2] \leq \sigma_\varepsilon^2$. To infer an appropriate σ_ε^2, gene-ε fits a K-mixture of normal distributions over the regularized effect sizes with successively smaller variances (i.e., $\sigma_1^2 > \cdots > \sigma_K^2 = 0$). In this study as in Cheng et al.[53], we assume that associated SNPs will appear in the first set, while spurious and non-associated SNPs appear in the latter sets. As a final step, gene-ε computes its gene-level association test statistic for the g-th gene by conformably partitioning the regularized GWA effect size estimates and computing the quadratic form $\tilde{Q}_g = \tilde{\boldsymbol{\beta}}_g^\intercal \tilde{\boldsymbol{\beta}}_g$. Corresponding p-values are then derived using Imhof's method. This assumes the common gene-level null $H_0 : Q_g = 0$, where the null distribution of Q_g is dependent upon the eigenvalues from the scaled LD matrix $\sigma_\varepsilon^2 \boldsymbol{\Sigma}$. For details on implementation, validation and performance comparison with simulations, and empirical application to UK Biobank white British individuals in six traits, see Cheng et al.[53].

S0.3 Regression with Summary Statistics (RSS) Enrichment.

Consider a GWA study with N individuals typed on P SNPs. For the j-th SNP, assume that we are given corresponding effect sizes $\widehat{\beta}_j$ and standard error $\widehat{s}_j$ via a single-SNP linear model fit using OLS. RSS then implements the following likelihood to model the GWA summary statistics[54]

$$\widehat{\boldsymbol{\beta}} \sim \mathcal{N}(\widehat{\mathbf{S}}\boldsymbol{\Sigma}\widehat{\mathbf{S}}^{-1}\boldsymbol{\beta}, \widehat{\mathbf{S}}\boldsymbol{\Sigma}\widehat{\mathbf{S}}) \tag{1}$$

where $\widehat{\mathbf{S}} = \text{diag}(\widehat{\mathbf{s}})$ is a $J \times J$ diagonal matrix of standard errors, $\boldsymbol{\Sigma}$ is again used to represent some empirical estimate of the LD matrix (i.e., using some external reference panel with ancestry matching the cohort of interest), and $\boldsymbol{\beta}$ are the true (unobserved) SNP-level effect sizes. To model gene-level enrichment, RSS assumes the following hierarchical prior structure on the true effect sizes

$$\beta_j \sim \pi_j \mathcal{N}(0, \sigma_\beta^2) + (1 - \pi_j)\, \delta_0, \tag{2}$$

$$\sigma_\beta^2 = h^2 \left(\sum_{j=1}^{J} \pi_j \, N^{-1} \widehat{s}_j^{-2} \right)^{-1}, \tag{3}$$

$$\pi_j = \left(1 + 10^{-(\theta_0 + a_j \theta)}\right)^{-1}, \tag{4}$$

where δ_0 is point mass centered at zero, h^2 denotes the narrow-sense heritability of the trait, a_j is an indicator detailing whether the j-th SNP is inside a particular gene, θ_0 is the background proportion of trait-associated SNPs, and θ reflects the increase in probability (on the $\log_{10}$-odds scale) when a SNP within a gene has non-zero effect. Here, the authors follow earlier works[78] and place independent uniform grid priors on the

hyper-parameters $\{h^2, \theta_0, \theta\}$. Note that, unlike other methods, RSS does not calculate a P-value for assessing gene-level association. Instead, RSS produces a posterior enrichment probability that at least one SNP in a given gene boundary is associated with the trait

$$P_g := 1 - \Pr\left[\beta_j = 0, \forall j \in \mathcal{J}_g \,|\, \mathbf{D}\right] \tag{5}$$

where $\mathbf{D}$ represents all of the input data including the GWA summary statistics $\{\widehat{\boldsymbol{\beta}}, \widehat{\mathbf{s}}\}$, the estimated LD matrix $\boldsymbol{\Sigma}$, and any applicable SNP annotations or weights $\mathbf{a} = (a_1, \ldots, a_J)$. See[54,79] for more details on preferred hyper-parameter settings. As noted in the main text, RSS is relies on a Markov chain Monte Carlo (MCMC) scheme for sampling posterior distributions and estimating model parameters. As a result, its algorithm can be subject to convergence issues if these (or the random seed) are not chosen properly.

S0.4 SNP-set (Sequence) Kernel Association Test (SKAT).

The implementation of SKAT required access to raw phenotype $\mathbf{y}$ and genotype $\mathbf{X}$ information for N individuals typed on J SNPs. To assess enrichment of the $|\mathcal{J}_g|$ variants within gene g, consider the linear model with sub-matrix $\mathbf{X}_g$

$$\mathbf{y} = \beta_0 + \mathbf{X}_g\boldsymbol{\beta}_g + \mathbf{e}, \qquad \mathbf{e} \sim \mathcal{N}(\mathbf{0}, \tau^2\mathbf{I}) \tag{6}$$

where β_0 is an intercept term, $\boldsymbol{\beta}_g = (\beta_1, \ldots, \beta_{|\mathcal{J}_g|})$ is a vector of regression coefficients for the SNPs within the gene of interest, and $\mathbf{e}$ is a normally distributed error term with mean zero and scaled variance τ^2. For model flexibility, gene-specific SNP effects β_j are assumed to follow an arbitrary distribution with mean zero and marginal variances $a_j\sigma_\beta^2$, where σ_β^2 is a variance component and a_j is a pre-specified weight for the j-th SNP. To this end, SKAT uses a variance component scoring approach and tests the null hypothesis $H_0 : \boldsymbol{\beta} = \mathbf{0}$, or equivalently $H_0 : \sigma_\beta^2 = 0$. The corresponding gene-level test statistic $\widehat{Q}_g$ then takes on the familiar quadratic form

$$\widehat{Q}_g = (\mathbf{y} - \widehat{\beta}_0)^\intercal \mathbf{K}_g (\mathbf{y} - \widehat{\beta}_0) \tag{7}$$

where $\widehat{\beta}_0$ is the predicted mean of trait under the null hypothesis, and is computed by projecting $\mathbf{y}$ onto the column space of the intercept (i.e., a vector of ones). The term $\mathbf{K}_g = \mathbf{X}_g\mathbf{A}_g\mathbf{A}_g\mathbf{X}_g^\intercal$ is commonly referred to as an $N \times N$ kernel matrix, where $\mathbf{A}_g = \text{diag}(a_1, \ldots, a_{|\mathcal{J}_g|})$ is used to denote a diagonal weight matrix that

changes for each gene g. Each element of $\mathbf{K}_g$ is computed via the linear kernel function

$$k(\mathbf{x}_i, \mathbf{x}_{i'}) = \sum_{j=1}^{|\mathcal{J}_g|} a_j x_{ij} x_{i'j}. \tag{8}$$

While implementing SKAT in this work, we follow previous works and set each weight to be $\sqrt{a_j} = \text{Beta}(\text{MAF}_j, 1, 25)$ — the beta distribution density function with pre-specified parameters evaluated at the sample minor allele frequency (MAF) for the j-th SNP in the gene region. For more details, see[55,80,82].

Clustering traits sharing a core set of associated genes using the WINGS algorithm

We used the WINGS algorithm[83] to identify clusters of traits sharing a core set of genes enriched for associated mutations. WINGS takes as input a gene (M) by trait (N) matrix and uses the Ward distance metric to find the distance among vectors of gene scores for different phenotypes; in this study, we used gene-ε gene-level association statistics as the input to WINGS. The more significantly associated genes that two traits share, the closer they will be in the gene-dimensional space. Applying WINGS to a matrix of gene scores for each ancestry separately, we examined whether the same traits clustered together, separately in each ancestry. We constructed matrices of gene-ε gene-level association statistics for the UK Biobank European, African, South Asian (from the UK Biobank) and East Asian (Biobank Japan) ancestry cohorts. Each of these matrices contained gene-level association statistics for all 25 quantitative traits of interest. The total number of genes and regulatory regions included were: European (23,603), African (23,575), South Asian(23,671), and East Asian (21,435). For the East Asian ancestry cohort, we limited the genes to the intersection of genes with gene-ε gene-level association statistics across all 25 traits. The number of gene scores calculated for each trait in the East Asian ancestry cohort varies due to the heterogeneity in imputed and genotype SNP arrays in the Biobank Japan studies (Table S5 and Table S16). Figure S21 shows the resulting dendrograms displaying prioritized phenotypes identified using the WINGS algorithm on each cohort's gene score matrix. The WINGS algorithm is designed to run on 25 phenotypes or more (see McGuirl et al.[83] for details), and we therefore did not apply the WINGS algorithm to the AIAN, Native Hawaiian, or Hispanic and Latin American cohorts as there was not data for enough phenotypes (Table S6, Table S10).

Analysis of GWAS Catalog Metadata and Previous GWA Publications

We cross-referenced our results from association testing at multiple genomic scales against previously published results in the GWAS catalog (`https://www.ebi.ac.uk/gwas/`) and in PubMed using the following processes.

In order to collect PubMed IDs (PMIDs) for publications associated with the UK Biobank, a two-part

data collection process was used. The first process was to directly search for publications with variations of the term "UK Biobank" (e.g., U.K. Biobank, United Kingdom Biobank) from PubMed using the Entrez Programming Utilities (E-Utilities) API. The E-Utilities API is the public API to the NCBI Entrez system and allows direct access to all Entrez databases including PubMed. Search queries were formulated by narrowing publications using year published and then further narrowing to those publications with variations of the search term "UK Biobank" in either the title or abstract. The open-source Python package Entrez (https://biopython.org/DIST/docs/api/Bio.Entrez-module.html) from the Biopython Project was used to facilitate interaction with the E-Utilities API.

The second data collection process was to gather information from publications listed directly on the UK Biobank website (https://www.ukbiobank.ac.uk/). Since the majority of publications on the website did not have an easily accessible PMID, identifying information including publication title and year was scraped and used to retrieve a publication's corresponding PMID (again using the E-Utilities API). The HTML/XML document parsing Python library Beautiful Soup (https://www.crummy.com/software/BeautifulSoup/bs4/doc/) was used to parse the HTML of the various UK Biobank webpages, and the Python Requests library (https://requests.readthedocs.io/en/master/) was used to programatically send HTTP calls to the server hosting the website. PMIDs were retrieved directly from the XML output of the E-Utilities API calls.

The PMIDs retrieved from both processes were aggregated into a single set of unique PMIDs, as some publications were identified by both processes. Publications that could not get associated PMIDs from the second data collection process were flagged for manual processing. The PMIDs that were retrieved from PubMed directly but could not be found based on the publication information provided on the UK Biobank website were noted. Conversely, the PMIDs that could be retrieved from publication information found on the UK Biobank website but not directly from PubMed were also noted.

Using the compiled list of PMIDs, analyses of the UK Biobank data set reported in the GWAS catalog association data were compiled. Previous genotype-to-phenotype association data and sample ancestry descriptions were downloaded from https://www.ebi.ac.uk/gwas/docs/file-downloads. Unique genotype-to-phenotype associations were parsed using a set of custom python scripts. All scripts used in the curation of PMIDs, parsing of GWAS catalog summary data, and determination of previously published genotype-to-phenotype associations from UK Biobank studies are available on GitHub (https://github.com/ramachandran-lab/redefining_replication).

Simulation design to test the power and false discovery rate of GWA and gene-level association analyses

Simulations of a single population

In our simulation studies, we used the following general simulation scheme to generate quantitative traits using real genotype data on chromosome 1 from N randomly sampled individuals of European ancestry in the UK Biobank. This pipeline follows from previous studies[53,84]. We will use $\mathbf{X}$ to denote the $N \times J$ genotype matrix, with J denoting the number of single nucleotide polymorphisms (SNPs) encoded as $0, 1, 2$ copies of a reference allele at each locus and $\mathbf{x}_j$ representing the genotypic vector for the j-th SNP. Following quality control procedures detailed in the Supplemental Information, our simulations included J = 36,518 SNPs distributed across genome. We used the NCBI's RefSeq database in the UCSC Genome Browser to assign SNPs to genes which resulted in G = 1,408 genes in the simulation studies.

After the annotation step, we simulated phenotypes by first assuming that the total phenotypic variance $\mathbb{V}[\mathbf{y}] = 1$, and that all observed genetic effects explained a fixed proportion of this value (i.e., narrow-sense heritability, h^2). Next, we randomly selected a certain percentage of genes to be enriched fotr associations and denoted the sets of SNPs that they contained as $\mathcal{C}$. Within $\mathcal{C}$, we selected causal SNPs in a way such that each associated gene at least contains one SNP with non-zero effect size. Quantitative continuous traits were then generated under the following two general linear models:

- Standard Model: $\mathbf{y} = \sum_{c \in \mathcal{C}} \mathbf{x}_c \beta_c + \mathbf{e}$
- Population Structure Model: $\mathbf{y} = \mathbf{W}\mathbf{b} + \sum_{c \in \mathcal{C}} \mathbf{x}_c \beta_c + \mathbf{e}$

where $\mathbf{y}$ is an N-dimensional vector containing all the phenotype states; $\mathbf{x}_c$ is the genotype for the c-th causal SNP; β_c is the additive effect size for the c-th SNP; and $\mathbf{e} \sim \mathcal{N}(0, \tau^2\mathbf{I})$ is an N-dimensional vector of normally distributed environmental noise. Additionally, in the model with population structure, $\mathbf{W}$ is an $N \times M$ matrix of the top $M = 10$ principal components (PCs) from the genotype matrix and represents additional population structure with corresponding fixed effects $\mathbf{b}$. The effect sizes of SNPs in genes enriched for associations are randomly drawn from standard normal distributions and then rescaled so they explain a fixed proportion of the narrow-sense heritability $\mathbb{V}[\sum \mathbf{x}_c \beta_c] = h^2$. The coefficients for the genotype PCs are also drawn from standard normal distributions and rescaled such that $\mathbb{V}[\mathbf{W}\mathbf{b}] = 10\%$ of the total phenotypic variance, with the variance of all non-genetic effects contributing $\mathbb{V}[\mathbf{W}\mathbf{b}] + \mathbb{V}[\mathbf{e}] = (1 - h^2)$. For any simulations conducted under the population structure model, genotype PCs are not included in any of the model fitting procedures, and no other preprocessing normalizations were carried out to account for the additional population structure. More specifically, GWA summary statistics are then computed by fitting a

single-SNP univariate linear model via ordinary least squares (OLS):

$$\widehat{\beta}_j = (\mathbf{x}_j^\intercal \mathbf{x}_j)^{-1} \mathbf{x}_j^\intercal \mathbf{y}; \tag{9}$$

for every SNP in the data $j = 1, \ldots J$. These OLS effect size estimates, along with an empirically LD matrix $\mathbf{\Sigma}$ computed directly from the full $N \times J$ genotype matrix $\mathbf{X}$, are given to gene-ε. We also retain standard errors and p-values for the implementation of competing methods: RSS[54], SKAT[55], and the standard GWA SNP-level association test. Given the simulation procedure above, we simulate a wide range of scenarios for comparing the performance of gene-level association approaches by varying the following parameters:

- Number of individuals: N = 5,000 and 10,000;
- Narrow-sense heritability: $h^2 = 0.2$ and 0.6;
- Percentage of enriched genes: 1% (sparse) and 10% (polygenic);

Furthermore, we set the number of causal SNPs with non-zero effects to be some fixed percentage of all SNPs located within the designated genes enriched for associations. We set this percentage to be 0.125% in the 1% associated SNP-set case, and 3% in the 10% associated SNP-set case. All performance comparisons are based on 100 different simulated runs for each parameter combination. Lastly, for each simulated dataset, we also selected some number of intergenic SNPs (i.e., SNPs not mapped to any gene) to have non-zero effect sizes. This was done to mimic genetic associations in unannotated regulatory elements. Specifically, five randomly selected intergenic SNPs were given non-zero contributions to the trait heritability in the 1% enriched genes case, and 30 intergenic SNPs were selected in the 10% enriched genes case.

All performance comparisons are based on 100 different simulated runs for each parameter combination. We computed gene-level p-values for gene-ε, SKAT, and the single-SNP GWAS. For evaluating the performance of RSS, we compute posterior enrichment probabilities. For all approaches, we assessed the power and false discovery rates when identifying enriched genes at either a Bonferroni-corrected threshold ($p = 0.05/1,408$ genes $= 3.55 \times 10^{-5}$) or according to the median probability model (posterior enrichment probability > 0.5)[85]. Figure S6 and Figure S7 show the mean performances (and standard errors) across all simulated replicates. Figure S8 illustrates that both GWAS and gene-ε are limited by the sample size of the cohort of interest. Specifically, when the sample size is set to 2,000 individuals power is low and false discovery rates are high for both the standard GWA framework and gene-ε.

Simulations of genetic trait architecture in two populations

We used the African (UKB) cohort and a subset of the European cohort and simulation studies to test the ability of GWAS and gene-ε to detect shared causal SNPs (in the case of gene-ε, genes containing causal SNPs) in a multi-ancestry study. Using the same simulation protocol as that described for testing power of different enrichment analysis methods, described in *Simulations in a single population*, we labeled all genes containing at least one causal SNP as "causal". We first determined the power of gene-ε to identify SNPs or genes that are causal in each cohort under a variety of genomic architectures. The total amount of variance explained in the phenotype by the causal SNPs (i.e. the narrow-sense heritability) to be equal to 0.2 or 0.6. In each of these contexts, the sparsity of causal variants as a function of the total number of variants was set to either 0.1 or 0.5. These values of causal SNP sparsity were selected in order to ensure that an ample number of SNPs were associated with the phenotype in both cohorts. Finally, the overlap in causal SNPs between the two cohorts was tested at proportions equal to 0 (no overlap in causal between SNPs cohorts) 0.25, 0.5, and 1 (complete overlap in causal SNPs between cohorts). For each of these parameter sets, 50 replicate simulations were performed of two cohorts derived from 10,000 European individuals and 4,967 African individuals, respectively. We summarize the performance of the standard GWA framework and gene-ε across the parameter space. Generally, gene-ε performs better on the European cohort than it does in the African cohort, but is better powered in the African cohort when the causal SNPs are the same in both cohorts (Figure S9 and Figure S10). Additionally, gene-ε performs better when identifying causal genes that are shared between the two cohorts - particularly when traits have high heritability Figure S11 - Figure S12.

References

[1] Terhi Kettunen, Carita Eklund, Mika Kähönen, Antti Jula, Hannu Päivä, Leo-Pekka Lyytikäinen, Mikko Hurme, and Terho Lehtimäki. Polymorphism in the c-reactive protein (crp) gene affects crp levels in plasma and one early marker of atherosclerosis in men: The health 2000 survey. Scandinavian journal of clinical and laboratory investigation, 71(5):353–361, 2011.

[2] Amy Z Fan, Ajay Yesupriya, Man-huei Chang, Meaghan House, Jing Fang, Renée Ned, Donald Hayes, Nicole F Dowling, and Ali H Mokdad. Gene polymorphisms in association with emerging cardiovascular risk markers in adult women. BMC medical genetics, 11(1):6, 2010.

[3] E Komurcu-Bayrak, N Erginel-Unaltuna, A Onat, B Ozsait, C Eklund, M Hurme, N Mononen, R Laak-

sonen, G Hergenc, and T Lehtimäki. Association of c-reactive protein (crp) gene allelic variants with serum crp levels and hypertension in turkish adults. Atherosclerosis, 206(2):474–479, 2009.

[4] AJ Szalai, J Wu, EM Lange, MA McCrory, CD Langefeld, A Williams, SO Zakharkin, Varghese George, DB Allison, GS Cooper, et al. Single-nucleotide polymorphisms in the c-reactive protein (crp) gene promoter that affect transcription factor binding, alter transcriptional activity, and associate with differences in baseline serum crp level. Journal of Molecular Medicine, 83(6):440–447, 2005.

[5] Shi-Chao Zhang, Ming-Yu Wang, Jun-Rui Feng, Yue Chang, Shang-Rong Ji, and Yi Wu. Reversible promoter methylation determines fluctuating expression of acute phase proteins. Elife, 9:e51317, 2020.

[6] S-N Chang, C-T Tsai, C-K Wu, J-K Lee, L-P Lai, S-W Huang, L-Y Huang, C-D Tseng, J-L Lin, F-T Chiang, et al. A functional variant in the promoter region regulates the c-reactive protein gene and is a potential candidate for increased risk of atrial fibrillation. Journal of internal medicine, 272(3):305–315, 2012.

[7] Hyoun-Ah Kim, Hye-Young Chun, Seung-Hyun Kim, Hae-Sim Park, and Chang-Hee Suh. C-reactive protein gene polymorphisms in disease susceptibility and clinical manifestations of korean systemic lupus erythematosus. The Journal of rheumatology, 36(10):2238–2243, 2009.

[8] Abbas Dehghan, Josée Dupuis, Maja Barbalic, Joshua C Bis, Gudny Eiriksdottir, Chen Lu, Niina Pellikka, Henri Wallaschofski, Johannes Kettunen, Peter Henneman, et al. Meta-analysis of genome-wide association studies in¿ 80 000 subjects identifies multiple loci for c-reactive protein levels. Circulation, 123(7):731–738, 2011.

[9] Paul M Ridker, Guillaume Pare, Alex Parker, Robert YL Zee, Jacqueline S Danik, Julie E Buring, David Kwiatkowski, Nancy R Cook, Joseph P Miletich, and Daniel I Chasman. Loci related to metabolic-syndrome pathways including lepr, hnf1a, il6r, and gckr associate with plasma c-reactive protein: the women's genome health study. The American Journal of Human Genetics, 82(5):1185–1192, 2008.

[10] Symen Ligthart, Ahmad Vaez, Urmo Võsa, Maria G Stathopoulou, Paul S De Vries, Bram P Prins, Peter J Van der Most, Toshiko Tanaka, Elnaz Naderi, Lynda M Rose, et al. Genome analyses of¿ 200,000 individuals identify 58 loci for chronic inflammation and highlight pathways that link inflammation and complex disorders. The American Journal of Human Genetics, 103(5):691–706, 2018.

[11] Alex P Reiner, Sandra Beleza, Nora Franceschini, Paul L Auer, Jennifer G Robinson, Charles Kooperberg, Ulrike Peters, and Hua Tang. Genome-wide association and population genetic analysis of c-

reactive protein in african american and hispanic american women. The American Journal of Human Genetics, 91(3):502–512, 2012.

[12] Paul Elliott, John C Chambers, Weihua Zhang, Robert Clarke, Jemma C Hopewell, John F Peden, Jeanette Erdmann, Peter Braund, James C Engert, Derrick Bennett, et al. Genetic loci associated with c-reactive protein levels and risk of coronary heart disease. Jama, 302(1):37–48, 2009.

[13] Deog Kyeom Kim, Michael H Cho, Craig P Hersh, David A Lomas, Bruce E Miller, Xiangyang Kong, Per Bakke, Amund Gulsvik, Alvar Agustí, Emiel Wouters, et al. Genome-wide association analysis of blood biomarkers in chronic obstructive pulmonary disease. American journal of respiratory and critical care medicine, 186(12):1238–1247, 2012.

[14] William J Astle, Heather Elding, Tao Jiang, Dave Allen, Dace Ruklisa, Alice L Mann, Daniel Mead, Heleen Bouman, Fernando Riveros-Mckay, Myrto A Kostadima, et al. The allelic landscape of human blood cell trait variation and links to common complex disease. Cell, 167(5):1415–1429, 2016.

[15] Juraj Sokol, Kamil Biringer, Maria Skerenova, Miroslav Hasko, Lenka Bartosova, Jan Stasko, Jan Danko, and Peter Kubisz. Platelet aggregation abnormalities in patients with fetal losses: the gp6 gene polymorphism. Fertility and sterility, 98(5):1170–1174, 2012.

[16] Andrew D Johnson, Lisa R Yanek, Ming-Huei Chen, Nauder Faraday, Martin G Larson, Geoffrey Tofler, Shiow J Lin, Aldi T Kraja, Michael A Province, Qiong Yang, et al. Genome-wide meta-analyses identifies seven loci associated with platelet aggregation in response to agonists. Nature genetics, 42(7):608–613, 2010.

[17] Takao Shimizu. Lipid mediators in health and disease: enzymes and receptors as therapeutic targets for the regulation of immunity and inflammation. Annual review of pharmacology and toxicology, 49: 123–150, 2009.

[18] Yuji Shimizu, Kazuhiko Arima, Yuko Noguchi, Shin-Ya Kawashiri, Hirotomo Yamanashi, Mami Tamai, Yasuhiro Nagata, and Takahiro Maeda. Potential mechanisms underlying the association between single nucleotide polymorphism (brap and aldh2) and hypertension among elderly japanese population. Scientific Reports, 10(1):1–9, 2020.

[19] John D Eicher, Nathalie Chami, Tim Kacprowski, Akihiro Nomura, Ming-Huei Chen, Lisa R Yanek, Salman M Tajuddin, Ursula M Schick, Andrew J Slater, Nathan Pankratz, et al. Platelet-related variants identified by exomechip meta-analysis in 157,293 individuals. The American Journal of Human Genetics, 99(1):40–55, 2016.

[20] Rehan Qayyum, Beverly M Snively, Elad Ziv, Michael A Nalls, Yongmei Liu, Weihong Tang, Lisa R Yanek, Leslie Lange, Michele K Evans, Santhi Ganesh, et al. A meta-analysis and genome-wide association study of platelet count and mean platelet volume in african americans. PLoS Genet, 8(3):e1002491, 2012.

[21] Raymond Noordam, Maxime M Bos, Heming Wang, Thomas W Winkler, Amy R Bentley, Tuomas O Kilpeläinen, Paul S de Vries, Yun Ju Sung, Karen Schwander, Brian E Cade, et al. Multi-ancestry sleep-by-snp interaction analysis in 126,926 individuals reveals lipid loci stratified by sleep duration. Nature communications, 10(1):1–13, 2019.

[22] Tom G Richardson, Eleanor Sanderson, Tom M Palmer, Mika Ala-Korpela, Brian A Ference, George Davey Smith, and Michael V Holmes. Evaluating the relationship between circulating lipoprotein lipids and apolipoproteins with risk of coronary heart disease: A multivariable mendelian randomisation analysis. PLoS medicine, 17(3):e1003062, 2020.

[23] Alexander M Kulminski, Jian Huang, Yury Loika, Konstantin G Arbeev, Olivia Bagley, Arseniy Yashkin, Matt Duan, and Irina Culminskaya. Strong impact of natural-selection–free heterogeneity in genetics of age-related phenotypes. Aging (Albany NY), 10(3):492, 2018.

[24] Thomas J Hoffmann, Elizabeth Theusch, Tanushree Haldar, Dilrini K Ranatunga, Eric Jorgenson, Marisa W Medina, Mark N Kvale, Pui-Yan Kwok, Catherine Schaefer, Ronald M Krauss, et al. A large electronic-health-record-based genome-wide study of serum lipids. Nature genetics, 50(3):401–413, 2018.

[25] Aldi T Kraja, Dhananjay Vaidya, James S Pankow, Mark O Goodarzi, Themistocles L Assimes, Iftikhar J Kullo, Ulla Sovio, Rasika A Mathias, Yan V Sun, Nora Franceschini, et al. A bivariate genome-wide approach to metabolic syndrome: Stampeed consortium. Diabetes, 60(4):1329–1339, 2011.

[26] Cassandra N Spracklen, Peng Chen, Young Jin Kim, Xu Wang, Hui Cai, Shengxu Li, Jirong Long, Ying Wu, Ya Xing Wang, Fumihiko Takeuchi, et al. Association analyses of east asian individuals and trans-ancestry analyses with european individuals reveal new loci associated with cholesterol and triglyceride levels. Human molecular genetics, 26(9):1770–1784, 2017.

[27] Makoto Kurano, Kazuhisa Tsukamoto, Shigeo Kamitsuji, Naoyuki Kamatani, Masumi Hara, Toshio Ishikawa, Bong-Jo Kim, Sanghoon Moon, Young Jin Kim, and Tamio Teramoto. Genome-wide association study of serum lipids confirms previously reported associations as well as new associations of common snps within pcsk7 gene with triglyceride. Journal of human genetics, 61(5):427–433, 2016.

[28] Paul S De Vries, Michael R Brown, Amy R Bentley, Yun J Sung, Thomas W Winkler, Ioanna Ntalla, Karen Schwander, Aldi T Kraja, Xiuqing Guo, Nora Franceschini, et al. Multiancestry genome-wide association study of lipid levels incorporating gene-alcohol interactions. American journal of epidemiology, 188(6):1033–1054, 2019.

[29] Amy R Bentley, Yun J Sung, Michael R Brown, Thomas W Winkler, Aldi T Kraja, Ioanna Ntalla, Karen Schwander, Daniel I Chasman, Elise Lim, Xuan Deng, et al. Multi-ancestry genome-wide gene–smoking interaction study of 387,272 individuals identifies new loci associated with serum lipids. Nature genetics, 51(4):636–648, 2019.

[30] Ida Surakka, Momoko Horikoshi, Reedik Mägi, Antti-Pekka Sarin, Anubha Mahajan, Vasiliki Lagou, Letizia Marullo, Teresa Ferreira, Benjamin Miraglio, Sanna Timonen, et al. The impact of low-frequency and rare variants on lipid levels. Nature genetics, 47(6):589–597, 2015.

[31] Tanya M Teslovich, Kiran Musunuru, Albert V Smith, Andrew C Edmondson, Ioannis M Stylianou, Masahiro Koseki, James P Pirruccello, Samuli Ripatti, Daniel I Chasman, Cristen J Willer, et al. Biological, clinical and population relevance of 95 loci for blood lipids. Nature, 466(7307):707–713, 2010.

[32] Cristen J Willer, Ellen M Schmidt, Sebanti Sengupta, Gina M Peloso, Stefan Gustafsson, Stavroula Kanoni, Andrea Ganna, Jin Chen, Martin L Buchkovich, Samia Mora, et al. Discovery and refinement of loci associated with lipid levels. Nature genetics, 45(11):1274, 2013.

[33] Rita PS Middelberg, Manuel AR Ferreira, Anjali K Henders, Andrew C Heath, Pamela AF Madden, Grant W Montgomery, Nicholas G Martin, and John B Whitfield. Genetic variants in lpl, oasl and tomm40/apoe-c1-c2-c4 genes are associated with multiple cardiovascular-related traits. BMC medical genetics, 12(1):123, 2011.

[34] Sekar Kathiresan, Olle Melander, Candace Guiducci, Aarti Surti, Noël P Burtt, Mark J Rieder, Gregory M Cooper, Charlotta Roos, Benjamin F Voight, Aki S Havulinna, et al. Six new loci associated with blood low-density lipoprotein cholesterol, high-density lipoprotein cholesterol or triglycerides in humans. Nature genetics, 40(2):189–197, 2008.

[35] Jaspal S Kooner, John C Chambers, Carlos A Aguilar-Salinas, David A Hinds, Craig L Hyde, Gregory R Warnes, Francisco J Gómez Pérez, Kelly A Frazer, Paul Elliott, James Scott, et al. Genome-wide scan identifies variation in mlxipl associated with plasma triglycerides. Nature genetics, 40(2):149, 2008.

[36] Sekar Kathiresan, Cristen J Willer, Gina M Peloso, Serkalem Demissie, Kiran Musunuru, Eric E Schadt, Lee Kaplan, Derrick Bennett, Yun Li, Toshiko Tanaka, et al. Common variants at 30 loci contribute to polygenic dyslipidemia. Nature genetics, 41(1):56–65, 2009.

[37] Maria Keller, Dorit Schleinitz, Julia Förster, Anke Tönjes, Yvonne Böttcher, Antje Fischer-Rosinsky, Jana Breitfeld, Kerstin Weidle, Nigel W Rayner, Ralph Burkhardt, et al. Thoc5: a novel gene involved in hdl-cholesterol metabolism. Journal of lipid research, 54(11):3170–3176, 2013.

[38] Richa Saxena, Benjamin F Voight, Valeriya Lyssenko, Noël P Burtt, Paul IW de Bakker, Hong Chen, Jeffrey J Roix, Sekar Kathiresan, Joel N Hirschhorn, Mark J Daly, et al. Genome-wide association analysis identifies loci for type 2 diabetes and triglyceride levels. Science, 316(5829):1331–1336, 2007.

[39] Yurii S Aulchenko, Samuli Ripatti, Ida Lindqvist, Dorret Boomsma, Iris M Heid, Peter P Pramstaller, Brenda WJH Penninx, A Cecile JW Janssens, James F Wilson, Tim Spector, et al. Loci influencing lipid levels and coronary heart disease risk in 16 european population cohorts. Nature genetics, 41(1): 47, 2009.

[40] Rubina Tabassum, Joel T Rämö, Pietari Ripatti, Jukka T Koskela, Mitja Kurki, Juha Karjalainen, Priit Palta, Shabbeer Hassan, Javier Nunez-Fontarnau, Tuomo TJ Kiiskinen, et al. Genetic architecture of human plasma lipidome and its link to cardiovascular disease. Nature communications, 10(1):1–14, 2019.

[41] Liang He, Yelena Kernogitski, Irina Kulminskaya, Yury Loika, Konstantin G Arbeev, Elena Loiko, Olivia Bagley, Matt Duan, Arseniy Yashkin, Svetlana V Ukraintseva, et al. Pleiotropic meta-analyses of longitudinal studies discover novel genetic variants associated with age-related diseases. Frontiers in genetics, 7:179, 2016.

[42] Derek Klarin, Scott M Damrauer, Kelly Cho, Yan V Sun, Tanya M Teslovich, Jacqueline Honerlaw, David R Gagnon, Scott L DuVall, Jin Li, Gina M Peloso, et al. Genetics of blood lipids among˜ 300,000 multi-ethnic participants of the million veteran program. Nature genetics, 50(11):1514–1523, 2018.

[43] Dawn M Waterworth, Sally L Ricketts, Kijoung Song, Li Chen, Jing Hua Zhao, Samuli Ripatti, Yurii S Aulchenko, Weihua Zhang, Xin Yuan, Noha Lim, et al. Genetic variants influencing circulating lipid levels and risk of coronary artery disease. Arteriosclerosis, thrombosis, and vascular biology, 30(11): 2264–2276, 2010.

[44] Gina M Peloso, Paul L Auer, Joshua C Bis, Arend Voorman, Alanna C Morrison, Nathan O Stitziel, Jennifer A Brody, Sumeet A Khetarpal, Jacy R Crosby, Myriam Fornage, et al. Association of low-

frequency and rare coding-sequence variants with blood lipids and coronary heart disease in 56,000 whites and blacks. The American Journal of Human Genetics, 94(2):223–232, 2014.

[45] Tuomas O Kilpeläinen, Amy R Bentley, Raymond Noordam, Yun Ju Sung, Karen Schwander, Thomas W Winkler, Hermina Jakupović, Daniel I Chasman, Alisa Manning, Ioanna Ntalla, et al. Multi-ancestry study of blood lipid levels identifies four loci interacting with physical activity. Nature communications, 10(1):1–11, 2019.

[46] Yoichiro Kamatani, Koichi Matsuda, Yukinori Okada, Michiaki Kubo, Naoya Hosono, Yataro Daigo, Yusuke Nakamura, and Naoyuki Kamatani. Genome-wide association study of hematological and biochemical traits in a japanese population. Nature genetics, 42(3):210, 2010.

[47] Marc A Coram, Qing Duan, Thomas J Hoffmann, Timothy Thornton, Joshua W Knowles, Nicholas A Johnson, Heather M Ochs-Balcom, Timothy A Donlon, Lisa W Martin, Charles B Eaton, et al. Genome-wide characterization of shared and distinct genetic components that influence blood lipid levels in ethnically diverse human populations. The American Journal of Human Genetics, 92(6):904–916, 2013.

[48] Deepti Gurdasani, Tommy Carstensen, Segun Fatumo, Guanjie Chen, Chris S Franklin, Javier Prado-Martinez, Heleen Bouman, Federico Abascal, Marc Haber, Ioanna Tachmazidou, et al. Uganda genome resource enables insights into population history and genomic discovery in africa. Cell, 179(4):984–1002, 2019.

[49] Elisabeth M van Leeuwen, Aniko Sabo, Joshua C Bis, Jennifer E Huffman, Ani Manichaikul, Albert V Smith, Mary F Feitosa, Serkalem Demissie, Peter K Joshi, Qing Duan, et al. Meta-analysis of 49 549 individuals imputed with the 1000 genomes project reveals an exonic damaging variant in angptl4 determining fasting tg levels. Journal of medical genetics, 53(7):441–449, 2016.

[50] Matthew A Reyna, Mark DM Leiserson, and Benjamin J Raphael. Hierarchical hotnet: identifying hierarchies of altered subnetworks. Bioinformatics, 34(17):i972–i980, 2018.

[51] Christoph Heiring, Björn Dahlbäck, and Yves A Muller. Ligand recognition and homophilic interactions in tyro3 structural insights into the axl/tyro3 receptor tyrosine kinase family. Journal of Biological Chemistry, 279(8):6952–6958, 2004.

[52] Alice B Popejoy and Stephanie M Fullerton. Genomics is failing on diversity. Nature News, 538(7624): 161, 2016.

[53] Wei Cheng, Sohini Ramachandran, and Lorin Crawford. Estimation of non-null snp effect size distributions enables the detection of enriched genes underlying complex traits. PLoS genetics, 16(6):e1008855, 2020.

[54] Xiang Zhu and Matthew Stephens. Bayesian large-scale multiple regression with summary statistics from genome-wide association studies. The annals of applied statistics, 11(3):1561, 2017.

[55] Michael C Wu, Seunggeun Lee, Tianxi Cai, Yun Li, Michael Boehnke, and Xihong Lin. Rare-variant association testing for sequencing data with the sequence kernel association test. The American Journal of Human Genetics, 89(1):82–93, 2011.

[56] Jake R Conway, Alexander Lex, and Nils Gehlenborg. Upsetr: an r package for the visualization of intersecting sets and their properties. Bioinformatics, 33(18):2938–2940, 2017.

[57] Antonio Fabregat, Konstantinos Sidiropoulos, Phani Garapati, Marc Gillespie, Kerstin Hausmann, Robin Haw, Bijay Jassal, Steven Jupe, Florian Korninger, Sheldon McKay, et al. The reactome pathway knowledgebase. Nucleic acids research, 44(D1):D481–D487, 2016.

[58] Sabry Razick, George Magklaras, and Ian M Donaldson. irefindex: a consolidated protein interaction database with provenance. BMC bioinformatics, 9(1):405, 2008.

[59] Masahiro Kanai, Masato Akiyama, Atsushi Takahashi, Nana Matoba, Yukihide Momozawa, Masashi Ikeda, Nakao Iwata, Shiro Ikegawa, Makoto Hirata, Koichi Matsuda, et al. Genetic analysis of quantitative traits in the japanese population links cell types to complex human diseases. Nature genetics, 50 (3):390–400, 2018.

[60] Masato Akiyama, Yukinori Okada, Masahiro Kanai, Atsushi Takahashi, Yukihide Momozawa, Masashi Ikeda, Nakao Iwata, Shiro Ikegawa, Makoto Hirata, Koichi Matsuda, et al. Genome-wide association study identifies 112 new loci for body mass index in the japanese population. Nature genetics, 49(10): 1458, 2017.

[61] Masato Akiyama, Kazuyoshi Ishigaki, Saori Sakaue, Yukihide Momozawa, Momoko Horikoshi, Makoto Hirata, Koichi Matsuda, Shiro Ikegawa, Atsushi Takahashi, Masahiro Kanai, et al. Characterizing rare and low-frequency height-associated variants in the japanese population. Nature communications, 10 (1):1–11, 2019.

[62] Alexander Gusev, Arthur Ko, Huwenbo Shi, Gaurav Bhatia, Wonil Chung, Brenda WJH Penninx, Rick Jansen, Eco JC De Geus, Dorret I Boomsma, Fred A Wright, et al. Integrative approaches for large-scale transcriptome-wide association studies. Nature genetics, 48(3):245, 2016.

[63] Pak C Sham and Shaun M Purcell. Statistical power and significance testing in large-scale genetic studies. Nature Reviews Genetics, 15(5):335–346, 2014.

[64] Huwenbo Shi, Kathryn S Burch, Ruth Johnson, Malika K Freund, Gleb Kichaev, Nicholas Mancuso, Astrid M Manuel, Natalie Dong, and Bogdan Pasaniuc. Localizing components of shared transethnic genetic architecture of complex traits from gwas summary data. The American Journal of Human Genetics, 106(6):805–817, 2020.

[65] Gao Wang, Abhishek Sarkar, Peter Carbonetto, and Matthew Stephens. A simple new approach to variable selection in regression, with application to genetic fine mapping. Journal of the Royal Statistical Society: Series B (Statistical Methodology), 82(5):1273–1300, 2020.

[66] David H Alexander, John Novembre, and Kenneth Lange. Fast model-based estimation of ancestry in unrelated individuals. Genome research, 19(9):1655–1664, 2009.

[67] Christopher C Chang, Carson C Chow, Laurent CAM Tellier, Shashaank Vattikuti, Shaun M Purcell, and James J Lee. Second-generation plink: rising to the challenge of larger and richer datasets. Gigascience, 4(1):s13742–015, 2015.

[68] Akiko Nagai, Makoto Hirata, Yoichiro Kamatani, Kaori Muto, Koichi Matsuda, Yutaka Kiyohara, Toshiharu Ninomiya, Akiko Tamakoshi, Zentaro Yamagata, Taisei Mushiroda, et al. Overview of the biobank japan project: study design and profile. Journal of epidemiology, 27(Supplement_III):S2–S8, 2017.

[69] Genevieve L Wojcik, Mariaelisa Graff, Katherine K Nishimura, Ran Tao, Jeffrey Haessler, Christopher R Gignoux, Heather M Highland, Yesha M Patel, Elena P Sorokin, Christy L Avery, et al. Genetic analyses of diverse populations improves discovery for complex traits. Nature, 570(7762):514–518, 2019.

[70] Peter H Sudmant, Tobias Rausch, Eugene J Gardner, Robert E Handsaker, Alexej Abyzov, John Huddleston, Yan Zhang, Kai Ye, Goo Jun, Markus Hsi-Yang Fritz, et al. An integrated map of structural variation in 2,504 human genomes. Nature, 526(7571):75–81, 2015.

[71] Anders Bergström, Shane A McCarthy, Ruoyun Hui, Mohamed A Almarri, Qasim Ayub, Petr Danecek, Yuan Chen, Sabine Felkel, Pille Hallast, Jack Kamm, et al. Insights into human genetic variation and population history from 929 diverse genomes. Science, 367(6484), 2020.

[72] Huwenbo Shi, Steven Gazal, Masahiro Kanai, Evan M Koch, Armin P Schoech, Katherine M Siewert, Samuel S Kim, Yang Luo, Tiffany Amariuta, Hailiang Huang, et al. Population-specific causal disease

effect sizes in functionally important regions impacted by selection. Nature Communications, 12(1): 1–15, 2021.

[73] Iain Mathieson. The omnigenic model and polygenic prediction of complex traits. The American Journal of Human Genetics, 2021.

[74] Matthew Stephens. False discovery rates: a new deal. Biostatistics, 18(2):275–294, 2017.

[75] Sarah M Urbut, Gao Wang, Peter Carbonetto, and Matthew Stephens. Flexible statistical methods for estimating and testing effects in genomic studies with multiple conditions. Nature genetics, 51(1): 187–195, 2019.

[76] Farhad Hormozdiari, Emrah Kostem, Eun Yong Kang, Bogdan Pasaniuc, and Eleazar Eskin. Identifying causal variants at loci with multiple signals of association. Genetics, 198(2):497–508, 2014.

[77] Alicia R Martin, Meng Lin, Julie M Granka, Justin W Myrick, Xiaomin Liu, Alexandra Sockell, Elizabeth G Atkinson, Cedric J Werely, Marlo Möller, Manjinder S Sandhu, et al. An unexpectedly complex architecture for skin pigmentation in africans. Cell, 171(6):1340–1353, 2017.

[78] Peter Carbonetto and Matthew Stephens. Integrated enrichment analysis of variants and pathways in genome-wide association studies indicates central role for il-2 signaling genes in type 1 diabetes, and cytokine signaling genes in crohn's disease. PLoS genetics, 9(10):e1003770, 2013.

[79] Xiang Zhu and Matthew Stephens. Large-scale genome-wide enrichment analyses identify new trait-associated genes and pathways across 31 human phenotypes. Nature communications, 9(1):1–14, 2018.

[80] Michael C Wu, Peter Kraft, Michael P Epstein, Deanne M Taylor, Stephen J Chanock, David J Hunter, and Xihong Lin. Powerful snp-set analysis for case-control genome-wide association studies. The American Journal of Human Genetics, 86(6):929–942, 2010.

[81] Seunggeun Lee, Mary J Emond, Michael J Bamshad, Kathleen C Barnes, Mark J Rieder, Deborah A Nickerson, ESP Lung Project Team, David C Christiani, Mark M Wurfel, Xihong Lin, et al. Optimal unified approach for rare-variant association testing with application to small-sample case-control whole-exome sequencing studies. The American Journal of Human Genetics, 91(2):224–237, 2012.

[82] Iuliana Ionita-Laza, Seunggeun Lee, Vlad Makarov, Joseph D Buxbaum, and Xihong Lin. Sequence kernel association tests for the combined effect of rare and common variants. The American Journal of Human Genetics, 92(6):841–853, 2013.

[83] Melissa R McGuirl, Samuel Pattillo Smith, Björn Sandstede, and Sohini Ramachandran. Detecting shared genetic architecture among multiple phenotypes by hierarchical clustering of gene-level association statistics. Genetics, 2020.

[84] Lorin Crawford, Ping Zeng, Sayan Mukherjee, and Xiang Zhou. Detecting epistasis with the marginal epistasis test in genetic mapping studies of quantitative traits. PLoS genetics, 13(7):e1006869, 2017.

[85] Maria Maddalena Barbieri, James O Berger, et al. Optimal predictive model selection. The annals of statistics, 32(3):870–897, 2004.